Chapter 2

Nickel-Catalyzed Asymmetric Reductive Cross-Coupling to Access 1,1-Diarylalkanes[◊]

2.1 INTRODUCTION

2.1.1 Background and significance

1,1-Diarylalkanes are a common pharmacophore, present in biologically active natural products as well as marketed drugs for a diverse range of applications (Figure 2.1). These products are active against cancer, osteoporosis, smallpox, tuberculosis, and insomnia and are present in natural products and pharmaceutical agents such as sertraline (**51**), lasofoxifene (**52**), and tolterodine (**53**), among others.[1–5] As such, methods for the enantioselective preparation of diarylalkanes have become a proving ground in

◊ Portions of this chapter have been reproduced from published studies (see reference **37**) and the supporting information found therein. The research presented in this chapter was completed in collaboration with Dr. Nathaniel Kadunce, a former graduate student in the Reisman group. Preliminary investigations discussed herein were conducted by Dr. Alan Cherney, a former graduate student in the Reisman lab.

asymmetric catalysis, with methods to afford these products being reported by many synthetic laboratories.[6–9] Enantioenriched 1,1-diarylalkanes have been prepared via Ni-catalyzed stereospecific,[1,10–15] as well as stereoconvergent,[16–18] cross-couplings. However, conditions for their preparation via asymmetric reductive cross-coupling remain elusive.

Figure 2.1. *Examples of bioactive chiral 1,1-diarylalkanes.*

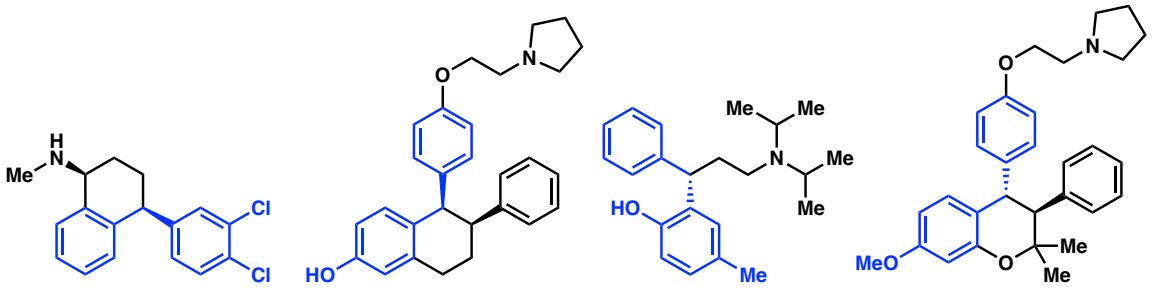

Sertraline (51)
serotonin reuptake inhibitor used as antidepressant and anti-anxiety

Lasofoxifene (52)
non-steroidal selective estrogen receptor modulator (SERM) used for treatment of osteoporosis

Tolterodine (53)
antimuscarinic drug used to treat urinary incontinence

Ormeloxifene (54)
SERM, non-hormonal, non-steroidal oral contraceptive

2.1.2 Previous Ni-catalyzed cross-coupling strategies

Due to the ubiquity of the 1,1-diarylalkane motif in bioactive molecules, significant effort has been devoted to the enantioselective synthesis of this substructure. As a complementary approach to methods such as asymmetric hydrogenation[19,20] and conjugate addition,[21–24] Ni-catalyzed stereospecific and stereoconvergent cross-coupling reactions have been developed (Scheme 2.1). In these strategies, redox-neutral couplings of a C(sp^3) benzyl electrophile and a nucleophilic organometallic C(sp^2) aryl partner are employed. For example, in 2013, Fu and coworkers reported the enantioselective Negishi coupling of benzyl mesylates with aryl zinc halides to furnish 1,1-diarylalkane products in good yields and high enantioselectivity.[16] In 2014, Jarvo and coworkers reported the

stereospecific Kumada-type coupling of enantioenriched benzyl ethers with aryl Grignard reagents using an achiral ligand.[10]

Scheme 2.1. *Examples of asymmetric cross-coupling strategies to access 1,1-diarylalkanes.*

a) Fu, 2013

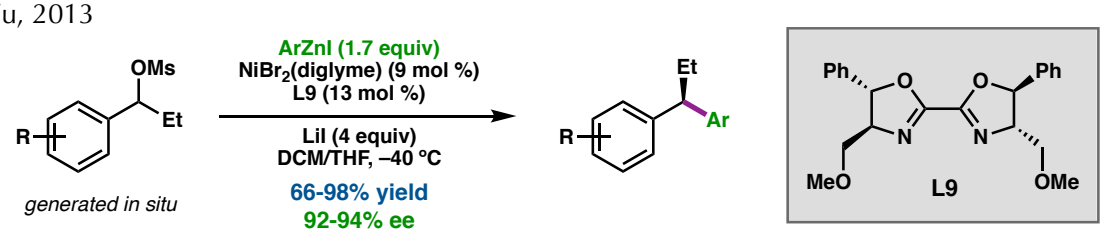

b) Jarvo, 2014

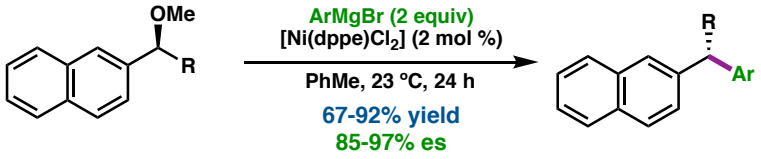

Efforts to prepare enantioenriched 1,1-diarylalkanes via asymmetric reductive coupling or Ni/Ir synergistic catalysis have proved challenging. In 2015, Weix reported a reductive cross-electrophile coupling between primary mesylates and aryl bromides;[25] this report contained a single enantioselective coupling of (1-chloroethyl)benzene (**24**) with 4-bromoacetophenone (**55**) using BnBiOX (**L2**) as the chiral ligand, which proceeded in both modest yield and ee (Scheme 2.2). Similarly, Molander reported that the coupling of (1-phenylethyl) potassium trifluoroborate (**11**) with methyl 3-bromobenzoate (**12**) proceeds in 50% ee, and coupling of more electron deficient arenes occurs with lower enantioselectivity.[18,26]

***Scheme 2.2**. Attempts to access enantioenriched 1,1-diarylalkanes.*

a) Weix, 2015

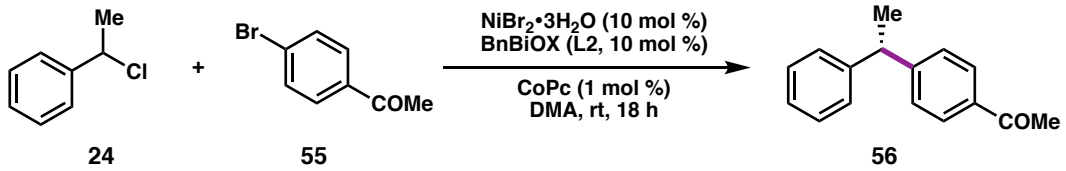

24 **55** **56**
41% yield
43% ee

b) Molander, 2014

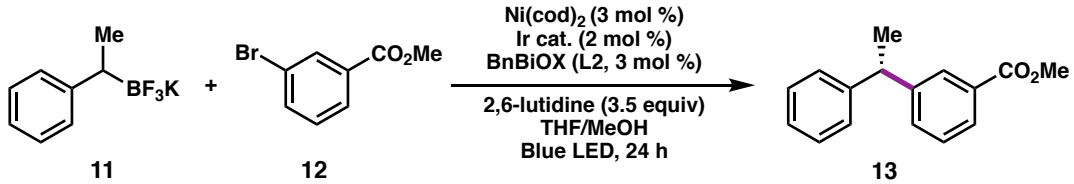

11 **12** **13**
52% yield
50% ee

2.2 REACTION DEVELOPMENT

2.2.1 Application of previously developed conditions

Based on our previously disclosed research,[27,28] we hypothesized that we could develop conditions for the Ni-catalyzed asymmetric reductive cross-coupling of benzyl chlorides and aryl iodides to access heterocycle-containing products. However, a challenge in the development of such enantioselective reactions is that as one changes electrophile class (e.g. from alkenyl halides to aryl halides), or as one alters the ligand, the product yield and ee can decrease dramatically. Consistent with the challenges encountered by others, submission of a mixture of (1-chloropropyl)benzene (**35**) and 5-iodo-2-methoxypyridine (**36**) to the optimal conditions identified for the Ni-catalyzed asymmetric reductive cross-coupling of benzyl chlorides with alkenyl bromides provided **37** in only 12% yield and 10% ee (Scheme 2.3a). Similarly, use of the conditions developed for the reductive cross-coupling of heteroaryl iodides with α-chloronitriles failed to deliver detectable amounts of **37** (Scheme 2.3b). Despite these discouraging

preliminary results, we decided to focus our initial optimization efforts on reaction conditions similar to the precedent set by our lab for related transformations.

Scheme 2.3. *Application of previously developed cross-coupling conditions.*

a) Conditions for cross-coupling of benzyl chlorides with alkenyl bromides

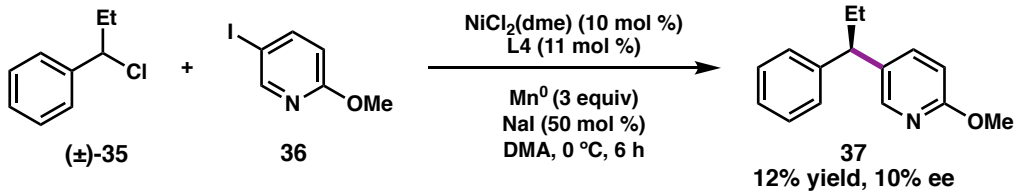

(±)-35 36 37
12% yield, 10% ee

b) Conditions for cross-coupling of chloronitriles with heteroaryl iodides

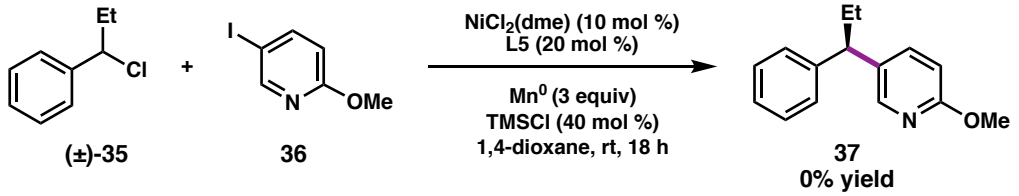

(±)-35 36 37
0% yield

2.2.2 Initial optimization

We initiated studies focusing on the cross-coupling between benzyl chlorides and aryl iodides by screening a variety of chiral bidentate ligands under both sets of conditions shown in Scheme 2.3. Employing $NiCl_2$(dme) as the Ni source and Mn^0 as the superstoichiometric reductant, we investigated the cross-coupling of **9** and **24** in DMA at room temperature (Table 2.1). We observed poor chemoselectivity across a variety of chiral ligand classes, with the formation of homocoupled dimers of both coupling partners. Modest enantioselectivities were observed with both BOX (**L3**, 49% ee) and BiOX (**L2**, 33% ee) ligand scaffolds, suggesting promise for this enantioconvergent transformation. However, further optimization employing bis(oxazoline) ligand **L3** was unsuccessful. Other ligand scaffolds such as PyBOX (**L27)**, CyanoBOX (**L1)**, PyOx (**L28)**, QuinOx (**L29)**, and PHOX (**L30)** did not induce higher enantioselectivity.

***Table 2.1**. Initial ligand investigation with 4-bromobenzonitrile (**9**).*

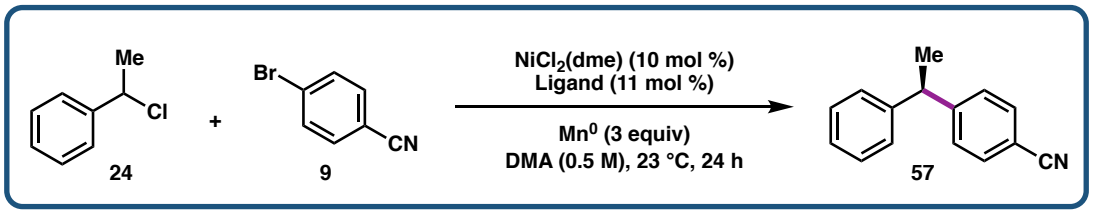

Bis(oxazoline) Ligand Scaffold

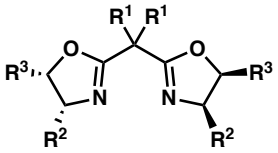

Ligand	R^1	R^2	R^3	% ee 57
L10	Me	^{i}Pr	H	19
L11	Me	^{t}Bu	H	0
L12	Me	Bn	H	1
L3	Me	Ph	H	49
L13	Me	Ph	Ph	14
L14	H	Ph	Ph	11
L15	H	Ph	H	1
L16	H	^{t}Bu	H	1
L17	H	indanyl		1
L18	Me	indanyl		3
L4	-CH_2CH_2-	indanyl		7

Bi(oxazoline) Ligand Scaffold

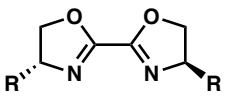

Ligand	R	% ee 57
L19	^{i}Pr	24
L20	^{t}Bu	8
L2	Bn	33
L21	Ph	1
L22	Cy	25
L23	^{s}Bu	23
L24	$CHPh_2$	3
L25	CH_2(1-naph)	20
L26	CH_2(2-naph)	29

Other Ligand Scaffolds

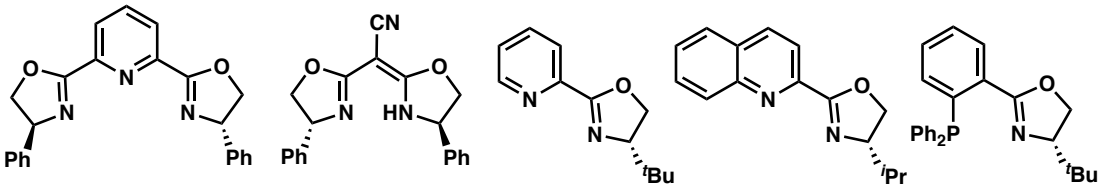

L27 3% ee | L1 39% ee | L28 14% ee | L29 8% ee | L30 12% ee

2.2.3 Application of 1,4-dioxane/TMSCl conditions

Given these results, we moved away from conditions similar to those shown in Scheme 2.3a in DMA, and focused instead on different chiral ligand classes in 1,4-dioxane with TMSCl as an activator, conditions more closely related to the cross-

coupling of heteroaryl iodides with α-chloronitriles (Scheme 2.3b). We explored several chiral bidentate ligand classes under these conditions and discovered that performing the reaction with bi(oxazoline) ligand **L22** in 1,4-dioxane with TMSCl as an activator[29,30] produced **59** in 74% yield and 74% ee (Table 2.2). Studying now the cross-coupling of (1-chloroethyl)benzene (**24**) and 2-chloro-5-iodopyridine (**58**), a solvent screen with **L22** confirmed 1,4-dioxane to give the highest level of yield and enantioselectivity with a clean reaction profile, delivering diminished amounts of homocoupled side product **60** (Table 2.2). Polar solvents, such as DMA and DMPU, gave product **59** in low to moderate enantioselectivity (Table 2.2).

Table 2.2. *Solvent investigation with bi(oxazoline) ligand (**L22**).*

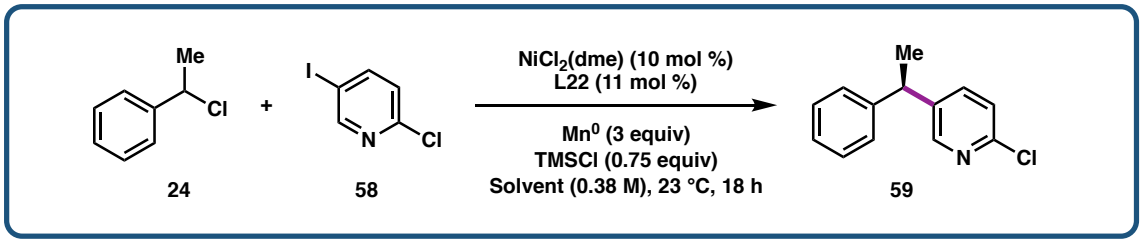

24 58 59

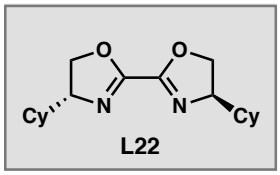

L22

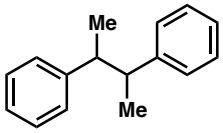

60
rac and meso

with 11 mol % CyBiOX (L22):

Solvent	Yield HC 60 (%)	Yield 59 (%)	ee 59 (%)
DMA	72	25	31
DMPU	33	60	49
THF	51	49	43
DME	41	54	55
MeCN	47	44	6
DCM	50	10	44
MeOH	77	13	73
1,4-Dioxane	26	74	74

Encouraged by these results, we explored several more bi(oxazoline) ligand scaffolds bearing both aryl and alkyl substituents at room temperature (Table 2.3).[31] We

were surprised to observe that ligands bearing aryl substituents, such as phenyl (**L2**, **L21**, and **L24**) or naphthal (**L25** and **L26**), afforded poor yields of product in moderate ee. We note that BnBiOX (**L2**), the ligand used by used by Weix and Molander, perform poorly under these conditions. However, branched-alkyl ligands bearing groups such as cyclohexyl (**L22**), *sec*-butyl (**L23**), and *iso*-butyl (**L8**), furnished **59** in significantly improved yields and enantioselectivities over the aryl-substituted BiOX ligands (Table 2.3).

Table 2.3. *Bi(oxazoline) ligand investigation.*

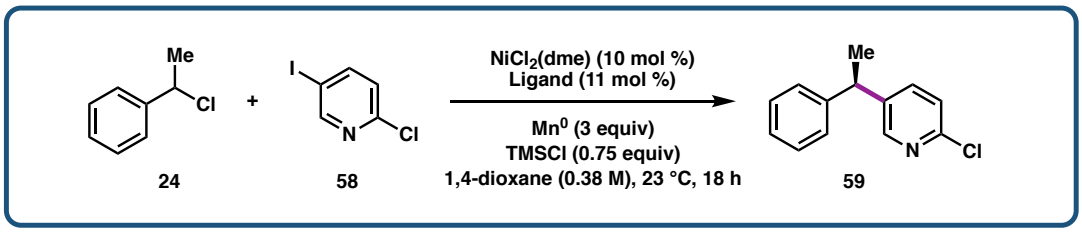

Bi(oxazoline) Ligand Scaffold

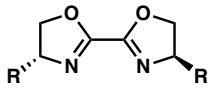

Ligand	R	Yield HC 60 (%)	Yield 59 (%)	ee 59 (%)
L21	Ph	0	0	–
L24	$CHPh_2$	43	37	67
L25	CH_2-1-Nap	3	17	44
L26	CH_2-2-Nap	5	32	50

Ligand	R	Yield HC 60 (%)	Yield 59 (%)	ee 59 (%)
L2	Bn	54	39	44
L22	Cy	32	68	69
L23	*s*-Bu	0	35	76
L8	*i*-Bu	6	68	56

Our lab has had success employing chiral BOX ligands in the cross-coupling of various C(sp^3) electrophiles with alkenyl halides,[32–34] but these results, as well as results described in **Chapter 3**, suggest that while BOX ligands are optimal for an alkenyl halide coupling partner, BiOX ligands provide the best reactivity for the cross-coupling of aryl halides. Comparison of the BOX and BiOX structures reveals that the larger bite angle of the BiOX ligands directs the substituents on the oxazoline ring farther away from the

metal center, reducing steric encumbrance at the reaction site, creating a larger chiral cavity that can tolerate the larger steric profile of aryl halides (than a disubstituted *E*-alkenyl halide). While this larger bite angle might be responsible for increased reactivity, it is possible that the more distal substituents are less effective at transferring chiral information, resulting in moderate ee's.

2.2.4 Novel bi(oxazoline) ligand synthesis

Given these exciting results, we aimed to incorporate several more alkyl groups onto the bi(oxazoline) scaffold in the hopes of improving the enantioselectivity of the cross-coupling. The usual method to synthesize bi(oxazoline) ligands is a four step sequence from the commercially available amino acid, or three steps from the amino alcohol (Scheme 2.4). However, we did not want to limit ourselves to alkyl groups found on commercially available amino acids and so developed an asymmetric route to introduce novel alkyl groups onto an amino alcohol backbone using Ellman's chiral auxiliary to perform diastereoselective Grignard additions of *sec*-alkyl reagents to access protected 1,2-amino alcohols.[35]

Scheme 2.4. *Bi(oxazoline) ligand synthesis from chiral amino alcohol.*

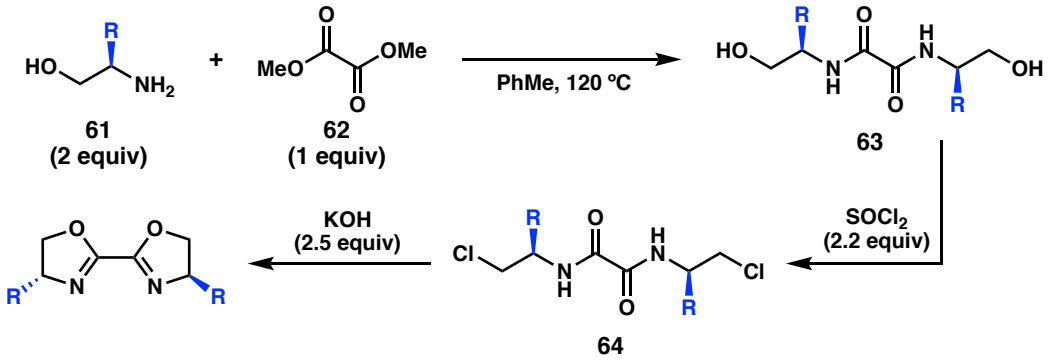

Known chiral sulfinimine **65** was synthesized in three steps from commercially available cis-2-butene-1,4-diol. From this compound, we were able to successfully perform several Grignard additions to introduce both cyclic and acyclic alkyl groups, such as cyclopentyl, cycloheptyl, 3-pentyl, and 4-heptyl, with high diastereoselectivity (Scheme 2.5). Cleavage of the chiral auxiliary with HCl/dioxane could be performed smoothly to furnish amine **67**. Finally, deprotection of the benzyl group was performed through a hydrogenolysis with Pd/C to access the desired amino alcohol (**61**), which could then taken through the three-step BiOX synthesis (Scheme 2.4). Condensation with dimethyl oxalate to give the polar diamide **63**, chlorination with thionyl chloride, and subsequent base-mediated cyclization provided the novel alkyl-substituted bi(oxazoline) ligands. Unfortunately, this route requires nine steps in the longest linear sequence and an early divergence point. Efforts to design a shorter synthesis of these ligands are ongoing in our laboratory.

Scheme 2.5. *Synthesis of novel enantioenriched alkyl-substituted amino alcohols.*

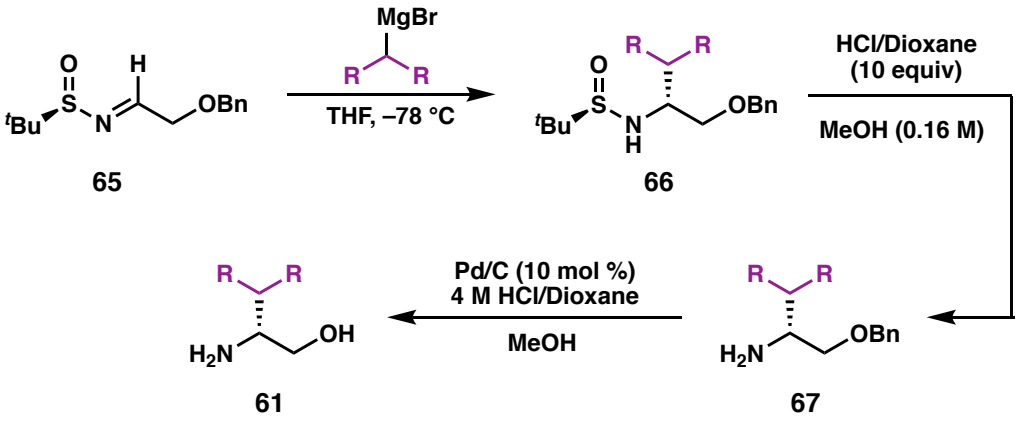

Gratifyingly, these novel branched-alkyl ligands performed well in the asymmetric reductive cross-coupling reaction, improving upon the yield and ee observed with CyBiOX (**L22**). CyPentyl (**L31**), CyHeptyl (**L32**), and 3-PentylBiOX (**L33**) gave

the desired product **59** in 75% ee and good yields with suppressed homocoupled product **60** (Table 2.4). We were pleased to observe that 4-HeptylBiOX (**L6**) provided the desired diarylalkane **59** in 81% yield with 80% ee, the highest yield and ee observed to that point.

Table 2.4. *Novel bi(oxazoline) ligand investigation.*

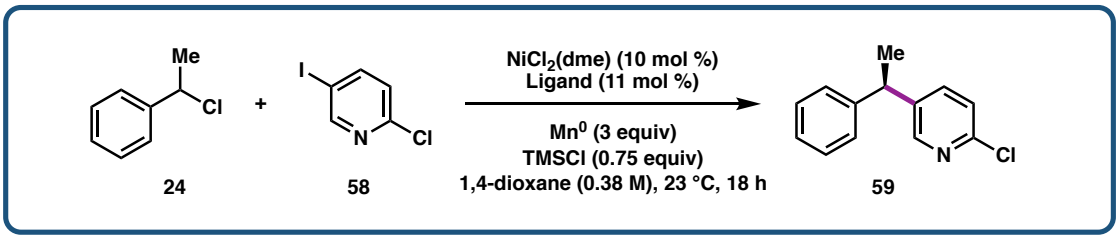

Bi(oxazoline) Ligand Scaffold

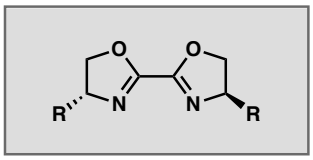

Ligand	R	Yield HC 60 (%)	Yield 59 (%)	ee 59 (%)
L31	Cy-Pentyl	15	81	75
L22	Cy-Hexyl	32	68	69
L32	Cy-Heptyl	28	72	75
L33	3-Pentyl	23	65	75
L6	4-Heptyl	16	81	80

2.2.5 Evaluation of remaining reaction parameters

With these promising ligand results in hand, we turned our attention to the optimization of the remaining reaction parameters. Due to the lengthy synthesis required to access noncommercial amino acid-derived branched ligands (such as **L6**), we chose to perform further reaction optimization using the analogous ligand, CyBiOX (**L22**), which can be readily accessed in four steps from the commercially available amino acid. A screen of Ni precatalysts revealed a significant improvement in yield and selectivity upon switching to $NiBr_2$(diglyme), the first time that a Ni source other than $NiCl_2$(dme) has been optimal in our hands (Table 2.5). Employing this Ni salt, we conducted a screen of metal/ligand ratios and catalyst loading. This survey revealed a remarkable tolerance for

variability in these parameters. However a catalyst loading of 10 mol % with a 2:1 ligand:metal ratio gave the most reproducible results and was chosen as the standard condition for further studies.

Table 2.5. *Evaluation of Ni sources and catalyst loadings.*

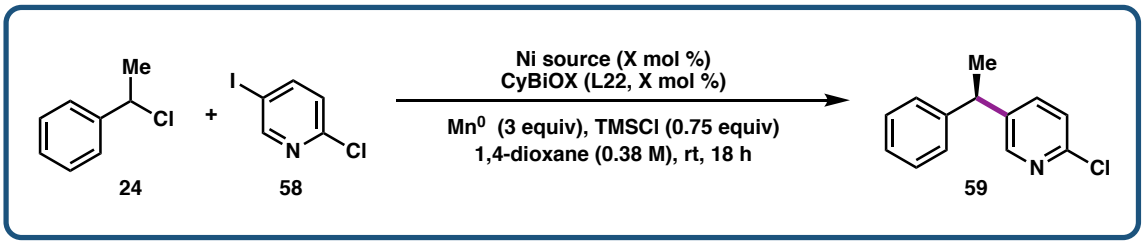

with 11 mol % CyBiOX (LXX):

Ni Source (10 mol %)	Yield HC 60 (%)	Yield 59 (%)	ee 59 (%)
$NiCl_2$(dme)	30	69	69
$Ni(OAc)_2 \cdot 4H_2O$	0	22	72
$Ni(BF_4)_2 \cdot 6H_2O$	5	0	-
$Ni(acac)_2$	30	69	69
$NiBr_2$(dme)	25	74	72
$NiBr_2$(diglyme)	20	81	74

with $NiBr_2$(diglyme):

% Ni	M:L	Yield HC 60 (%)	Yield 59 (%)	ee 59 (%)
5%	1:1	15	71	75
5%	1:2	22	77	75
10%	1:1	16	68	74
10%	1:1.5	23	77	72
10%	1:2	25	75	74
10%	1:3	27	78	74
15%	1:1	29	71	71
15%	1:2	29	71	74

In a survey of reductants, Mn^0 emerged as the most efficacious in this series, with Zn^0 giving lower yield and selectivity (Table 2.6). The difference in reactivity may be attributed to the difference in reduction potential between the metals. However, the change in enantioselectivity is more difficult to rationalize. It is possible that the reductants favor different mechanisms, or one can imagine that the stoichiometric Lewis-acidic salt byproducts may exert significant influence over the course of the reaction. Poor yields were achieved employing the soluble organic reductant TDAE (entry 5),[36]

with lower selectivity. Other activating reagents in place of TMSCl, such as TFA or TfOH (entries 8 and 10),[29,30] resulted in minimal product formation with no enantioinduction, while TMSOTf and 4 M HCl/dioxane delivered **59** with moderate enantioselectivity, albeit in low yields (Table 2.6, entries 9 and 11).

Table 2.6. *Evaluation of reductants and activating reagents.*

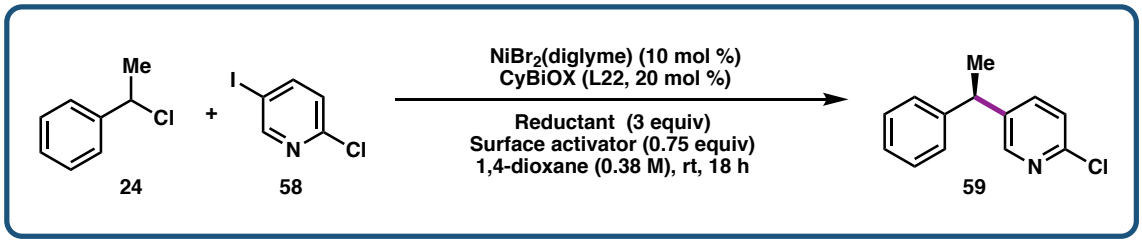

with TMSCl:

Entry	Reductant	Yield (%)	ee (%)
1	Mn^0	83	72
2	Zn^0	20	30
3	Zn^0 + $MgCl_2$	6	0
4	In^0	0	-
5	TDAE	6	31
6	TDAE (-TMSCl)	6	43

with Mn^0:

Entry	Surface activator	Yield (%)	ee (%)
7	TMSCl	74	74
8	TFA	3	0
9	TMSOTf	18	64
10	TfOH	1	3
11	4 M HCl/dioxane	4	60

Next, we screened the reaction at various temperatures. We observed a decrease in yield and ee with increasing temperature (Table 2.7, entries 2 and 3), with increased formation of homocoupled product **60**. Since the freezing point of 1,4-dioxane is 12 °C, it was necessary to employ a co-solvent to run the reaction at low temperature. DCM and DMA proved to be competent co-solvents at room temperature, and allowed us to explore the reactivity at 10 °C and 0 °C (Table 2.7). Regardless of the identity or ratio of co-solvent, the yield of **59** was greatly diminished at lower temperatures, even with allowing the reaction to run longer for 24 hours, with little benefit to the enantioinduction. The ee of **59** increased slightly to 76% with 30% DCM at both 10 °C and 0 °C, while only

resulting in approximately 25% yield of **59** (Table 2.7, entries 4 and 6). Increasing the ratio of DCM to 50% resulted in an increase in yield, but a decrease in ee (Table 2.7, entry 5). Finally, the use of DMA as a co-solvent resulted in a decrease in both yield and ee of **59** (Table 2.7, entry 7).

Table 2.7*. Temperature investigation.*

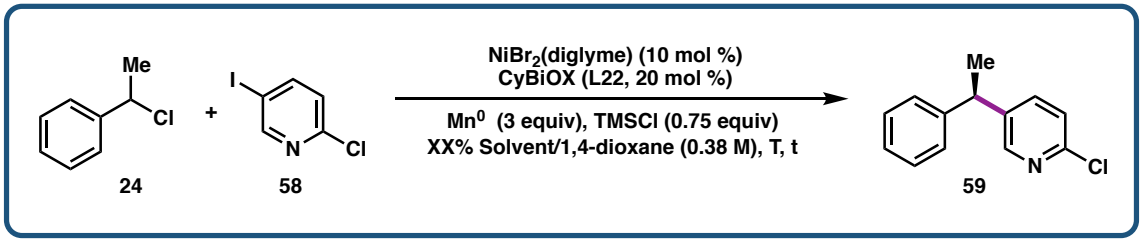

Entry	Solvent	T (°C)	t (h)	% Yield 59	% ee 59
1	–	23	18	74	70
2	–	40	18	65	62
3	–	60	18	56	55
4	30% DCM	10	24	23	76
5	50% DCM	10	24	52	55
6	30% DCM	0	24	27	78
7	30% DMA	0	24	28	53

2.2.6 Investigation into sec-alkyl ligand effect

With optimized conditions in hand, we returned to the ligand effect on this reaction. The novel sec-alkyl bi(oxazoline) ligands that we synthesized provided a markedly improved effect on both the reactivity and selectivity of this reaction, suppressing homocoupling to favor the formation of the desired product, while also achieving the highest levels of enantioselectivity among various chiral ligand classes. Looking specifically at the cross-coupling of (1-chloropropyl)benzene (**35**) with 5-iodo-2-methoxypyridine (**36**) across a series of these acyclic *sec*-alkyl substituted BiOX ligands produces a fascinating trend in reactivity and selectivity (Table 2.8). As the

length of the alkyl chains increase incrementally by two methylenes from ^{i}Pr (**L19**) to 3-pentyl (**L33**) to 4-heptyl (**L6**), the enantioselectivity increases by 10% with each homologation. We observe a significant increase in yield from **L19** (22% yield) to **L33** (74% yield), and then a further 10% increase with **L6** (84% yield).

Table 2.8. *Sec-alkyl bi(oxazoline) ligand investigation.*

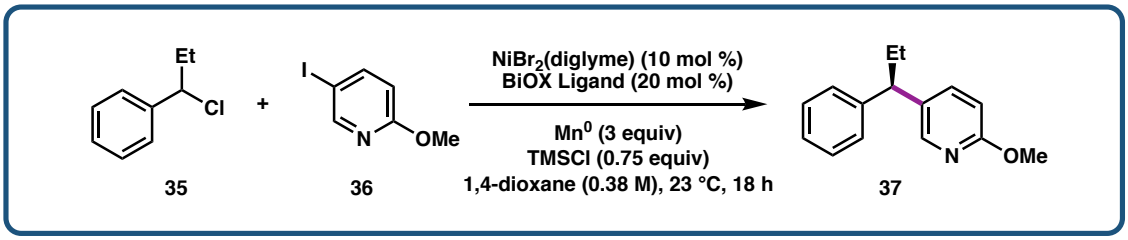

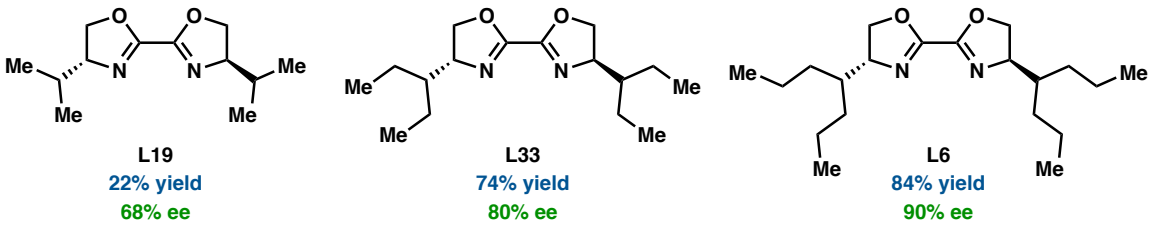

The effect of these longer alkyl groups on both the chemoselectivity and yield remains unclear at this stage. The hydrophobic alkyl chains could provide flexible, steric blocking, resulting in increased enantioinduction. During the development of this transformation,[37] the Doyle group at Princeton University reached out to us to request material of **L6**. Interestingly, **L6** was the optimal ligand in their stereoconvergent cross-coupling of racemic aziridines and aryl iodides (Scheme 2.6).[38]

Scheme 2.6. *Sigman and Doyle's reductive cross-coupling of racemic aziridines.*

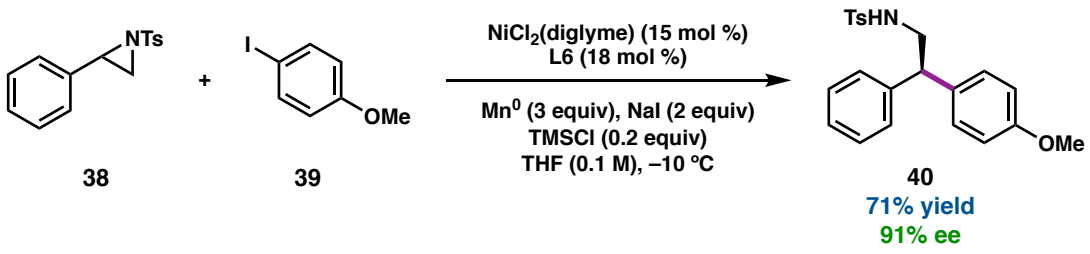

A collaboration between the Doyle and Sigman group at the University of Utah revealed parameters such as the minimum width of the ligand substituent (steric effects), electronic character, and polarizability of the ligand (presence of non-covalent interactions) were primarily responsible for the enantioselectivity of the reaction (Scheme 2.6). Our lab is currently collaborating with the Sigman group to apply their multivariate analysis tools to determine if the alkyl-substituents are inducing non-covalent interactions with the coupling partners, significantly altering the ligand bite angles, or influencing some other mechanistic parameter to produce the observed effects in our transformations.

2.2.7 Reproducibility issues on scale

Finally, this reaction proved extremely sensitive to an increase in scale. When we increased the scale of the reaction from 0.05 mmol to 0.2 mmol, we observed a significant decrease in yield of the desired product, independent of reaction time, with no change in ee (Table 2.9). After exploring several variables, such as purity of substrates and reagents, vessel and stir bar size, stirring speed, concentration, catalyst loading, and activation of the reductant on 0.2 mmol scale, we discovered the method in which the reagents were added was essential to the success of the reaction.

Table 2.9. *Reproducibility and conversion issues on 0.2 mmol scale.*

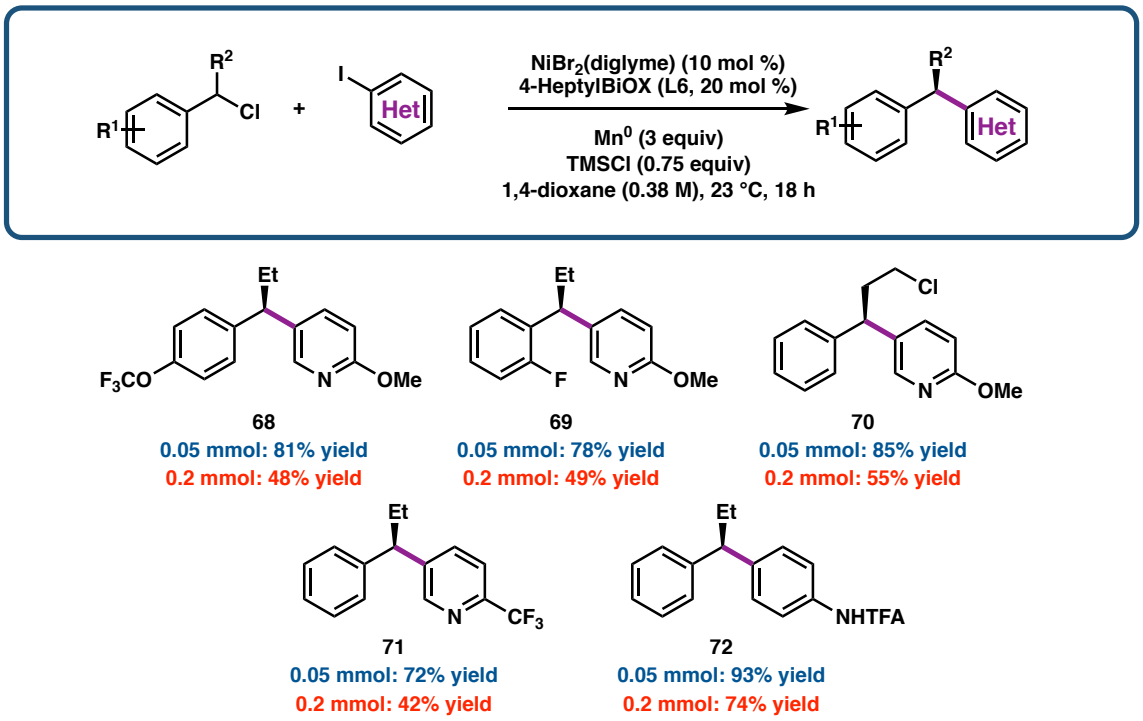

The reaction setup consists of the addition of solid reagents, including the Ni catalyst, ligand, and reductant, which are then dissolved in 1,4-dioxane. After several minutes of stirring, the aryl iodide (**36**), benzyl chloride (**73**), and lastly TMSCl are added. On scale, it was necessary to stir the reaction for 20 min before addition of the coupling partners and the activating reagent in order for the reaction to go to full conversion (Table 2.10, entries 2 and 3). Addition of the TMSCl before either coupling partner leads to reaction failure (Table 2.10, entry 4). Interestingly, this mirrors the setup of multiple reactions on the 0.05 mmol screening scale, which inherently requires more time for setup.

Table 2.10. *Effect of pre-stir of reagents on 0.2 mmol scale.*

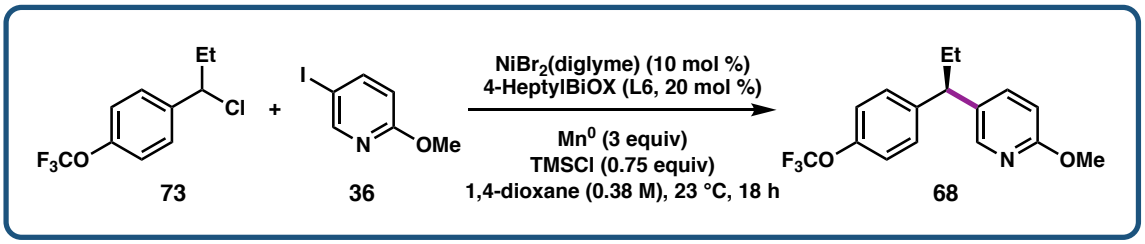

Entry	Pre-stir Conditions	% Yield 68	% ee 68
1	Control: Stir 2 min, then 36, 73, TMSCl	48	87
2	Stir 20 min, then 36, 73, TMSCl	76	87
3	36, stir 20 min, then 73, TMSCl	80	87
4	36, TMSCl, stir 20 min, then 73	0	—

2.3 SUBSTRATE SCOPE

Before investigating a wide range of substrates, we first sought to assess the strategy of functional group incorporation to access these pseudosymmetric products. That is, informed substrate selection in which substitution is introduced on either the benzyl component or the aryl partner depending on reaction tolerance, may allow us to prepare a variety of differently substituted mono-substituted 1,1-diarylalkane. This disconnection versatility is an advantage of this cross-coupling methodology, allowing us to leverage the ideal disconnection of the target. Therefore, we initially explored a short series of mono-substituted electrophiles to compare the functional group performance on each coupling partner. Benzyl chlorides bearing conjugated electron-withdrawing groups such as nitriles (**74**) underwent rampant decomposition, affording low yields and messy reaction profiles (Figure 2.2). Fortunately, these groups were well tolerated when incorporated via the aryl iodide partner. The opposite trend was observed with *ortho*-coordinating groups, such as *o*-methoxy **75**. These groups afforded good yields and high

ee's when installed on the benzyl chloride partner, but gave low enantioselectivity from the corresponding aryl iodide. Non-conjugated groups at the *para*- and *meta*-positions gave only slight and unpredictable variability between the two partners, as observed in the *para*-methoxy containing substrate **76**. Finally, non-coordinating *ortho*-substituents, such as methyl, performed poorly on both substrates (not shown).

Figure 2.2. *Strategic disconnection of pseudosymmetric 1,1-diarylalkanes.*

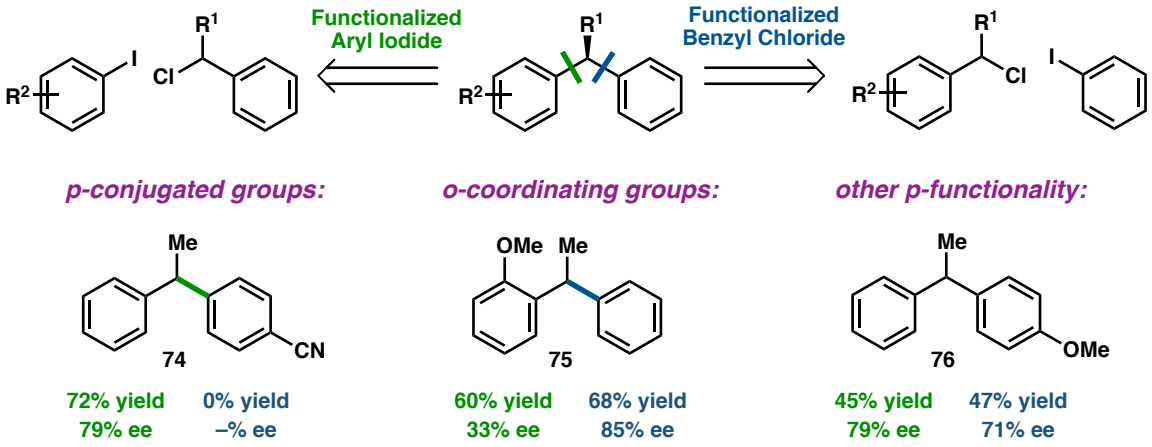

With preliminary knowledge of substrate-dependent functional group tolerance, we evaluated the substrate scope of the aryl iodide coupling partner (Table 2.11). Pyridyl iodides bearing substitution at the 2-position couple smoothly (**37**, **77–79**, **90**), as do pyrimidines (**88**, **89**) and indoles (**87**). Non-heteroaryl iodides bearing either electron-rich (**83, 84**) or electron-poor (**81**, **82**, **85–86**) functional groups couple smoothly, although slightly lower ee is observed with more electron-rich arenes. It is notable that acidic protons are tolerated (**84**); no protodehalogenated byproducts observed. The cross-coupling is orthogonal to aryl boronates and triflates, affording **80** and **81** in excellent yields and providing handles for further derivatization. Interestingly, use of the

corresponding aryl bromide, instead of **36**, delivered **37** in only slightly reduced yield and comparable ee (72% yield, 89% ee).

Table 2.11. *Scope of (hetero)aryl iodides.*[a]

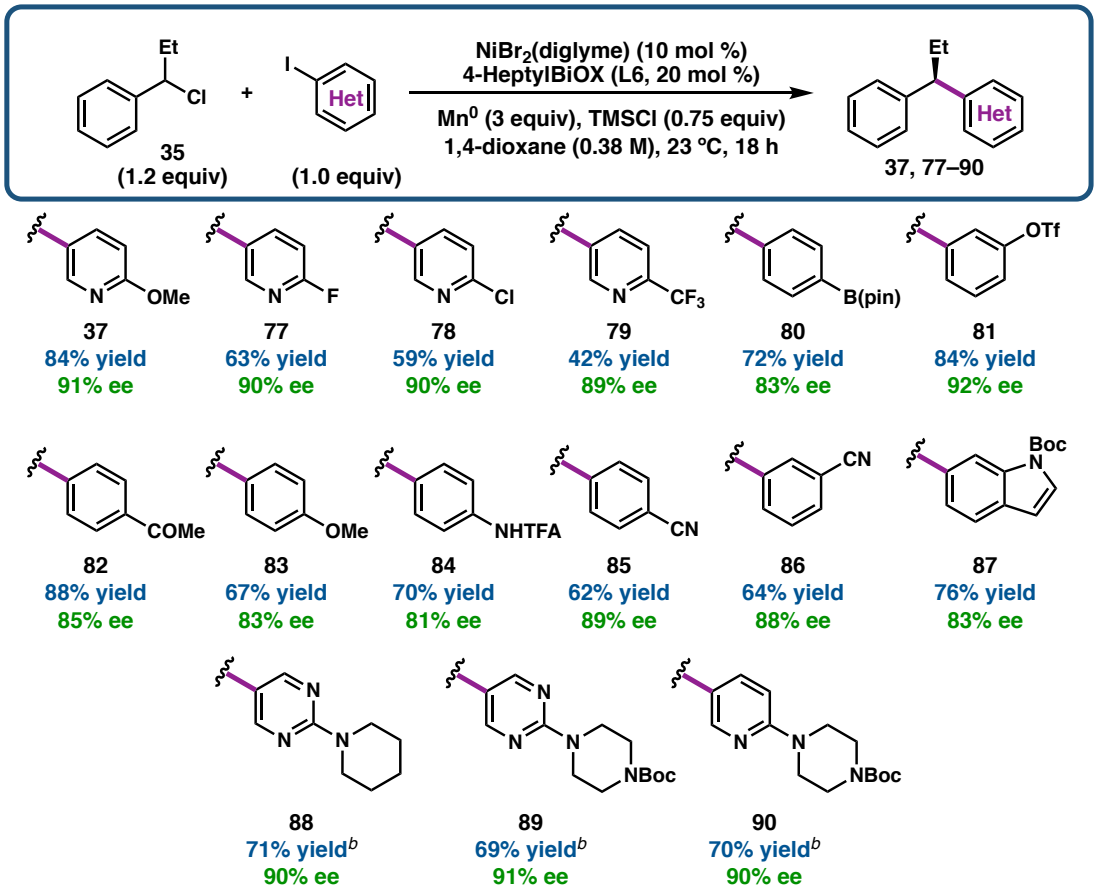

[a] Isolated yields, reactions conducted on 0.2 mmol scale under an N_2 atmosphere in a glovebox. % ee determined by SFC using a chiral stationary phase. [b] 2.4 equiv of 35 is used.

Next, we turned our attention to the scope of the benzyl chloride coupling partners (Table 2.12). Substrates with either electron-donating or -withdrawing substituents at the *para* position couple in comparable yields and enantioselectivity (**91**–**95**). In addition, *o*-substitution with either methoxy (**94**) or fluorine (**95**) is tolerated, although the products are formed in decreased yields. Substituents of varying steric encumbrance can be incorporated at the α-position of the benzyl halide (**96**–**101**). Of particular interest, good

chemoselectivity is observed for coupling of the benzyl chloride in preference to the primary chloride (**97**). *N*-Boc-piperidine (**101**) and dibenzofuran (**102**) groups are also tolerated, providing the products in serviceable yields and excellent ee. Employing the corresponding benzyl bromide in place of **35** increased formation of dibenzyl homocoupling product at the expense of **37** with slightly lower ee (8% yield, 81% ee).

Table 2.12. *Scope of benzyl chlorides.*[a]

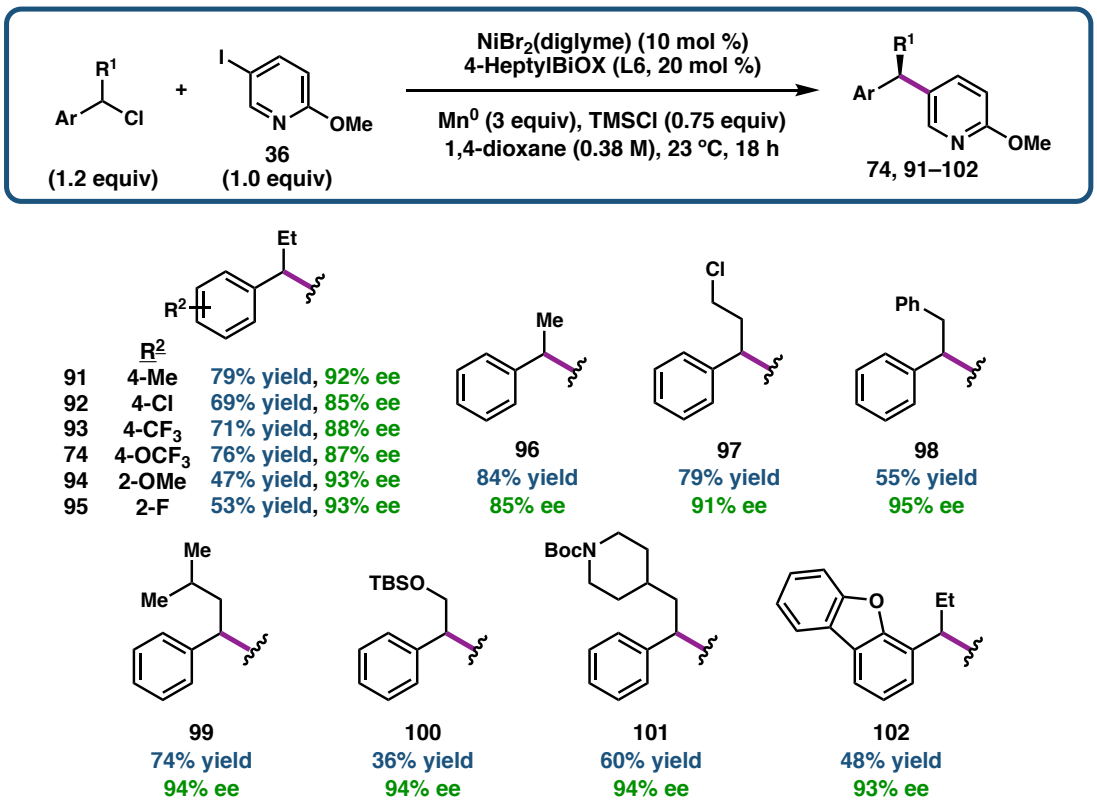

[a] Isolated yields, reactions conducted on 0.2 mmol scale under an N_2 atmosphere in a glovebox. % ee determined by SFC using a chiral stationary phase.

We were pleased to see the heterogeneous reaction performed well on a 2.0 mmol scale in a round bottom flask, producing pyridine **37** in 63% yield and 91% ee. To further demonstrate the potential synthetic utility of our method, we synthesized diarylalkane **107**, an intermediate in the synthesis of the commercial anti-depressant sertraline (Scheme 2.7).[39] Unfortunately, the cross-coupling of tetralone **103** with commercially

available iodobenzene **104** under our standard reaction conditions afforded product **105** in only 23% yield and 54% ee. This poor yield could be due to the instability of the benzyl chloride coupling partner, which was prone to decomposition into the corresponding naphthol. Fortunately, cross-coupling of 1-chloro-1,2,3,4-tetrahydronaphthalene (**106**) with **104** provides chiral tetrahydronaphthalene **107** in 70% yield, and 84% ee. Subsequent benzylic oxidation of **107** using 3 equiv of CrO_3 in $AcOH/H_2O$ afforded tetralone **108** in 51% yield (unoptimized) with no erosion of ee.[40] This oxidation suffered from both poor conversion, as well as the formation of over-oxidized side products. Tetralone **108** is a known intermediate in the synthesis of sertraline.[41–44]

Scheme 2.7. *Synthesis of sertraline intermediate.*

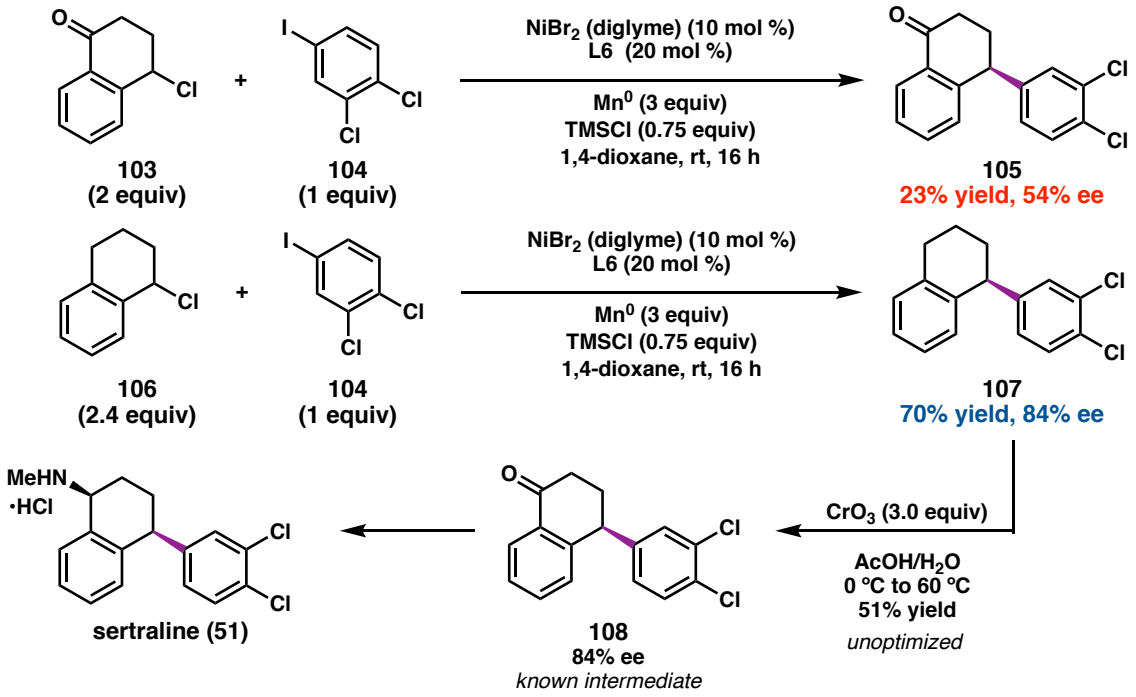

2.4 MECHANISTIC STUDIES

Confident in the range and utility of the substrate scope, we next sought to probe the mechanism of this transformation. As described in **Chapter 1**, we hypothesize that asymmetric reductive cross-couplings of radical-stabilized C(sp^3) electrophiles may proceed through the intermediacy of prochiral radicals generated from a halide abstraction event. This can occur in either a sequential reduction mechanism, in which halide abstraction and radical addition occur rapidly in a radical rebound process (Figure 2.3a), or a radical chain reaction mechanism with a long-lived, cage escaped radical intermediate (Figure 2.3b).

Figure 2.3. *Mechanistic hypotheses for the asymmetric reductive cross-coupling.*

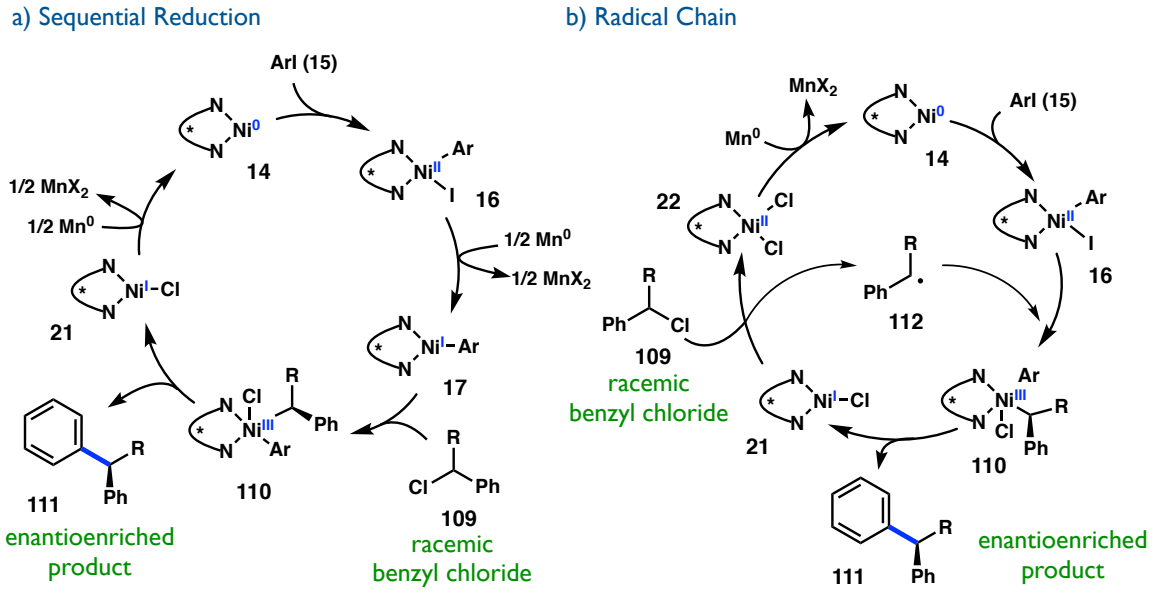

In order to determine the presence and nature of benzylic radical intermediates in the reductive cross-coupling of benzyl chlorides and aryl halides, we conducted a series of mechanistic investigations. First, when cyclopropyl chloride **113** was subjected to the standard cross-coupling conditions, alkene **115** was obtained in 57% yield (Scheme 2.8).

We hypothesize that a cyclopropyl carbinyl radical (**116**) is generated from halide abstraction by Ni(I) species **17**. This benzylic radical can then reversibly open the cyclopropane to give a primary homoallylic radical,[45,46] which can be intercepted by Ni(II) species **118** to form Ni(III) **110**. Ideally, both **116** and **117** could add to the Ni(II) complex and a ratio of the unrearranged (**114**) and rearranged (**115**) products would form. Varying the Ni loading would then support one mechanistic hypothesis over the other depending on the behavior of the ratio of these products formed.[47] However, we were not able to observe the formation of **114**, likely due to steric interference of the cyclopropyl group, and thus cannot conclusively favor one mechanistic hypothesis. However, these findings are consistent with a mechanism that proceeds through a non-persistent alkyl radical, though we cannot rule out the possibility of a Ni-mediated cyclopropane opening pathway at this time.

Scheme 2.8. *Radical clock studies.*

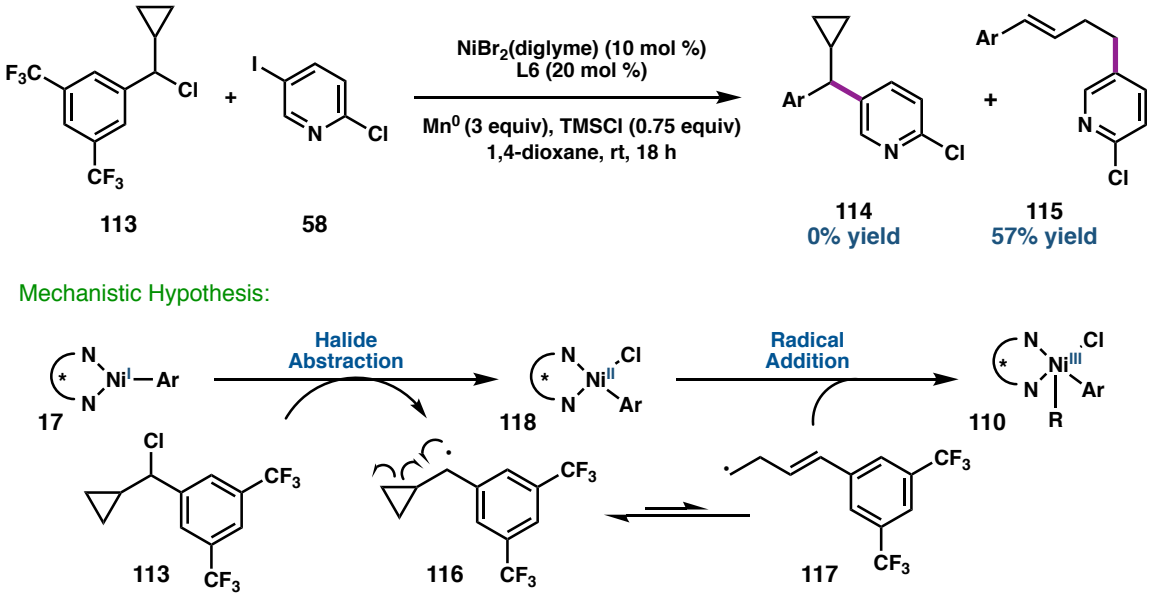

Next, the reaction was conducted in the presence of TEMPO, which has been used to trap carbon-centered radical species. However, no significant decrease in yield

was observed, and no TEMPO trapping adducts were detected (Scheme 2.9). A control experiment in which TEMPO was treated with Mn^0 and TMSCl in 1,4-dioxane indicated that TEMPO is stable under the reaction conditions, however we cannot rule out the possibility that reduction of TEMPO precludes trapping. Likewise, other known radical inhibitors, BHT and DHA, did not cause inhibition of the reaction at 50 mol % loading (Scheme 2.9). These findings suggest a non-persistent alkyl radical.

Scheme 2.9. *Radical inhibitor studies.*

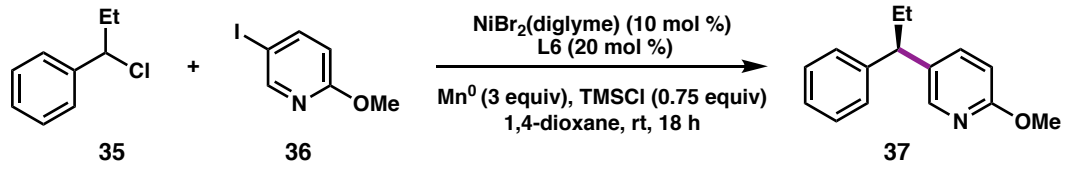

35 36 37

Control: 84% yield, 90% ee
50 mol % BHT: 83% yield, 89% ee
50 mol % DHA: 78% yield, 88% ee
50 mol % TEMPO: 72% yield, 91% ee

Further studies of the mechanism are ongoing; it is unclear at this time whether the absolute stereochemistry is determined by addition to form a Ni(III) species or reductive elimination from Ni(III). Fu and coworkers have demonstrated that chiral Ni catalysts can promote stereoconvergent cross-couplings of racemic *sec*-alkyl electrophiles and organometallic reagents due to the stereoablative interaction of the *sec*-alkyl electrophile with Ni.[48–51] We can imagine that enantioinduction arises during either the oxidative addition of the C(sp^3) electrophile to generate the Ni(III) complex or, if oxidative addition is reversible, during reductive elimination.[18]

2.5 CONCLUSION

In conclusion, we have developed a Ni-catalyzed asymmetric reductive cross-coupling between (hetero)aryl iodides and benzyl chlorides. This transformation enables the synthesis of enantioenriched 1,1-diarylalkanes from simple organic halide starting materials. The reaction tolerates a wide range of functionality, including heterocyclic substrates. Key differences in the substrate scopes of the two partners highlight the advantage of this disconnection in synthetic planning, exploiting the pseudosymmetry of the products to select optimal coupling substrates. The success of this effort hinged on the development of a new chiral bi(oxazoline) ligand, 4-HeptylBiOX (**L6**), which provides 1,1-diarylalkanes with both improved yield and enantioselectivity relative to previously disclosed BiOX ligands.

2.6 EXPERIMENTAL SECTION

2.6.1 *Materials and Methods*

Unless otherwise stated, reactions were performed under a nitrogen atmosphere using freshly dried solvents. Methylene chloride (DCM), diethyl ether (Et_2O), tetrahydrofuran (THF), 1,4-dioxane and toluene (PhMe) were dried by passing through activated alumina columns. All other commercially obtained reagents were used as received unless specifically indicated. Aryl iodides were purchased from Sigma Aldrich, Combi-Blocks, or Astatech. Manganese powder (>99.9%) was purchased from Sigma Aldrich. $NiBr_2$(diglyme) was purchased from Strem. All reactions were monitored by thin-layer chromatography using EMD/Merck silica gel 60 F254 pre-coated plates (0.25 mm). Silica gel and basic alumina column chromatography was performed as described by Still et al. (W. C. Still, M. Kahn, A. Mitra, *J. Org. Chem*. **1978**, *43*, 2923.) using silica gel (particle size 0.032–0.063) purchased from Silicycle and aluminum oxide (activated, basic, Brockmann I, 58 Å pore size, powder) purchased from Sigma-Aldrich. ^1H and ^{13}C NMR were recorded on a Varian Inova 500 (at 500 MHz and 125 MHz respectively) or a Bruker Avance III HD with Prodigy cyroprobe (at 400 MHz and 101 MHz respectively). ^1H and ^{19}F NMR spectra were recorded on a Varian Inova 300 (at 300 MHz and 282 MHz, respectively). NMR data is reported relative to internal chloroform (^1H, δ = 7.26, ^{13}C, δ = 77.0) and C_6F_6 (^{19}F, δ = –164.9). Data for ^1H NMR spectra are reported as follows: chemical shift (δ ppm) (multiplicity, coupling constant (Hz), integration). Multiplicity and qualifier abbreviations are as follows: s = singlet, d = doublet, t = triplet, q = quartet, m = multiplet, br = broad. IR spectra were recorded on a Perkin Elmer Paragon 1000 spectrometer and are reported in frequency of absorption (cm^{-1}). Analytical

SFC was performed with a Mettler SFC supercritical CO_2 analytical chromatography system with Chiralcel AD-H, OD-H, AS-H, OB-H, and IA columns (4.6 mm x 25 cm). SFC analysis performed at 100.0 bar and 40 ºC. HRMS were acquired using either an Agilent 6200 Series TOF with an Agilent G1978A Multimode source in electrospray ionization (ESI), atmospheric pressure chemical ionization (APCI), or mixed (MM) ionization mode. Low-temperature diffraction data (φ- and ω-scans) were collected on a Bruker AXS D8 VENTURE KAPPA diffractometer coupled to a PHOTON 100 CMOS detector or a PHOTON II CPAD detector with Cu-K_α radiation (λ = 1.54178 Å) from a $I_\mu S$ HB micro-focus sealed X-ray tube. All diffractometer manipulations, including data collection, integration, and scaling were carried out using the Bruker APEXII software. Absorption corrections were applied using SADABS. The structure was solved by intrinsic phasing using SHELXT and refined against F^2 on all data by full-matrix least squares with SHELXL-2014[3] using established refinement techniques. All non-hydrogen atoms were refined anisotropically. Unless otherwise noted, all hydrogen atoms were included into the model at geometrically calculated positions and refined using a riding model. The isotropic displacement parameters of all hydrogen atoms were fixed to 1.2 times the *U* value of the atoms they are linked to (1.5 times for methyl groups). Crystallographic data for **L6** and **84** can be obtained free of charge from The Cambridge Crystallographic Data Centre (CCDC) via www.ccdc.cam.ac.uk/data_request/cif under CCDC deposition number 1819175 and 1533022, respectively. Graphical representation of the structure with 50% probability thermal ellipsoids was generated using Mercury visualization software.

2.6.2 Ligand Synthesis

2.6.2.1 Preparation of (4R,4′R)-4,4′-diheptan-4-yl)-4,4′,5,5′-tetrahydro-2,2′bioxazole (L6, (R,R′)-4-HeptylBiOX)

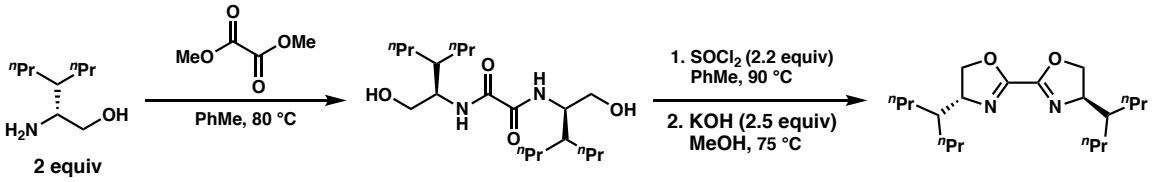

(*R,R*)-4-HeptylBiOX (L6): The synthesis of this ligand was adapted from procedures described by Denmark and coworkers. (*R*)-2-amino-3-propylhexan-1-ol (2 equiv, 2.80 g, 17.6 mmol) and dimethyloxalate (1 equiv, 1.04 g, 8.80 mmol) were dissolved in PhMe (200 mL) and heated to 80 °C. The reaction was allowed to stir overnight with the diamide precipitating out of solution as a white solid. Reaction was cooled to room temperature and concentrated *in vacuo* to afford the crude diol as a sticky white solid (3.3 g, 8.86 mmol). The crude diol was dissolved in PhMe (60 mL) and heated to 70 °C whereupon thionyl chloride (1.4 mL, 19.2 mmol) was added. Reaction was stirred at 70 °C for 30 minutes then heated to 90 °C for 90 minutes. The reaction was cooled to room temperature and poured into 20% KOH solution cooled to 0 °C. The aqueous layer was separated and extracted (3x) with DCM and the combined organic layers were washed with 20% KOH solution, $NaHCO_3$ and brine. The organic layer was dried with Na_2SO_4, filtered through a pad of Celite, and concentrated under reduced pressure to afford the dichloride as a sticky brown solid. The crude dichloride (3.6 g, 8.8 mmol) was immediately dissolved in MeOH (90 mL) and KOH (1.23 g, 21.9 mmol) was added. The reaction was heated to reflux for 14 hours. The reaction was cooled to room temperature and concentrated to remove MeOH. The crude mixture was loaded directly onto a silica

gel column and eluted with 10–40% EtOAc/Hex. The pure ligand was obtained as an off-white solid (1.55 g, 53% over 3 steps, >99% ee).

$\mathbf{R_f}$ = 0.15 (silica gel, 20% EtOAc/Hex, UV).

$\mathbf{[\alpha]_D^{25}}$ = +119° (c = 1.0, $CHCl_3$).

^{1}H NMR (500 MHz, $CDCl_3$): δ 4.47 – 4.33 (m, 2H), 4.18 – 4.11 (m, 1H), 1.65 (q, *J* = 6.2, 5.6 Hz, 1H), 1.48 – 1.12 (m, 7H), 0.95 – 0.86 (m, 5H).

^{13}C NMR (101 MHz, $CDCl_3$): δ 154.6, 71.1, 70.0, 41.6, 32.5, 32.0, 20.3, 20.2, 14.6, 14.5.

FTIR (NaCl, thin film, cm^{-1}): 2955, 2926, 2870, 1620, 1456, 1378, 1120, 945.

HRMS (ESI, *m/z*): calc'd for $C_{20}H_{37}N_2O_2^+$ $(M+H)^+$: 337.2850, found: 337.2847.

2.6.2.2 SFC Traces of rac-, (S,S)-, and (R,R)-4-HeptylBiOX

(IC, 2.5 mL/min, 20% IPA in CO_2, λ = 254 nm): t_R = 3.5 min, t_R = 4.0 min.

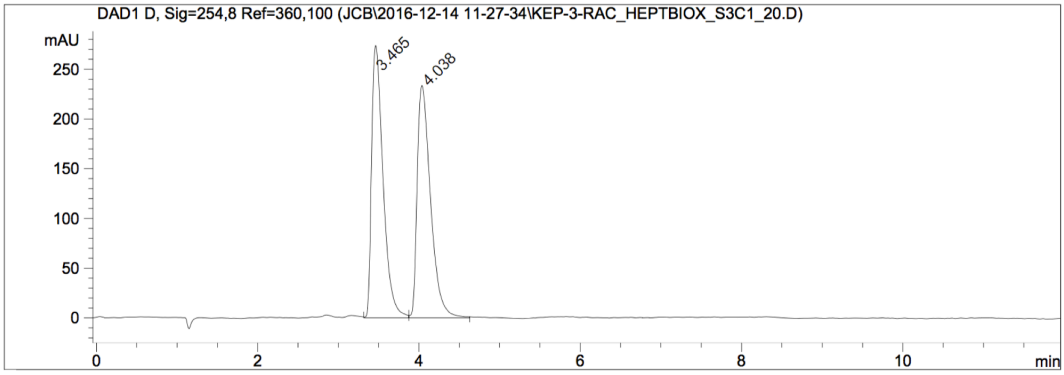

Peak #	RetTime [min]	Type	Width [min]	Area [mAU*s]	Height [mAU]	Area %
1	3.465	VV	0.1518	2709.62598	273.04416	50.1608
2	4.038	VB	0.1788	2692.25098	233.04976	49.8392

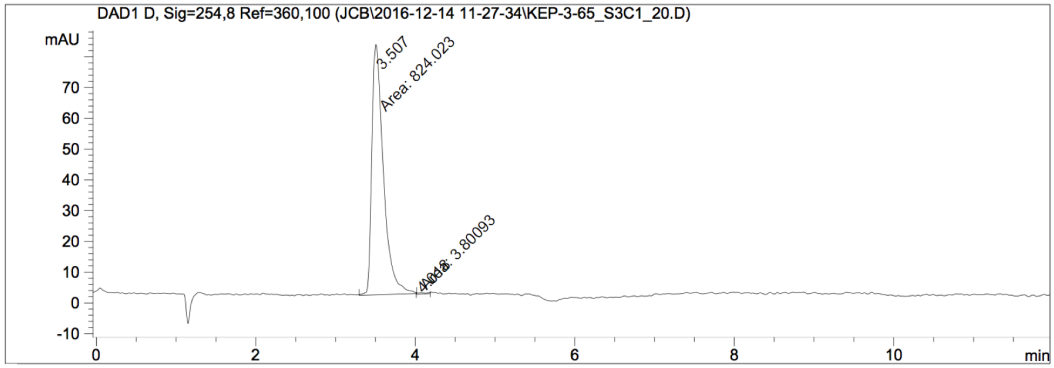

Peak #	RetTime [min]	Type	Width [min]	Area [mAU*s]	Height [mAU]	Area %
1	3.507	MM	0.1687	824.02258	81.41270	99.5409
2	4.018	MM	0.0891	3.80093	5.68225e-1	0.4591

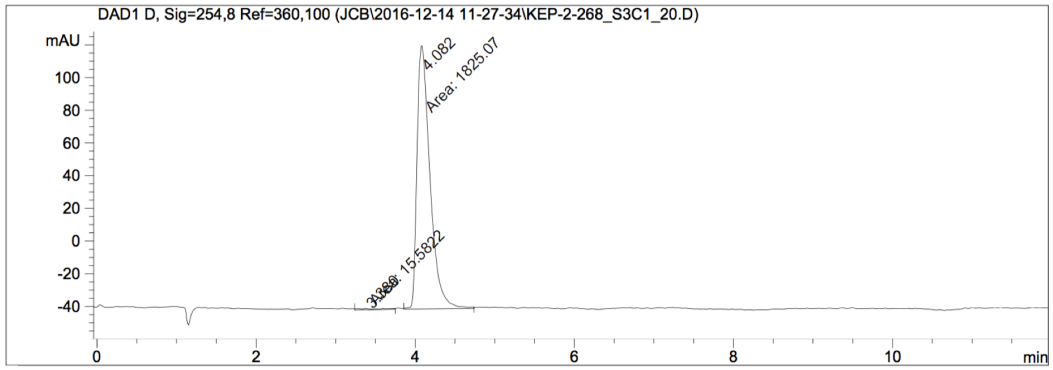

Peak #	RetTime [min]	Type	Width [min]	Area [mAU*s]	Height [mAU]	Area %
1	3.380	MM	0.2938	15.58221	8.83812e-1	0.8466
2	4.082	MM	0.1885	1825.06812	161.33264	99.1534

2.6.2.3 X-Ray crystal structure of (R,R)-4-HeptylBiOX

Suitable crystals of **L6** were grown by slow cooling in hexanes in the freezer for 4 weeks. Upon warming to room temperature, the crystals begin to dissolve in hexanes. The crystals also began to dissolve in Paratone oil, but were stable once they were removed from the oil. Compound **L6** crystallizes in the monoclinic space group $P2_1$ with three molecules in the asymmetric unit. Absolute configuration was determined by anomalous dispersion (Flack = 0.03(4)). The final R factor was refined to 3.63% with an average C–C bond e.s.d. value of 0.0022 Å. A second crystal was also analyzed by single-crystal X-ray diffraction, which was found to be in the same enantiomeric configuration (Flack = 0.05(4)). The second crystal was refined to a final R factor of 4.85% with an average C–C bond e.s.d. of 0.0032 Å. Taken together, we confirm the absolute stereochemistry of **L6** to be that of the R enantiomer.

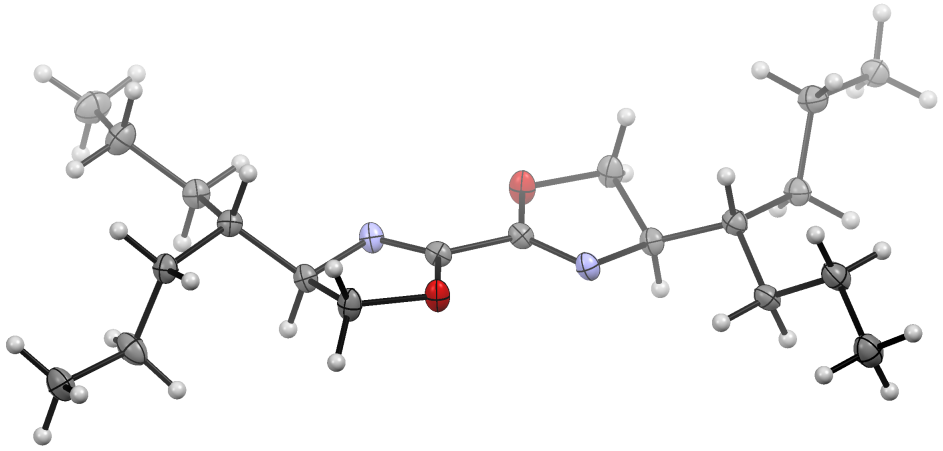

Table S2.1: Crystal data and structure refinement for **L6**.

Identification code	KEP-3-236
Empirical formula	$C_{20}H_{36}N_2O_2$
Formula weight	336.51
Temperature	100 K
Wavelength	1.54178 Å

Crystal system	Monoclinic	
Space group	P 1 21 1	
Unit cell dimensions	a = 17.2695(12) Å	a= 90°.
	b = 8.4949(6) Å	b= 108.140(3)°.
	c = 21.7390(15) Å	g = 90°.
Volume	3030.7(4) $Å^3$	
Z	6	
Density (calculated)	1.106 Mg/m^3	
Absorption coefficient	0.549 mm^{-1}	
F(000)	1116	
Crystal size	0.22 x 0.16 x 0.04 mm^3	
Theta range for data collection	2.692 to 80.579°.	
Index ranges	-22<=h<=21, -10<=k<=10, -27<=l<=27	
Reflections collected	97605	
Independent reflections	12703 [R(int) = 0.0468]	
Completeness to theta = 67.679°	99.8 %	
Absorption correction	Semi-empirical from equivalents	
Max. and min. transmission	0.7543 and 0.6514	
Refinement method	Full-matrix least-squares on F^2	
Data / restraints / parameters	12703 / 1 / 661	
Goodness-of-fit on F^2	1.047	
Final R indices [I>2sigma(I)]	R1 = 0.0363, wR2 = 0.0969	
R indices (all data)	R1 = 0.0387, wR2 = 0.0991	
Absolute structure parameter	0.03(4)	
Extinction coefficient	n/a	
Largest diff. peak and hole	0.377 and -0.163 $e.Å^{-3}$	

2.6.2.4 Preparation of (R)-2-amino-3-propylhexan-1-ol

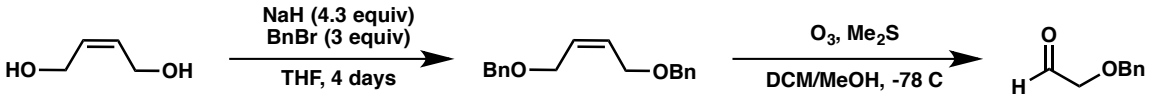

Benzyloxyacetaldehyde. Cis-1,4-dihydroxy-2-butene was benzyl protected under known literature procedure. The aldehyde was prepared following known literature procedure: (Z)-1,4-bis(benzyloxy)but-2-ene (1 equiv, 15 g, 56 mmol) was dissolved in 3:1 solution of DCM/MeOH (150 mL) and cooled to –78 °C. Ozone was bubbled through the reaction until the solution turned blue, signaling O_3 saturation. Reaction was sparged with O_2, then N_2 for 15 minutes. Dimethyl sulfide (12 equiv, 50 mL, 676 mmol) was added, and the reaction was allowed to warm to room temperature and stir for 14 hours. Reaction was concentrated under reduced pressure and purified by column chromatography (30% EtOAc/Hex) to afford the aldehyde as a yellow oil (16.6 g, 99% yield).

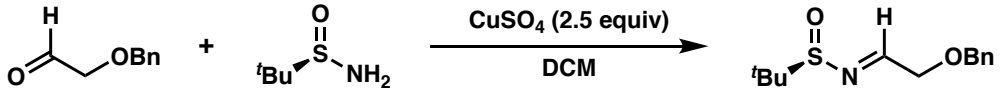

Preparation of (*R*)-2-amino-3-propylhexan-1-ol from benzyloxyacetaldehyde was based on the procedures described by Ellman and coworkers. 2-(benzyloxy)acetaldehyde (1 equiv, 16.6 g, 111 mmol) was dissolved in DCM (225 mL) at room temperature. (*R*)-(+)-*tert*-butylsulfinamide (1.1 equiv, 14.9 g, 123 mmol) and copper (II) sulfate (2.5 equiv, 44.1 g, 276 mmol) were added and the reaction was allowed to stir at room temperature for 36 hours. Reaction was filtered through a plug of Celite with DCM. The solution concentrated and purified by column chromatography (20% EtOAc/Hex) to afford imine product as a pale yellow oil (17.0 g, 61% yield).

$\mathbf{R}_f$ = 0.23 (silica gel, 20% EtOAc/Hex, UV).

^{1}H NMR (500 MHz, $CDCl_3$): δ 8.13 (t, *J* = 3.2 Hz, 1H), 7.41 – 7.27 (m, 5H), 4.64 (d, *J* = 1.1 Hz, 2H), 4.41 (t, *J* = 3.1 Hz, 2H), 1.22 (s, 9H).

^{13}C NMR (126 MHz, $CDCl_3$): δ 166.9, 137.3, 128.7, 128.2, 128.0, 73.4, 71.4, 57.1, 22.6.

$[\alpha]_D^{25}$ = –221° (c = 1.0, $CHCl_3$).

HRMS (ESI, *m/z*): calc'd for $C_{13}H_{20}NO_2S^+$ $(M+H)^+$: 254.1209, found: 254.1214.

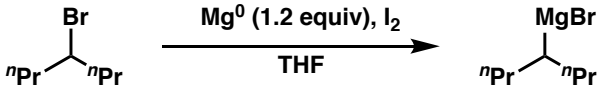

Grignard formation:

Magnesium (1.3 equiv, 4.00 g, 172 mmol) was activated by washing with minimal 1 M HCl, then washed with water, ethanol, and ether before transfer to a flame-dried 500 mL 3-neck flask, equipped with a reflux condenser and stir bar. The Mg^0 was stirred under vacuum overnight. THF (170 mL) and a fleck of I_2 was added and the stirring mixture was periodically heated to reflux with a heat gun over 20 minutes, until the brown solution turned dark, translucent gray. 4-Bromoheptane (1 equiv, 21 mL, 134 mmol) was added slowly, portion-wise, with manual heating to reflux in the intervals between additions. After addition of alkyl bromide, the reaction was stirred at 80 °C for 1 hour, then cooled to room temperature and titrated (0.36 M, 49% yield).

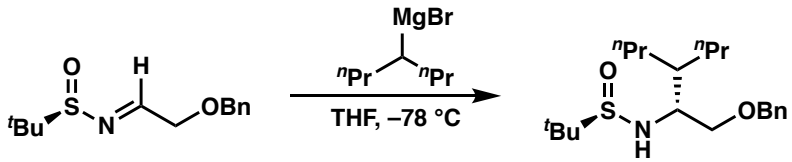

Sulfinamide (1 equiv, 7.33 g, 28.9 mmol) was dissolved in THF (260 mL) and cooled to –78 °C. Freshly prepared heptan-4-ylmagnesium bromide (1.6 equiv, 9.4 g, 46.2 mmol) was added via cannula. The reaction was stirred at –78 °C for 8 hours, then allowed to

stir overnight while the bath warmed slowly. The reaction mixture was quenched with water and Na_2SO_4 was added. The mixture was filtered through a plug of Celite and concentrated. The crude reaction was purified by silica gel chromatography (10% EtOAc/Hex to 30% EtOAc/Hex) to afford product (9.9 g, 97% yield, 97:3 d.r.).

R_f = 0.14 (silica gel, 20% EtOAc/Hex, UV).

^{1}H NMR (500 MHz, $CDCl_3$): δ 7.29 – 7.16 (m, 5H), 4.49 (d, *J* = 11.9 Hz, 1H), 4.41 (d, *J* = 11.9 Hz, 1H), 3.56 – 3.52 (m, 3H), 3.35 (dq, *J* = 7.3, 5.2 Hz, 1H), 1.63 (hept, *J* = 5.6, 5.1 Hz, 1H), 1.35 – 1.02 (m, 16H), 0.81 (td, *J* = 7.0, 4.9 Hz, 6H).

^{13}C NMR (126 MHz, $CDCl_3$): δ 137.8, 128.0, 127.5, 127.3, 72.7, 70.5, 57.3, 55.6, 38.7, 31.8, 31.6, 22.4, 22.4, 22.4, 22.3, 20.0, 19.9, 14.2, 14.1.

$[\alpha]_D^{25}$ = –38° (c = 6.7, $CHCl_3$).

FTIR (NaCl, thin film, cm^{-1}): 3216, 2065, 3032, 2960, 2871, 1720, 1455, 1363, 1073, 735.

HRMS (ESI, *m/z*): calc'd for $C_{20}H_{36}NO_2S^+$ $(M+H)^+$: 354.2461, found: 354.2469.

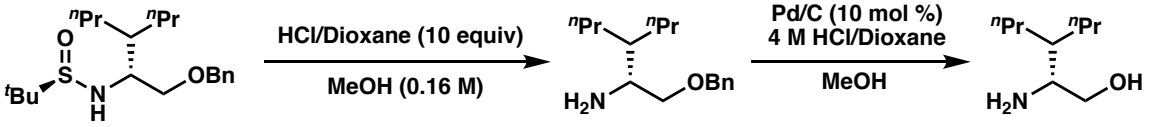

To a pale yellow solution of sulfinamine (1 equiv, 9.9 g, 28 mmol) in MeOH (175 mL) at room temperature, 4 M HCl/Dioxane (10 equiv, 70 mL) was added. The reaction was stirred for 1 hour and turned light amber. Reaction mixture was concentrated *in vacuo*. The crude oil was dissolved in minimal 50% EtOAc/Hex and loaded onto a silica gel column. 1 L of 50% EtOAc/Hex was eluted to remove sulfur impurities, then solvent

system was switched to 10% MeOH/DCM to elute brown product band from the top of the silica (6.2 g, 89% yield).

R_f = 0.17 (silica gel, 5% MeOH/DCM, Ninhydrin).

^{1}H NMR (400 MHz, $CDCl_3$): δ 8.53 (s, 3H), 7.43 – 7.23 (m, 5H), 4.70 – 4.43 (m, 2H), 3.68 (d, *J* = 5.5 Hz, 2H), 3.37 (s, 1H), 1.87 (q, *J* = 5.9 Hz, 1H), 1.58 (ddt, *J* = 12.9, 10.2, 4.6 Hz, 1H), 1.49 – 1.16 (m, 8H), 0.90 (td, *J* = 7.1, 3.0 Hz, 6H).

^{13}C NMR (126 MHz, $CDCl_3$): δ 137.9, 128.5, 127.8, 127.7, 73.4, 67.8, 54.0, 37.4, 31.6, 31.5, 20.2, 20.0, 14.3, 14.3.

$[\alpha]_D^{25}$ = +3° (c = 1.9, $CHCl_3$).

FTIR (NaCl, thin film, cm^{-1}): 2957, 2873, 1727, 1609, 1518, 1455, 1377, 1273, 1102, 737.

HRMS (ESI, *m/z*): calc'd for $C_{16}H_{28}NO^+$ $(M+H)^+$: 250.2165, found: 250.2166.

Pd/C (4.0 g) was added to the flask and dissolved in minimal EtOAc, then placed under N_2. Amine (1 equiv, 4.2 g, 16.8 mmol) was dissolved in MeOH (35 mL) and added to the reaction flask via cannula. 4 M HCl/Dioxane (35 mL) was added and the N_2 atmosphere was exchanged with H_2 and the reaction was allowed to stir 14 h under H_2. Upon completion, the reaction was sparged with argon and filtered through a pad of Celite with EtOAc. The filtrate was concentrated then dissolved in 250 mL EtOAc and added to 250 mL of 6 M NaOH. The organic layer was separated and extracted (x3) with EtOAc. The combined organic layers were dried, filtered, and concentrated under reduced pressure to afford pure amino alcohol (2.3 g, 86% yield).

R_f = 0.09 (silica gel, 5% MeOH/DCM, Ninhydrin).

^{1}H NMR (400 MHz, MeOD): δ 3.76 (dd, *J* = 11.6, 3.9 Hz, 1H), 3.57 (dd, *J* = 11.5, 8.4 Hz, 1H), 3.18 (ddd, *J* = 8.8, 5.3, 3.9 Hz, 1H), 1.91 (s, 3H), 1.67 (q, *J* = 5.5 Hz, 1H), 1.50 – 1.19 (m, 9H), 0.95 (td, *J* = 6.7, 3.9 Hz, 6H).

^{13}C NMR (101 MHz, MeOD): δ 61.0, 56.9, 39.0, 32.8, 32.4, 21.1, 21.1, 14.5, 14.5.

$[\alpha]_D^{25}$ = –11° (c = 2.1, $CHCl_3$).

FTIR (NaCl, thin film, cm^{-1}): 3283, 2957, 2922, 2345, 1570, 1466, 1378, 1051.

HRMS (ESI, *m/z*): calc'd for $C_9H_{22}NO^+$ $(M+H)^+$: 160.1696, found: 160.1701.

2.6.3 Substrate Synthesis

General Procedure 1: Benzyl Chloride Synthesis from Benzyl Alcohols

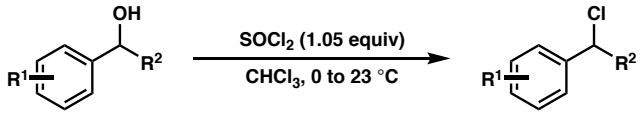

A flame-dried flask was charged with the benzyl alcohol substrate (1 equiv) and chloroform (0.30 M) and sealed with a rubber septum. This solution was cooled to 0 ºC in an ice bath and placed under a positive pressure of nitrogen. The flask was vented via a Teflon cannula into a saturated solution of $NaHCO_3$ to quench evolved SO_2 gas. To the cooled solution was slowly added thionyl chloride (1.05 equiv) via syringe. The reaction was allowed to stir overnight and the ice bath allowed to melt, unless otherwise noted. Reactions were then concentrated to typically afford the crude substrates as yellow oils containing a mixture of benzylic chloride and the styrenyl elimination product. Substrates were purified by column chromatography on silica gel in 100% hexanes to elute first the elimination product (strong staining by $KMnO_4$ and brightly fluorescent) followed by the desired chloride product (dimly fluorescent, no staining).

1-(1-chloropropyl)-4-(trifluoromethyl)benzene (119)

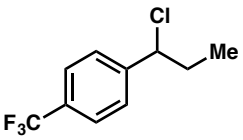

Prepared from 1-(4-(trifluoromethyl)phenyl)propan-1-ol (5.0 mmol, 1.02 g) following General Procedure 1 to yield 350 mg (31% yield, 1.57 mmol) as a mobile clear liquid. Benzyl chloride contained styrene elimination product and was used as 88% pure.

R_f= 0.6 (silica gel, hexane, UV)

^{1}H NMR (400 MHz, $CDCl_3$): δ 7.67 – 7.59 (m, 2H), 7.52 – 7.47 (m, 2H), 4.81 (dd, *J* = 7.8, 6.4 Hz, 1H), 2.23 – 1.98 (m, 2H), 1.01 (t, *J* = 7.3 Hz, 3H).

^{13}C NMR (101 MHz, $CDCl_3$): δ 145.7, 130.5 (q, *J* = 32.6 Hz), 127.5, 125.7 (q, *J* = 3.8 Hz), 124.1 (q, J = 272.2 Hz), 64.3, 33.3, 11.7.

^{19}F NMR (282 MHz, $CDCl_3$): δ –62.7

FTIR (NaCl, thin film, cm^{-1}): 2975, 1621, 1420, 1326, 1127, 1068, 849.

HRMS (EI+, m/z): calc'd for $C_{10}H_{10}ClF_3$ $[M+\bullet]^+$: 222.0423; found: 222.0408.

1-(1-chloropropyl)-4-(trifluoromethoxy)benzene (73)

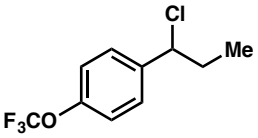

Prepared from 1-(4-(trifluoromethoxy)phenyl)propan-1-ol (13.1 mmol, 2.88 g) following General Procedure 1 to yield 2.51 g (80% yield, 10.48 mmol) as a mobile clear liquid.

R_f= 0.6 (silica gel, hexane, UV)

^{1}H NMR (400 MHz, $CDCl_3$): δ 7.47 – 7.36 (m, 2H), 7.25 – 7.16 (m, 2H), 4.78 (dd, *J* = 7.9, 6.4 Hz, 1H), 2.20 – 1.99 (m, 2H), 1.00 (t, *J* = 7.3 Hz, 3H).

^{13}C NMR (101 MHz, $CDCl_3$): δ 149.0 (d, *J* = 1.9 Hz), 140.6, 128.6, 121.2, 120.6 (q, *J* = 257.3 Hz), 64.4, 33.4, 11.8.

^{19}F NMR (282 MHz, $CDCl_3$): δ –57.9

FTIR (NaCl, thin film, cm^{-1}): 2973, 1508, 1262, 1220, 1165

HRMS (FAB+, m/z): calc'd for $C_{10}H_{10}ClF_3O$ $[M+H]^+$: 239.0464; found: 239.0465.

1-(1-chloropropyl)-2-fluorobenzene (120)

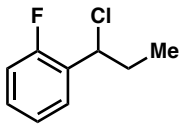

Prepared from 1-(2-fluorophenyl)propan-1-ol (19.7 mmol, 3.03 g) following General Procedure 1 to yield 2.63 g (77% yield, 15.2 mmol) as a mobile clear liquid.

R_f= 0.6 (silica gel, hexane, UV)

^{1}H NMR (500 MHz, $CDCl_3$): δ 7.51 (td, *J* = 7.6, 1.8 Hz, 1H), 7.32 – 7.25 (m, 1H), 7.17 (td, *J* = 7.6, 1.2 Hz, 1H), 7.04 (ddd, *J* = 10.3, 8.2, 1.2 Hz, 1H), 5.17 (dd, *J* = 8.0, 6.4 Hz, 1H), 2.24 – 2.02 (m, 2H), 1.03 (t, *J* = 7.3 Hz, 3H).

^{13}C NMR (101 MHz, $CDCl_3$): δ 159.65 (d, *J* = 247.5 Hz), 129.79 (d, *J* = 8.4 Hz), 128.94 (d, *J* = 13.0 Hz), 128.61 (d, *J* = 3.3 Hz), 124.57 (d, *J* = 3.7 Hz), 115.61 (d, *J* = 22.1 Hz), 57.61 (d, *J* = 3.7 Hz), 32.4, 11.6.

^{19}F NMR (282 MHz, $CDCl_3$): δ –118.6 (ddd, *J* = 10.3, 7.4, 5.1 Hz).

FTIR (NaCl, thin film, cm^{-1}): 3436, 3088, 2974, 2879, 1616, 1588, 1492, 1457, 1233, 1118, 755.

HRMS (EI+, m/z): calc'd for $C_9H_{10}ClF$ $[M+\bullet]^+$: 172.0455; found: 172.0445.

***tert*-butyl 4-(2-chloro-2-phenylethyl)piperidine-1-carboxylate (121)**

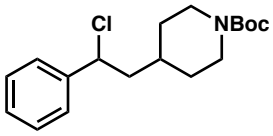

Prepared from *tert*-butyl 4-(2-hydroxy-2-phenylethyl)piperidine-1-carboxylate (6.2 mmol, 1.89 g) following General Procedure 1. The reaction was concentrated and loaded onto a silica plug. Elution with $CHCl_3$ delivered degradation products. Subsequent elution with 10% MeOH/DCM afforded the deprotected HCl salt as a tan solid 68% yield (4.22 mmol, 1.02 g). This product was not competent in the cross-coupling reaction. Reprotection with Boc_2O (1.05 equiv) in DCM with Et_3N (4 equiv) afforded the desired product containing 10% styrene and was used without further purification.

R_f= 0.3 (silica gel, 10% EtOAc/hexane, UV)

^{1}H NMR (400 MHz, $CDCl_3$): δ 7.44 – 7.29 (m, 5H), 4.98 (dd, *J* = 9.2, 5.9 Hz, 1H), 4.10 (s, 3H), 2.69 (t, *J* = 12.8 Hz, 2H), 2.14 (ddd, *J* = 14.5, 9.3, 5.6 Hz, 1H), 1.90 (ddd, *J* = 14.0, 7.7, 5.9 Hz, 1H), 1.85 – 1.65 (m, 2H), 1.47 (s, 9H), 1.27 – 1.07 (m, 2H).

^{13}C NMR (101 MHz, $CDCl_3$): δ 154.8, 141.7, 128.7, 128.4, 126.9, 79.4, 61.0, 46.6, 33.5, 28.5, 28.5, 27.4.

FTIR (NaCl, thin film, cm^{-1}): 3448, 2930, 1810, 1692, 1424, 1366, 1168, 698.

HRMS (FAB+, m/z): calc'd for $C_{18}H_{26}ClNO_2$ $[M+H]^+$: 324.1730; found: 324.1740.

4-(1-chloropropyl)dibenzo[*b*,*d*]furan (122)

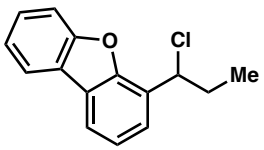

Prepared from 1-(dibenzo[*b*,*d*]furan-4-yl)propan-1-ol (9.2 mmol, 2.08 g) following General Procedure 1 to yield 1.74 g (84% yield, 7.7 mmol) as a mobile clear liquid. Benzyl chloride contained styrene elimination product and was used as 78% pure.

R_f= 0.3 (silica gel, hexane, UV)

^{1}H NMR (300 MHz, $CDCl_3$): δ 7.95 (dddd, *J* = 7.6, 2.6, 1.4, 0.7 Hz, 1H), 7.90 (dd, *J* = 7.7, 1.3 Hz, 1H), 7.65 – 7.54 (m, 2H), 7.48 (ddd, *J* = 8.3, 7.3, 1.4 Hz, 1H), 7.40 – 7.32 (m, 2H), 5.50 (dd, *J* = 7.8, 6.5 Hz, 1H), 2.48 – 2.19 (m, 2H), 1.08 (t, *J* = 7.3 Hz, 3H).

^{13}C NMR (101 MHz, $CDCl_3$): δ 156.2, 153.1, 127.5, 126.0, 125.5, 124.6, 124.2, 123.2, 123.0, 120.9, 120.5, 112.0, 59.4, 32.2, 11.9.

FTIR (NaCl, thin film, cm^{-1}): 2971, 1588, 1451, 1424, 1326, 1272, 1189, 1108, 1055, 846, 749.

HRMS (FAB+, m/z): calc'd for $C_{15}H_{13}ClO$ $[M+H]^+$: 245.0733; found: 245.0731.

2.6.4 Enantioselective Reductive Cross-Coupling

2.6.4.1 General Procedures for Enantioselective Cross-Coupling of Benzyl Chlorides and (Hetero)aryl Iodides

General Procedure 2: Cross-Coupling on 0.05 mmol scale

On a bench-top, to a 1-dram vial was added a stir bar,* the appropriate ligand (20 mol %, 0.01 mmol), reductant (3 equiv, 0.15 mmol), and aryl iodide (1.0 equiv, 0.05 mmol). The vial was transferred into a N_2-filled glovebox and charged with $NiBr_2$(diglyme) (10 mol %, 0.005 mmol) and the appropriate solvent (0.14 mL, 0.36 M). Reaction was allowed to stir at 250 rpm for 20 minutes before addition of benzyl chloride (1.2 equiv, 0.06 mmol). After one minute of stirring, TMSCl (5 uL, 0.8 equiv) was added. The vial was sealed with a Teflon cap and removed from the glovebox. The mixture was stirred at 480 rpm over a period of 14 hours over which time the heterogeneous solution turned from dark gray to a light green, orange, or gray color (depending on substrate). The reaction was quenched by loading directly onto a short plug of basic alumina, eluting with 20% Et_2O/hexanes. The solution was concentrated to afford a clear oil. The crude residue was analyzed by chiral SFC and NMR. Dibenzyl ether was used as an internal NMR standard.

***Stir bar size is critically important to the success of the reaction**. The 2-dram sized (3 mm x 12 mm) stir bars are added to 1-dram vials in order to span the full diameter of the vial. Not all stir bars sold as 3 mm x 12 mm will be successful in every 1-dram vial. Manufacturing differences in stir bars and vials lead to certain stir bars fitting certain vials. To check for appropriate size: place the stir bar into the empty vial and shake it back and forth; a clinking noise will result if the stir bar is sufficiently small. If no clinking is heard, that stir bar will stick when Mn^0 is added and the reaction will result in no conversion. Vials should be placed on the stir plate such that the stir bar lies flat while stirring (completely centered or just off-center). Stir bars smaller than 3 mm x 12 mm will result in the Mn^0 settling on the outside perimeter of the vial and poor reaction conversion.

General Procedure 3: Cross-Coupling on 0.2 mmol scale

On the bench-top, a 20 mL scintillation vial was charged with a 1.0 x 1.9 cm cross stir bar, Mn^0 powder (3 equiv, 33 mg, 0.6 mmol), aryl iodide (*if solid*, 1 equiv, 0.2 mmol), and **L6** (0.2 equiv, 13.5 mg, 0.04 mmol). The vial was transferred into a N_2-filled glovebox and charged with $NiBr_2$(diglyme) (10 mol %, 7.1 mg, 0.02 mmol), 1,4-dioxane (0.56 mL, 0.36 M), and aryl iodide (*if liquid*, 1 equiv, 0.2 mmol). The reaction was allowed to stir at 250 rpm for **20 minutes** before addition of benzyl chloride (1.2 equiv, 0.24 mmol). After one minute of stirring, TMSCl (20 uL, 0.75 equiv) was added. The vial was sealed with a Teflon cap, taped, and removed from the glovebox. The mixture was stirred at 480 rpm over a period of 14 hours, over which time the heterogeneous solution turned from dark gray to a light green, deep red, or light gray color (depending on substrate). The reaction was quenched by loading directly onto a short plug of silica or basic alumina (if heteroatom present on arene), eluting with either 20% ethyl acetate/hexane or 20% Et_2O/hexane, respectively. The solution was concentrated to afford a clear oil. The oil was dissolved in DCM and dry loaded with Celite onto a silica gel or basic alumina column (if heteroatom present on arene) and eluted in a hexane/EtOAc or hexane/Et_2O gradient, respectively. The remaining benzyl homodimer could be collected in the first couple fractions, with biaryl homocoupled product being the most polar component. Reaction success is *critically dependent* on stirring. A stir bar too small for the reaction vessel will fail to suspend the Mn^0 powder and lead to low conversions. The reaction vessel should be sufficiently large (solvent height should be sufficiently low) to allow for even distribution of Mn^0 powder with vigorous stirring. *Short or no prestir before addition of benzyl chloride results in low yields on this scale.*

General Procedure 4: Cross-Coupling on 2.0 mmol scale

On the bench-top, a 100-mL flask with a 24/40 ground glass neck was charged with a large, 1.7 x 4.0 cm football-shaped stir bar, Mn^0 powder (3 equiv, 0.327 g, 6.0 mmol), and **L6** (0.2 equiv, 0.135 g, 0.4 mmol). The flask was transferred into a N_2-filled glovebox and charged with $NiBr_2$(diglyme) (10 mol %, 0.071 g, 0.2 mmol), 1,4-dioxane (5.6 mL, 0.36 M), and aryl iodide (1 equiv, 0.470 g, 2.0 mmol). Reaction was allowed to stir at 250 rpm for **30 minutes** before addition of benzyl chloride (1.2 equiv, 0.370 g, 2.4 mmol). After one minute of stirring, TMSCl (0.190 mL, 0.75 equiv) was added. The vial was sealed with a septum, taped, removed from the glovebox and a N_2 inlet needle inserted. The mixture was stirred at 1000 rpm over a period of 3 days, over which time the heterogeneous solution turned from green to dark gray. The reaction was quenched by loading directly onto a short plug of basic Alumina, eluting with 20% Et_2O/hexane. The solution was concentrated to afford a clear oil. The oil was dissolved in DCM and dry loaded with Celite onto a basic alumina column and eluted in a hexane/Et_2O gradient. Remaining benzyl homodimer could be collected in the first couple fractions, with biaryl homocoupled product being the most polar component. Reaction success is *critically dependent* on stirring. The stir bar was large enough and the correct shape to fit right along the bottom of the flask with minimal space between the stir bar and glass.

2.6.4.2 Characterization of Reaction Products

2-methoxy-5-(1-phenylpropyl)pyridine (37)

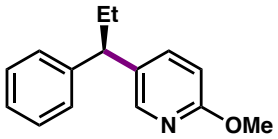

Prepared from 5-iodo-2-methoxypyridine (1 equiv, 47 mg, 0.2 mmol) and 1-(chloropropyl)benzene (1.2 equiv, 37 mg, 0.24 mmol) following General Procedure 3. The crude residue was purified by column chromatography to yield **37** (38 mg, 84% yield) in 91% ee as a colorless oil.

$\mathbf{R_f}$ = 0.35 (silica gel, 10% EtOAc/Hex, UV).

Chiral SFC: (OJ-H, 2.5 mL/min, 4% IPA in CO_2, λ = 210 nm): t_R(minor) = 6.0 min, t_R(major) = 6.7 min.

$\mathbf{[\alpha]_D^{25}}$ = +10.6° (c = 1.0, $CHCl_3$).

^{1}H NMR (400 MHz, $CDCl_3$): δ 8.06 (dt, *J* = 2.5, 0.7 Hz, 1H), 7.40 (ddd, *J* = 8.6, 2.5, 0.5 Hz, 1H), 7.33 – 7.24 (m, 2H), 7.24 – 7.14 (m, 3H), 6.66 (dd, *J* = 8.5, 0.7 Hz, 1H), 3.90 (s, 3H), 3.79 – 3.69 (m, 1H), 2.17 – 1.93 (m, 2H), 0.90 (t, *J* = 7.3 Hz, 3H).

^{13}C NMR (101 MHz, $CDCl_3$): δ 162.9, 145.8, 144.7, 138.4, 133.3, 128.6, 127.9, 126.4, 110.8, 53.5, 50.0, 28.5, 12.8.

FTIR (NaCl, thin film, cm^{-1}): 2963, 2874, 1605, 1572, 1492, 1392, 1287, 1262, 1028, 699.

HRMS (ESI-TOF, *m/z*): calc'd for $C_{15}H_{17}NO$ $[M+H]^+$: 228.1383; found: 228.1379.

2-fluoro-5-(1-phenylpropyl)pyridine (77)

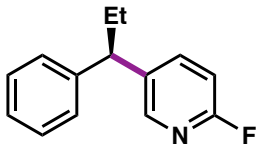

Prepared from 2-fluoro-5-iodopyridine (1 equiv, 45.0 mg, 0.2 mmol) and 1-(chloropropyl)benzene (1.2 equiv, 37 mg, 0.24 mmol) following General Procedure 3. The crude residue was purified by column chromatography to yield **77** (27 mg, 63% yield) in 90% ee as a colorless oil.

$\mathbf{R_f}$ = 0.35 (silica gel, 10% EtOAc/Hex, UV).

Chiral SFC: (AD-H, 2.5 mL/min, 5% IPA in CO_2, λ = 254 nm): t_R(major) = 5.1 min, t_R(minor) = 5.6 min.

$\mathbf{[\alpha]_D^{25}}$ = +3.3° (c = 1.0, $CHCl_3$).

^{1}H NMR (500 MHz, $CDCl_3$): δ 8.14 – 8.04 (m, 1H), 7.57 (ddd, *J* = 8.7, 7.8, 2.6 Hz, 1H), 7.32 – 7.25 (m, 2H), 7.22 – 7.14 (m, 3H), 6.81 (dd, *J* = 8.5, 3.0 Hz, 1H), 3.79 (t, *J* = 7.8 Hz, 1H), 2.15 – 1.95 (m, 2H), 0.88 (t, *J* = 7.3 Hz, 3H).

^{13}C NMR (101 MHz, $CDCl_3$): δ 162.41 (d, *J* = 237.3 Hz), 146.82 (d, *J* = 14.3 Hz), 143.7, 140.55 (d, *J* = 7.7 Hz), 138.28 (d, *J* = 4.6 Hz), 128.8, 127.9, 126.7, 109.38 (d, *J* = 37.4 Hz), 50.0, 50.0, 28.6, 12.7.

^{19}F NMR (282 MHz, $CDCl_3$): δ -71.9.

FTIR (NaCl, thin film, cm^{-1}): 2964, 2931, 2875, 1595, 1482, 1453, 1396, 1249, 700.

HRMS (ESI-TOF, *m/z*): calc'd for $C_{14}H_{14}FN$ $[M+H]^+$: 216.1183; found: 216.1181.

2-chloro-5-(1-phenylpropyl)pyridine (78)

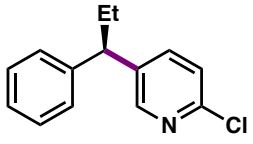

Prepared from 2-chloro-5-iodopyridine (1 equiv, 48.0 mg, 0.2 mmol) and 1-(chloropropyl)benzene (1.2 equiv, 37 mg, 0.24 mmol) following General Procedure 3. The crude residue was purified by column chromatography to yield **78** (27 mg, 59% yield) in 90% ee as a colorless oil.

R_f = 0.4 (silica gel, 20% Et_2O/Hex, UV).

Chiral SFC: (AD-H, 2.5 mL/min, 8% IPA in CO_2, λ = 254 nm): t_R (major) = 6.3 min, t_R (minor) = 7.5 min.

$[\alpha]_D^{25}$ = –1.8° (c = 1.0, $CHCl_3$).

^{1}H NMR (400 MHz, $CDCl_3$): δ 8.30 (dt, *J* = 2.6, 0.6 Hz, 1H), 7.47 (ddd, *J* = 8.2, 2.5, 0.6 Hz, 1H), 7.35 – 7.27 (m, 2H), 7.24 – 7.16 (m, 4H), 3.80 (t, *J* = 7.8 Hz, 1H), 2.18 – 1.98 (m, 2H), 0.91 (t, *J* = 7.3 Hz, 3H).

^{13}C NMR (101 MHz, $CDCl_3$): δ 149.4, 149.3, 143.4, 139.6, 138.3, 128.9, 127.9, 126.8, 124.2, 50.1, 28.4, 12.7.

FTIR (NaCl, thin film, cm^{-1}): 2931, 2963, 2874, 1581, 1563, 1456, 1386, 1106, 1022, 700.

HRMS (ESI-TOF, *m/z*): calc'd for $C_{14}H_{14}ClN$ $[M+H]^+$: 232.0888; found: 232.0888.

5-(1-phenylpropyl)-2-(trifluoromethyl)pyridine (79)

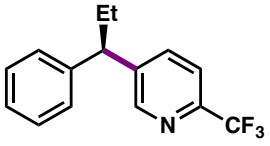

Prepared from 5-iodo-2-(trifluoromethyl)pyridine (1 equiv, 55.0 mg, 0.2 mmol) and 1-(chloropropyl)benzene (1.2 equiv, 37 mg, 0.24 mmol) following General Procedure 3. The crude residue was purified by column chromatography to yield **79** (22 mg, 42% yield) in 89% ee as a colorless oil.

R_f = 0.27 (silica gel, 10% EtOAc/Hex, UV).

Chiral SFC: (AD-H, 2.5 mL/min, 5% IPA in CO_2, λ = 210 nm): t_R(major) = 3.2 min, t_R(minor) = 3.6 min.

$[\alpha]_D^{25}$ = +2.29° (c = 1.0, $CHCl_3$).

^{1}H NMR (400 MHz, $CDCl_3$): δ 8.64 (d, *J* = 2.1 Hz, 1H), 7.68 (ddt, *J* = 8.2, 2.3, 0.7 Hz, 1H), 7.59 (dd, *J* = 8.2, 0.8 Hz, 1H), 7.38 – 7.27 (m, 2H), 7.22 (td, *J* = 7.1, 1.1 Hz, 3H), 3.91 (t, *J* = 7.8 Hz, 1H), 2.26 – 2.01 (m, 2H), 0.93 (t, *J* = 7.3 Hz, 3H).

^{13}C NMR (101 MHz, $CDCl_3$): δ 150.0, 146.2 (q, *J* = 34.7 Hz), 144.0, 142.8, 136.4, 129.0, 127.9, 127.0, 121.7 (q, *J* = 273.2 Hz), 120.4 (q, *J* = 2.7 Hz), 50.7, 28.3, 12.7.

^{19}F NMR (282 MHz, $CDCl_3$): δ –67.8.

FTIR (NaCl, thin film, cm^{-1}): 2967, 2933, 2878, 1336, 1174, 1136, 1087, 1026, 700.

HRMS (ESI-TOF, *m/z*): calc'd for $C_{15}H_{14}F_3N$ $[M+H]^+$: 266.1151; found: 266.1151.

4,4,5,5-tetramethyl-2-(4-(1-phenylpropyl)phenyl)-1,3,2-dioxaborolane (80)

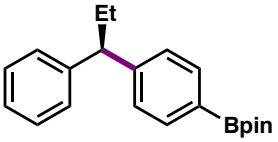

Prepared from 2-(4-iodophenyl)-4,4,5,5-tetramethyl-1,3,2-dioxaborolane (1 equiv, 66.0 mg, 0.2 mmol) and 1-(chloropropyl)benzene (1.2 equiv, 37 mg, 0.24 mmol) following General Procedure 3. The crude residue was purified by column chromatography to yield **80** (47 mg, 72% yield) in 83% ee as a white solid.

R_f = 0.42 (silica gel, 10% EtOAc/Hex, UV).

Chiral SFC: (AD-H, 2.5 mL/min, 7% IPA in CO_2, λ = 254 nm): t_R(minor) = 6.2 min, t_R(major) = 6.9 min.

$[\alpha]_D^{25}$ = –3.3° (c = 1.0, $CHCl_3$).

^{1}H NMR (400 MHz, $CDCl_3$): δ 7.81 – 7.73 (m, 2H), 7.34 – 7.22 (m, 6H), 7.22 – 7.15 (m, 1H), 3.84 (t, *J* = 7.8 Hz, 1H), 2.11 (p, *J* = 7.4 Hz, 2H), 1.36 (s, 12H), 0.93 (t, *J* = 7.3 Hz, 3H).

^{13}C NMR (101 MHz, $CDCl_3$): δ 148.6, 145.0, 135.1, 128.5, 128.0, 127.6, 126.2, 83.8, 53.5, 28.5, 25.0, 25.0, 12.9.

FTIR (NaCl, thin film, cm^{-1}): 2976, 2930, 1611, 1399, 1390, 1359, 1320, 1144, 1091, 660.

HRMS (+ESI, *m/z*): calc'd for $C_{21}H_{27}BO_2$ [M+H]-H_2: 321.2026; found: 321.2020.

3-(1-phenylpropyl)phenyl trifluoromethanesulfonate (81)

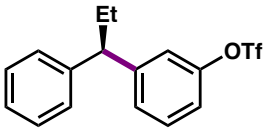

Prepared from 3-iodophenyl trifluoromethanesulfonate (1 equiv, 70.0 mg, 0.2 mmol) and 1-(chloropropyl)benzene (1.2 equiv, 37 mg, 0.24 mmol) following General Procedure 3. The crude residue was purified by column chromatography to yield **81** (58 mg, 84% yield) in 92% ee as a colorless oil.

R_f = 0.56 (silica gel, 10% EtOAc/Hex).

Chiral SFC: (OJ-H, 2.5 mL/min, 1% IPA in CO_2, λ = 254 nm): t_R(major) = 5.1 min, t_R(minor) = 5.8 min.

$[\alpha]_D^{25}$ = –5.6° (c = 1.0, $CHCl_3$).

^{1}H NMR (400 MHz, $CDCl_3$): δ 7.35 – 7.23 (m, 3H), 7.23 – 7.12 (m, 4H), 7.10 (t, *J* = 2.1 Hz, 1H), 7.04 (ddd, *J* = 8.2, 2.5, 1.1 Hz, 1H), 3.79 (t, *J* = 7.8 Hz, 1H), 2.03 (pd, *J* = 7.4, 2.5 Hz, 2H), 0.86 (t, *J* = 7.3 Hz, 3H).

^{13}C NMR (101 MHz, $CDCl_3$): δ 149.8, 148.5, 143.8, 130.2, 128.8, 128.2, 128.0, 126.7, 120.8, 119.0, 52.9, 28.6, 12.7.

^{19}F NMR (282 MHz, $CDCl_3$): δ -72.9.

FTIR (NaCl, thin film, cm^{-1}): 2967, 2934, 1612, 1579, 1484, 1422, 1249, 1212, 1142, 1120, 852.

HRMS (FAB+, *m/z*): calc'd for $C_{16}H_{15}F_3O_3S$ $[(M+H) - H_2]^+$: 343.0616; found: 343.0624.

1-(4-(1-phenylpropyl)phenyl)ethan-1-one (82)

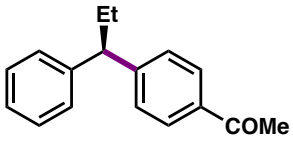

Prepared from 4-iodoacetophenone (1 equiv, 49.0 mg, 0.2 mmol) and 1-(chloropropyl)benzene (1.2 equiv, 37 mg, 0.24 mmol) following General Procedure 3. The crude residue was purified by column chromatography to yield **82** (42 mg, 88% yield) in 85% ee as a white solid.

$\mathbf{R}_f$ = 0.18 (silica gel, 10% Et_2O/hexanes, UV).

Chiral SFC: (OJ-H, 2.5 mL/min, 10% IPA in CO_2, λ = 254 nm): t_R (minor) = 5.4 min, t_R (major) = 6.1 min.

$[\alpha]_D^{25}$ = –3.0° (c = 1.0, $CHCl_3$).

^{1}H NMR (400 MHz, $CDCl_3$): δ 7.92 – 7.85 (m, 2H), 7.36 – 7.27 (m, 4H), 7.25 – 7.16 (m, 3H), 3.86 (t, *J* = 7.8 Hz, 1H), 2.56 (s, 3H), 2.19 – 2.01 (m, 2H), 0.91 (t, *J* = 7.3 Hz, 3H).

^{13}C NMR (101 MHz, $CDCl_3$): δ 197.9, 151.0, 144.2, 135.3, 128.7, 128.7, 128.2, 128.0, 126.5, 53.4, 28.4, 26.7, 12.8.

FTIR (NaCl, thin film, cm^{-1}): 2962, 2931, 2873, 1681, 1606, 1358, 1269, 700.

HRMS (FAB+, *m/z*): calc'd for $C_{17}H_{18}O$ $[M+H]^+$: 239.1436; found: 239.1446.

1-methoxy-4-(1-phenylpropyl)benzene (83)

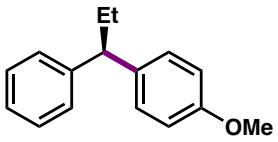

Prepared from 4-iodoanisole (1 equiv, 47.0 mg, 0.2 mmol) and 1-(chloropropyl)benzene (1.2 equiv, 37 mg, 0.24 mmol) following General Procedure 3. The crude residue was purified by column chromatography to yield **83** (30 mg, 67% yield) in 83% ee as a colorless oil.

$\mathbf{R}_f$ = 0.44 (silica gel, 10% Et_2O/hexanes, UV).

Chiral SFC: (OJ-H, 2.5 mL/min, 8% IPA in CO_2, λ = 235 nm): t_R(minor) = 7.9 min, t_R(major) = 9.9 min.

$[\alpha]_D^{25}$ = –3.7° (c = 1.0, $CHCl_3$).

^{1}H NMR (400 MHz, $CDCl_3$): δ 7.35 – 7.21 (m, 4H), 7.21 – 7.05 (m, 3H), 6.94 – 6.79 (m, 2H), 3.78 (m, 4H), 2.06 (p, *J* = 7.4 Hz, 2H), 0.91 (t, *J* = 7.3 Hz, 3H).

^{13}C NMR (101 MHz, $CDCl_3$): δ 157.9, 145.7, 137.5, 128.9, 128.5, 127.9, 126.0, 113.8, 55.3, 52.5, 28.9, 12.9.

FTIR (NaCl, thin film, cm^{-1}): 2960, 2931, 1610, 1507, 1452, 1248, 1178, 1037, 699.

HRMS (FAB+, *m/z*): calc'd for $C_{16}H_{18}O$ $[(M+H) - H_2]^+$: 225.1279; found: 225.1275.

2,2,2-trifluoro-*N*-(4-(1-phenylpropyl)phenyl)acetamide (84)

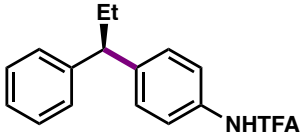

Prepared from 2,2,2-trifluoro-*N*-(4-iodophenyl)acetamide (1 equiv, 63.0 mg, 0.2 mmol) and 1-(chloropropyl)benzene (1.2 equiv, 37 mg, 0.24 mmol) following General Procedure 3. The crude residue was purified by column chromatography to yield **84** (43 mg, 70% yield) in 81% ee as a white solid. Recrystallized by vapor diffusion of pentane into a saturated solution of **84** in DCM to give white needles.

R$_f$ = 0.52 (silica gel, 10:45:45 Et_2O/PhMe/Pentane, UV).

Chiral SFC: (OD-H, 2.5 mL/min, 10% IPA in CO_2, λ = 254 nm): t_R(minor) = 6.6 min, t_R(major) = 10.4 min.

[α]$_D^{25}$ = –5.9° (c = 1.0, $CHCl_3$).

m.p. = 73.3–73.8 ºC

^{1}H NMR (500 MHz, $CDCl_3$): δ 7.91 (s, 1H), 7.50 – 7.45 (m, 2H), 7.33 – 7.24 (m, 4H), 7.24 – 7.16 (m, 3H), 3.80 (t, *J* = 7.8 Hz, 1H), 2.07 (pd, *J* = 7.4, 2.6 Hz, 2H), 0.90 (t, *J* = 7.3 Hz, 3H).

^{13}C NMR (101 MHz, $CDCl_3$): δ 154.84 (q, *J* = 37.4 Hz), 144.7, 143.7, 133.1, 128.9, 128.6, 127.9, 126.4, 120.7, 115.8 (q, *J* = 288.8 Hz) 52.8, 28.6, 12.8.

^{19}F NMR (282 MHz, $CDCl_3$): δ –75.7.

FTIR (NaCl, thin film, cm^{-1}): 3304, 2964, 1703, 1605, 1546, 1513, 1288, 1248, 1199, 1159, 699.

HRMS (FAB+, *m/z*): calc'd for $C_{17}H_{16}F_3NO$ $[M+H]^+$: 308.1262; found: 308.1266.

Compound **84** crystallizes in the monoclinic space group $P2_1$ with two molecules in the asymmetric unit. The coordinates for the hydrogen atoms bound to N1A and N1B were located in the difference Fourier synthesis and refined using a riding model. Absolute configuration was determined by anomalous dispersion (Flack = 0.05(7)).[6]

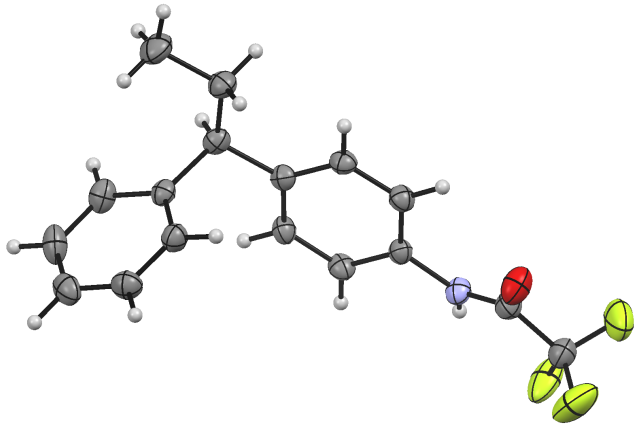

Table S2.2. Crystal data and structure refinement for 84.

Identification code	KEP-2-91	
Empirical formula	$C_{34}\ H_{32}\ F_6\ N_2\ O_2$	
Formula weight	614.61	
Temperature	200 K	
Wavelength	1.54178 Å	
Crystal system	Monoclinic	
Space group	P 1 21 1	
Unit cell dimensions	a = 12.5921(3) Å	α= 90°.
	b = 5.30640(10) Å	β= 99.0020(10)°.
	c = 22.4242(5) Å	γ = 90°.
Volume	1479.90(6) $Å^3$	
Z	2	
Density (calculated)	1.379 Mg/m^3	
Absorption coefficient	0.949 mm^{-1}	
F(000)	640	
Crystal size	0.208 x 0.115 x 0.08 mm^3	
Theta range for data collection	3.554 to 79.473°.	
Index ranges	-15<=h<=15, -6<=k<=6, -28<=l<=27	
Reflections collected	20749	
Independent reflections	6253 [R(int) = 0.0455]	
Completeness to theta = 67.679°	99.8 %	
Absorption correction	Semi-empirical from equivalents	
Max. and min. transmission	0.7542 and 0.6425	

Refinement method	Full-matrix least-squares on F^2
Data / restraints / parameters	6253 / 1 / 406
Goodness-of-fit on F^2	1.028
Final R indices [I>2sigma(I)]	R1 = 0.0390, wR2 = 0.0826
R indices (all data)	R1 = 0.0488, wR2 = 0.0872
Absolute structure parameter	0.05(7)
Extinction coefficient	0.0007(2)
Largest diff. peak and hole	0.154 and -0.161 e.$Å^{-3}$

4-(1-phenylpropyl)benzonitrile (85)

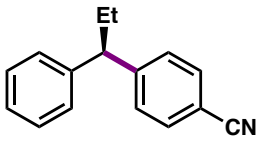

Prepared from 4-iodobenzonitrile (1 equiv, 46.0 mg, 0.2 mmol) and 1-(chloropropyl)benzene (1.2 equiv, 37 mg, 0.24 mmol) following General Procedure 3. The crude residue was purified by column chromatography to yield **85** (27 mg, 62% yield) in 89% ee as a colorless oil.

$\mathbf{R}_f$ = 0.21 (silica gel, 10% Et_2O/Hex, UV).

Chiral SFC: (OB-H, 2.5 mL/min, 10% IPA in CO_2, λ = 235 nm): t_R(major) = 5.4 min, t_R(minor) = 7.2 min.

$\mathbf{[\alpha]_D^{25}}$ = –1.9° (c = 1.0, $CHCl_3$).

^{1}H NMR (400 MHz, $CDCl_3$): δ 7.57 (s, 5H), 7.39 – 7.27 (m, 4H), 7.25 – 7.16 (m, 3H), 3.84 (t, *J* = 7.8 Hz, 1H), 2.20 – 1.98 (m, 2H), 0.90 (t, *J* = 7.3 Hz, 3H).

^{13}C NMR (101 MHz, $CDCl_3$): δ 150.9, 143.6, 132.4, 128.8, 128.8, 128.0, 126.7, 119.1, 110.0, 53.4, 28.3, 12.7.

FTIR (NaCl, thin film, cm^{-1}): 2963, 2930, 2874, 2226, 1606, 1503, 1493, 1462, 1452, 699.

HRMS (FAB+, *m/z*): calc'd for $C_{16}H_{15}N$ $[M+\bullet]^+$: 221.1204; found: 221.1202.

3-(1-phenylpropyl)benzonitrile (86)

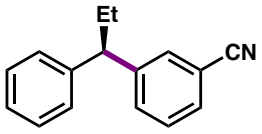

Prepared from 3-iodobenzonitrile (1 equiv, 46.0 mg, 0.2 mmol) and 1-(chloropropyl)benzene (1.2 equiv, 37 mg, 0.24 mmol) following General Procedure 3. The crude residue was purified by column chromatography to yield **86** (28 mg, 64% yield) in 88% ee as a colorless oil.

$\mathbf{R}_f$ = 0.26 (silica gel, 10:45:45 Et_2O/PhMe/Pentane, UV).

Chiral SFC: (OJ-H, 2.5 mL/min, 8% IPA in CO_2, λ = 235 nm): t_R (major) = 5.8 min, t_R (minor) = 6.5 min.

$\mathbf{[\alpha]_D^{25}}$ = –10.6° (c = 1.0, $CHCl_3$).

^{1}H NMR (400 MHz, $CDCl_3$): δ 7.56 – 7.42 (m, 3H), 7.42 – 7.27 (m, 3H), 7.25 – 7.16 (m, 3H), 3.82 (t, *J* = 7.8 Hz, 1H), 2.18 – 1.95 (m, 2H), 0.90 (t, *J* = 7.3 Hz, 3H).

^{13}C NMR (101 MHz, $CDCl_3$): δ 146.8, 143.7, 132.7, 131.6, 130.0, 129.3, 128.8, 127.9, 126.8, 119.2, 112.5, 52.9, 28.4, 12.7.

FTIR (NaCl, thin film, cm^{-1}): 3062, 3028, 2964, 2931, 2875, 2229, 1598, 1582, 1482, 1452, 701, 692.

HRMS (FAB+, *m/z*): calc'd for $C_{16}H_{15}N$ [M+•]$^+$: 221.1204; found: 221.1203.

tert-butyl-6-(1-phenylpropyl)-1*H*-indole-1-carboxylate (87)

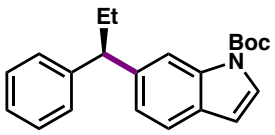

Prepared from *tert*-butyl 6-iodo-1*H*-indole-1-carboxylate (1 equiv, 69.0 mg, 0.2 mmol) and 1-(chloropropyl)benzene (1.2 equiv, 37 mg, 0.24 mmol) following General Procedure 3. The crude residue was purified by column chromatography to yield **87** (51 mg, 76% yield) in 83% ee as a colorless oil.

R$_f$ = 0.37 (silica gel, 10% Et_2O/Hex, UV).

Chiral SFC: (AD-H, 2.5 mL/min, 5% IPA in CO_2, λ = 254 nm): t_R(minor) = 5.2 min, t_R(major) = 5.5 min.

[α]$_D^{25}$ = –6.2° (c = 1.0, $CHCl_3$).

^{1}H NMR (400 MHz, $CDCl_3$): δ 8.09 (s, 1H), 7.45 (dd, *J* = 8.1, 0.7 Hz, 1H), 7.36 – 7.23 (m, 5H), 7.21 – 7.09 (m, 2H), 6.50 (dd, *J* = 3.7, 0.8 Hz, 1H), 3.93 (t, *J* = 7.8 Hz, 1H), 2.22 – 2.08 (m, 2H), 1.66 (s, 9H), 0.93 (t, *J* = 7.3 Hz, 3H).

^{13}C NMR (101 MHz, $CDCl_3$): δ 145.8, 141.8, 128.9, 128.5, 128.0, 126.0, 125.8, 123.2, 120.8, 114.5, 107.2, 83.6, 53.8, 29.0, 28.4, 13.0.

FTIR (NaCl, thin film, cm^{-1}): 2971, 2930, 1734, 1437, 1378, 1343, 1254, 1147, 1129, 1024.

HRMS (FAB+, *m/z*): calc'd for $C_{22}H_{25}NO_2$ [M+H]$^+$: 335.1885; found: 335.1899.

5-(1-phenylpropyl)-2-(piperidin-1-yl)pyrimidine (88)

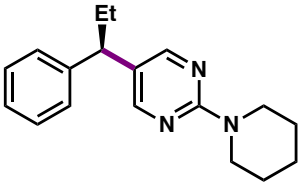

Prepared from 5-iodo-2-(piperidin-1-yl)pyrimidine (1 equiv, 58.0 mg, 0.2 mmol) and 1-(chloropropyl)benzene (2.4 equiv, 74 mg, 0.48 mmol) following General Procedure 3. The crude residue was purified by column chromatography to yield **88** (40 mg, 71% yield) in 90% ee as a clear oil.

R$_f$ = 0.44 (silica gel, 10% EtOAc/hexane, UV).

Chiral SFC: (OB-H, 2.5 mL/min, 15% IPA in CO_2, λ = 254 nm): t_R(minor) = 5.1 min, t_R(major) = 7.7 min.

$[\alpha]_D^{25}$ = –9° (c = 1.0, $CHCl_3$).

^{1}H NMR (400 MHz, $CDCl_3$): δ 8.18 (s, 2H), 7.33 – 7.24 (m, 2H), 7.23 – 7.13 (m, 3H), 3.80 – 3.68 (m, 4H), 3.60 (t, *J* = 7.8 Hz, 1H), 2.11 – 1.92 (m, 2H), 1.72 – 1.50 (m, 6H), 0.91 (t, *J* = 7.3 Hz, 3H).

^{13}C NMR (101 MHz, $CDCl_3$): δ 160.9, 157.3, 144.3, 128.7, 127.7, 126.4, 125.0, 48.1, 44.9, 28.3, 25.8, 25.0, 12.7.

FTIR (NaCl, thin film, cm^{-1}): 2931, 2852, 1599, 1537, 1505, 1462, 1446, 1364, 1271, 1255, 1022, 947.

HRMS (ESI-TOF, *m/z*): calc'd for $C_{18}H_{23}N_3$ $[M+H]^+$: 282.1965; found: 282.1960.

***tert*-butyl-4-(5-(1-phenylpropyl)pyrimidin-2-yl)piperazine-1-carboxylate (89)**

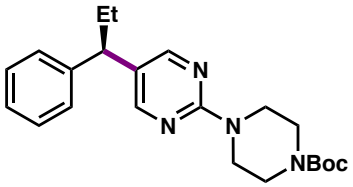

Prepared from *tert*-butyl 4-(5-iodopyrimidin-2-yl)piperazine-1-carboxylate (1 equiv, 78.0 mg, 0.2 mmol) and 1-(chloropropyl)benzene (2.4 equiv, 74 mg, 0.48 mmol) following General Procedure 3. The crude residue was purified by column chromatography to yield **89** (42 mg, 69% yield) in 91% ee as a clear oil.

R_f = 0.26 (silica gel, 10% EtOAc/hexane, UV).

Chiral SFC: (AD-H, 2.5 mL/min, 10% IPA in CO_2, λ = 254 nm): t_R(major) = 9.0 min, t_R(minor) = 10.1 min.

$[\alpha]_D^{25}$ = –7° (c = 1, $CHCl_3$).

^{1}H NMR (400 MHz, $CDCl_3$): δ 8.20 (s, 2H), 7.33 – 7.24 (m, 2H), 7.19 (d, *J* = 7.5 Hz, 3H), 3.75 (dd, *J* = 6.6, 4.0 Hz, 4H), 3.62 (t, *J* = 7.8 Hz, 1H), 3.47 (dd, *J* = 6.5, 4.0 Hz, 4H), 2.12 – 1.93 (m, 2H), 1.47 (s, 9H), 0.90 (t, *J* = 7.3 Hz, 3H).

^{13}C NMR (101 MHz, $CDCl_3$): δ 160.7, 157.3, 154.9, 144.1, 128.7, 127.7, 126.5, 126.3, 80.0, 48.0, 43.8, 28.5, 28.3, 12.7.

FTIR (NaCl, thin film, cm^{-1}): 2969, 2929, 2861, 1697, 1599, 1497, 1450, 1417, 1362, 1243, 1169, 1127, 998, 949.

HRMS (ESI-TOF, *m/z*): calc'd for $C_{22}H_{30}N_4O_2$ $[M+H]^+$: 383.2442; found: 383.2433.

***tert*-butyl-4-(5-(1-phenylpropyl)pyridin-2-yl)piperazine-1-carboxylate (90)**

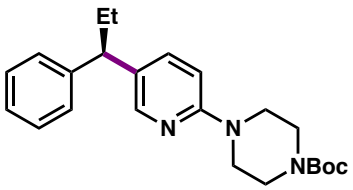

Prepared from *tert*-butyl 4-(5-iodopyridin-2-yl)piperazine-1-carboxylate (1 equiv, 78.0 mg, 0.2 mmol) and 1-(chloropropyl)benzene (2.4 equiv, 74 mg, 0.48 mmol) following General Procedure 3. The crude residue was purified by column chromatography to yield **90** (65 mg, 85% yield) in 86% ee as a clear oil.

$\mathbf{R}_f$ = 0.36 (silica gel, 20% EtOAc/hexane, UV).

Chiral SFC: (OJ-H, 2.5 mL/min, 15% IPA in CO_2, λ = 235 nm): t_R(major) = 7.8 min, t_R(minor) = 8.7 min.

$[\alpha]_D^{25}$ = 1.4° (c = 1.0, $CHCl_3$).

^{1}H NMR (400 MHz, $CDCl_3$): δ 8.18 (s, 2H), 7.34 – 7.23 (m, 2H), 7.23 – 7.13 (m, 3H), 3.85 – 3.66 (m, 4H), 3.60 (t, *J* = 7.8 Hz, 1H), 2.12 – 1.94 (m, 2H), 1.61 (dtt, *J* = 19.1, 7.5, 3.9 Hz, 6H), 0.91 (t, *J* = 7.3 Hz, 3H).

^{13}C NMR (101 MHz, $CDCl_3$): δ 160.5, 156.9, 144.0, 128.3, 127.4, 126.1, 124.7, 47.7, 44.6, 28.0, 25.5, 24.6, 12.4.

FTIR (NaCl, thin film, cm^{-1}): 2968, 2928, 2870, 2360, 2343, 1696, 1603, 1490, 1458, 1405, 1239, 1168, 1123, 99, 933.

HRMS (ESI-TOF, *m/z*): calc'd for $C_{23}H_{31}N_3O_2$ $[M+H]^+$: 382.2489; found: 382.2483.

5-(1-(*p*-tolyl)propyl)-2-methoxypyridine (91)

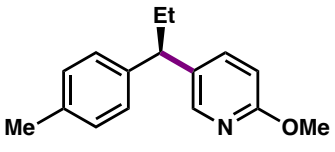

Prepared from 2-methoxy-5-iodopyridine (1 equiv, 47.0 mg, 0.2 mmol) and 1-(1-chloropropyl)-4-methylbenzene (1.2 equiv, 40 mg, 0.24 mmol) following General Procedure 3. The crude residue was purified by column chromatography to yield **91** (38 mg, 79% yield) in 92% ee as a colorless oil.

$\mathbf{R}_f$ = 0.32 (silica gel, 10% EtOAc/Hex, UV).

Chiral SFC: (OB-H, 2.5 mL/min, 5% IPA in CO_2, λ = 254 nm): t_R (major) = 5.3 min, t_R (minor) = 7.1 min.

$[\alpha]_D^{25}$ = +16.0° (c = 1.0, $CHCl_3$).

^{1}H NMR (400 MHz, $CDCl_3$): δ 8.05 (dt, *J* = 2.5, 0.7 Hz, 1H), 7.43 – 7.36 (m, 1H), 7.10 (s, 4H), 6.65 (dd, *J* = 8.5, 0.7 Hz, 1H), 3.90 (s, 3H), 3.70 (t, *J* = 7.8 Hz, 1H), 2.30 (s, 3H), 2.11 – 1.93 (m, 2H), 0.89 (t, *J* = 7.3 Hz, 3H).

^{13}C NMR (101 MHz, $CDCl_3$): δ 162.8, 145.7, 141.7, 138.3, 135.9, 133.5, 129.3, 127.7, 110.8, 53.4, 49.6, 28.5, 21.1, 12.8.

FTIR (NaCl, thin film, cm^{-1}): 2963, 2930, 2874, 1605, 1492, 1392, 1286, 1261, 1027, 820.

HRMS (ESI-TOF, *m/z*): calc'd for $C_{16}H_{19}NO$ $[M+H]^+$: 242.1539; found: 242.1542.

5-(1-(4-chlorophenyl)propyl)-2-methoxypyridine (92)

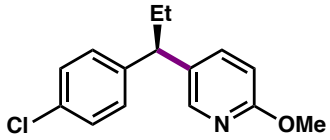

Prepared from 2-methoxy-5-iodopyridine (1 equiv, 47.0 mg, 0.2 mmol) and 1-chloro-4-(1-chloropropyl)benzene (1.2 equiv, 45 mg, 0.24 mmol) following General Procedure 3. The crude residue was purified by column chromatography to yield **92** (36 mg, 69% yield) in 85% ee as a colorless oil.

R_f = 0.24 (silica gel, 10% EtOAc/Hex, UV).

Chiral SFC: (OB-H, 2.5 mL/min, 5% IPA in CO_2, λ = 235 nm): t_R (minor) = 8.3 min, t_R (major) = 9.0 min.

$[\alpha]_D^{25}$ = 13.8° (c = 1.0, $CHCl_3$).

^{1}H NMR (400 MHz, $CDCl_3$): δ 8.03 (dt, *J* = 2.5, 0.7 Hz, 1H), 7.38 – 7.33 (m, 1H), 7.28 – 7.22 (m, 2H), 7.17 – 7.11 (m, 2H), 6.67 (dd, *J* = 8.6, 0.7 Hz, 1H), 3.90 (s, 3H), 3.71 (t, *J* = 7.8 Hz, 1H), 2.08 – 1.94 (m, 2H), 0.89 (t, *J* = 7.3 Hz, 3H).

^{13}C NMR (101 MHz, $CDCl_3$): δ 163.0, 145.8, 143.1, 138.2, 132.7, 132.1, 129.2, 128.8, 111.0, 53.5, 49.4, 28.4, 12.7.

FTIR (NaCl, thin film, cm^{-1}): 2964, 2932, 1605, 1572, 1489, 1461, 1392, 1291, 1262, 1027, 1014, 826.

HRMS (ESI-TOF, *m/z*): calc'd for $C_{15}H_{16}ClNO$ $[M+H]^+$: 262.0993; found: 262.0995.

2-methoxy-5-(1-(4-(trifluoromethyl)phenyl)propyl)pyridine (93)

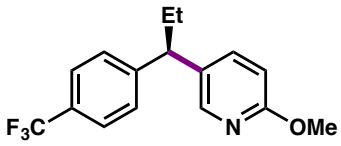

Prepared from 2-methoxy-5-iodopyridine (1 equiv, 47.0 mg, 0.2 mmol) and 1-(1-chloropropyl)-4-(trifluoromethyl)benzene (1.2 equiv, 53 mg, 0.24 mmol) following General Procedure 3. The crude residue was purified by column chromatography to yield **93** (42 mg, 71% yield) in 88% ee as a colorless oil.

R_f = 0.31 (silica gel, 10% EtOAc/Hex, UV).

Chiral SFC: (AD-H, 2.5 mL/min, 2% IPA in CO_2, λ = 254 nm): t_R (minor) = 5.9 min, t_R (major) = 6.4 min.

$[\alpha]_D^{25}$ = 9.0° (c = 1.0, $CHCl_3$).

^{1}H NMR (400 MHz, $CDCl_3$): δ 8.05 (dt, *J* = 2.5, 0.7 Hz, 1H), 7.61 – 7.48 (m, 2H), 7.37 (ddd, *J* = 8.6, 2.6, 0.5 Hz, 1H), 7.35 – 7.29 (m, 2H), 6.73 – 6.64 (m, 1H), 3.90 (s, 3H), 3.80 (t, *J* = 7.8 Hz, 1H), 2.13 – 1.99 (m, 2H), 0.91 (t, *J* = 7.3 Hz, 3H).

^{13}C NMR (101 MHz, $CDCl_3$): δ 163.1, 148.7, 145.9, 138.2, 132.2, 128.74 (q, *J* = 32.4 Hz), 128.2, 125.61 (q, *J* = 3.9 Hz), 124.3 (q, *J* = 271.7 Hz), 111.1, 53.5, 49.8, 28.3, 12.7.

^{19}F NMR (282 MHz, $CDCl_3$): δ –62.4.

FTIR (NaCl, thin film, cm^{-1}): 2967, 2937, 1618, 1605, 1493, 1325, 1289, 1165, 1122, 1068, 1018, 828.

HRMS (ESI-TOF, *m/z*): calc'd for $C_{16}H_{16}F_3NO$ $[M+H]^+$: 296.1257; found: 296.1265.

2-methoxy-5-(1-(4-(trifluoromethoxy)phenyl)propyl)pyridine (74)

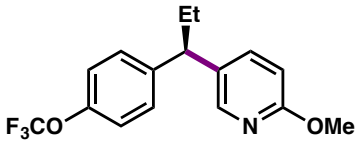

Prepared from 2-methoxy-5-iodopyridine (1 equiv, 47.0 mg, 0.2 mmol) and 1-(1-chloropropyl)-4-(trifluoromethoxy)benzene (1.2 equiv, 57 mg, 0.24 mmol) following General Procedure 3. The crude residue was purified by column chromatography to yield **74** (47 mg, 76% yield) in 87% ee as a colorless oil.

R_f = 0.26 (silica gel, 10% EtOAc/Hex, UV).

Chiral SFC: (AD-H, 2.5 mL/min, 5% IPA in CO_2, λ = 245 nm): t_R (minor) = 3.0 min, t_R (major) = 3.3 min.

$[\alpha]_D^{25}$ = +10.0° (c = 1.0, $CHCl_3$).

^{1}H NMR (400 MHz, $CDCl_3$): δ 8.04 (dt, *J* = 2.6, 0.7 Hz, 1H), 7.41 – 7.34 (m, 1H), 7.25 – 7.19 (m, 2H), 7.13 (ddt, *J* = 7.6, 2.1, 1.1 Hz, 2H), 6.68 (dd, *J* = 8.5, 0.7 Hz, 1H), 3.91 (s, 3H), 3.75 (t, *J* = 7.8 Hz, 1H), 2.11 – 1.94 (m, 2H), 0.90 (t, *J* = 7.3 Hz, 3H).

^{13}C NMR (101 MHz, $CDCl_3$): δ 163.0, 145.8, 143.4, 138.3, 132.6, 129.1, 128.2 (d, *J* = 62.1 Hz), 121.2, 120.6 (q, *J* = 257.7 Hz), 111.0, 53.5, 49.3, 28.5, 12.7.

^{19}F NMR (282 MHz, $CDCl_3$): δ –57.9.

FTIR (NaCl, thin film, cm^{-1}): 2967, 2935, 2877, 1605, 1508, 1493, 1259, 1222, 12264, 1027.

HRMS (ESI-TOF, *m/z*): calc'd for $C_{16}H_{16}F_3NO_2$ $[M+H]^+$: 312.1206; found: 312.1198.

2-methoxy-5-(1-(2-methoxyphenyl)propyl)pyridine (94)

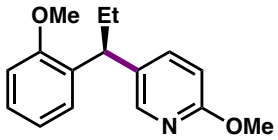

Prepared from 2-methoxy-5-iodopyridine (1 equiv, 47.0 mg, 0.2 mmol) and 1-(1-chloropropyl)-2-methoxybenzene (1.2 equiv, 44 mg, 0.24 mmol) following General Procedure 3. The crude residue was purified by column chromatography to yield **94** (24 mg, 47% yield) in 93% ee as a colorless oil.

R_f = 0.24 (silica gel, 10% EtOAc/Hex, UV).

Chiral SFC: (OB-H, 2.5 mL/min, 5% IPA in CO_2, λ = 235 nm): t_R (minor) = 4.9 min, t_R (major) = 5.7 min.

$[\alpha]_D^{25}$ = –24.6° (c = 1.0, $CHCl_3$).

^{1}H NMR (400 MHz, $CDCl_3$): δ 8.08 (dt, *J* = 2.5, 0.7 Hz, 1H), 7.42 (ddd, *J* = 8.6, 2.5, 0.5 Hz, 1H), 7.23 (dd, *J* = 7.6, 1.7 Hz, 1H), 7.17 (ddd, *J* = 8.2, 7.4, 1.7 Hz, 1H), 6.92 (td, *J* = 7.5, 1.2 Hz, 1H), 6.82 (dd, *J* = 8.2, 1.1 Hz, 1H), 6.66 – 6.60 (m, 1H), 4.18 (t, *J* = 7.8 Hz, 1H), 3.89 (s, 3H), 3.77 (s, 3H), 2.13 – 1.90 (m, 2H), 0.89 (t, *J* = 7.3 Hz, 3H).

^{13}C NMR (101 MHz, $CDCl_3$): δ 162.6, 157.1, 146.3, 138.5, 133.2, 133.1, 127.3, 127.2, 120.6, 110.7, 110.4, 55.5, 53.4, 42.2, 27.6, 12.8.

FTIR (NaCl, thin film, cm^{-1}): 2962, 2937, 1604, 1572, 1489, 1463, 1394, 1287, 1242, 1029, 753.

HRMS (ESI-TOF, *m/z*): calc'd for $C_{16}H_{19}NO_2$ $[M+H]^+$: 258.1489; found: 258.1487.

2-methoxy-5-(1-(2-fluorophenyl)propyl)pyridine (95)

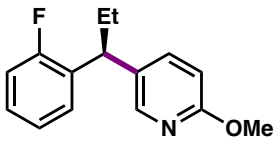

Prepared from 2-methoxy-5-iodopyridine (1 equiv, 47.0 mg, 0.2 mmol) and 1-(1-chloropropyl)-2-fluorobenzene (1.2 equiv, 41 mg, 0.24 mmol) following General Procedure 3. The crude residue was purified by column chromatography to yield **95** (26 mg, 53% yield) in 93% ee as a colorless oil.

R_f = 0.30 (silica gel, 10% EtOAc/Hex, UV).

Chiral SFC: (AD-H, 2.5 mL/min, 10% IPA in CO_2, λ = 254 nm): t_R (major) = 2.8 min, t_R (minor) = 3.3 min.

$[\alpha]_D^{25}$ = +5.9° (c = 0.97, $CHCl_3$).

^{1}H NMR (400 MHz, $CDCl_3$): δ 8.12 – 8.04 (m, 1H), 7.44 (dd, *J* = 8.6, 2.5 Hz, 1H), 7.29 – 7.20 (m, 1H), 7.17 (dddd, *J* = 8.1, 7.2, 5.2, 1.9 Hz, 1H), 7.09 (td, *J* = 7.5, 1.4 Hz, 1H), 6.99 (ddd, *J* = 10.5, 8.1, 1.4 Hz, 1H), 6.66 (dd, *J* = 8.6, 0.7 Hz, 1H), 4.09 (t, *J* = 7.9 Hz, 1H), 3.90 (s, 3H), 2.15 – 1.96 (m, 2H), 0.92 (t, *J* = 7.3 Hz, 3H).

^{13}C NMR (101 MHz, $CDCl_3$): δ 162.9, 162.1, 159.6, 146.1, 138.4, 132.1, 131.6 (d, *J* = 14.3 Hz), 128.2 (dd, J = 40.4, 4.2), 124.3 (d, J = 3.54Hz), 115.7 (d, *J* = 22.7 Hz), 110.7, 53.5, 42.5, 27.6, 12.7.

^{19}F NMR (282 MHz, $CDCl_3$): δ –117.9.

FTIR (NaCl, thin film, cm^{-1}): 2965, 2943, 1605, 1572, 1492, 1455, 1394, 1289, 1262, 1027, 755.

HRMS (ESI-TOF, *m/z*): calc'd for $C_{15}H_{16}FNO$ $[M+H]^+$: 246.1289; found: 246.1287.

2-methoxy-5-(1-phenylethyl)pyridine (96)

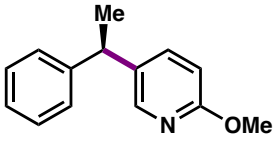

Prepared from 2-methoxy-5-iodopyridine (1 equiv, 47.0 mg, 0.2 mmol) and (1-chloroethyl)benzene (1.2 equiv, 34 mg, 0.24 mmol) following General Procedure 3. The crude residue was purified by column chromatography to yield **96** (36 mg, 84% yield) in 85% ee as a colorless oil.

R_f = 0.35 (silica gel, 20% Et_2O/Hex, UV).

Chiral SFC: (OJ-H, 2.5 mL/min, 4% IPA in CO_2, λ = 254 nm): t_R (minor) = 5.7 min, t_R (major) = 6.3 min.

$[\alpha]_D^{25}$ = +3.5° (c = 1.0, $CHCl_3$).

^{1}H NMR (500 MHz, $CDCl_3$): δ 8.07 (dt, *J* = 2.5, 0.7 Hz, 1H), 7.38 (ddd, *J* = 8.6, 2.5, 0.5 Hz, 1H), 7.33 – 7.27 (m, 2H), 7.23 – 7.17 (m, 3H), 6.66 (dt, *J* = 8.5, 0.5 Hz, 1H), 4.10 (q, *J* = 7.2 Hz, 1H), 3.91 (s, 3H), 1.63 (d, *J* = 7.2 Hz, 3H).

^{13}C NMR (126 MHz, $CDCl_3$): δ 162.8, 145.8, 145.4, 138.3, 134.5, 128.6, 127.6, 126.4, 110.7, 53.5, 41.7, 21.8.

FTIR (NaCl, thin film, cm^{-1}): 3026, 2966, 2927, 1606, 1571, 1492, 1390, 1284, 1025, 831, 699.

HRMS (ESI-TOF, *m/z*): calc'd for $C_{15}H_{15}NO$ $[M+H]^+$: 214.1226; found: 214.1220.

2-methoxy-5-(3-chloro-1-phenylpropyl)pyridine (97)

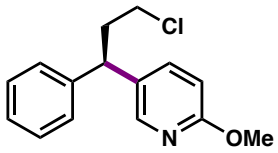

Prepared from 2-methoxy-5-iodopyridine (1 equiv, 47.0 mg, 0.2 mmol) and (1,3-dichloropropyl)benzene (1.2 equiv, 41.0 mg, 0.24 mmol) following General Procedure 3. The crude residue was purified by column chromatography to yield **97** (41 mg, 79% yield) in 91% ee as a colorless oil.

R_f = 0.28 (silica gel, 10% EtOAc/Hex, UV).

Chiral SFC: (AD-H, 2.5 mL/min, 8% IPA in CO_2, λ = 210 nm): t_R (major) = 6.0 min, t_R (minor) = 7.2 min.

$[\alpha]_D^{25}$ = +4.2° (c = 1.0, $CHCl_3$).

^{1}H NMR (400 MHz, $CDCl_3$): δ 8.09 (dt, *J* = 2.6, 0.7 Hz, 1H), 7.42 (ddd, *J* = 8.6, 2.6, 0.5 Hz, 1H), 7.34 – 7.27 (m, 2H), 7.25 – 7.18 (m, 3H), 6.68 (dd, *J* = 8.5, 0.7 Hz, 1H), 4.18 (t, *J* = 7.8 Hz, 1H), 3.91 (s, 3H), 3.45 (t, *J* = 6.5 Hz, 2H), 2.58 – 2.36 (m, 2H).

^{13}C NMR (101 MHz, $CDCl_3$): δ 163.1, 145.8, 143.0, 138.4, 131.8, 128.9, 127.9, 126.9, 111.1, 53.5, 44.7, 43.0, 37.9.

FTIR (NaCl, thin film, cm^{-1}): 2945, 1719, 1605, 1572, 1489, 1453, 1394, 1291, 1028, 829, 753, 700.

HRMS (ESI-TOF, *m/z*): calc'd for $C_{15}H_{16}ClNO$ $[M+H]^+$: 262.0993; found: 262.1003.

2-methoxy-5-(1,2-diphenylethyl)pyridine (98)

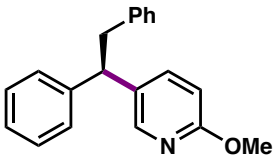

Prepared from 2-methoxy-5-iodopyridine (1 equiv, 47.0 mg, 0.2 mmol) and (1-chloro-1,2-diphenylethane (1.2 equiv, 52.0 mg, 0.24 mmol) following General Procedure 3. The crude residue was purified by column chromatography to yield **98** (26 mg, 55% yield) in 95% ee as a colorless oil.

$\mathbf{R}_f$ = 0.32 (silica gel, 10% EtOAc/Hex, UV, $KMnO_4$).

Chiral SFC: (AD-H, 2.5 mL/min, 12% IPA in CO_2, λ = 280 nm): t_R (major) = 5.7 min, t_R (minor) = 6.6 min.

$\mathbf{[\alpha]_D^{25}}$ = +37.9° (c = 0.865, $CHCl_3$).

^{1}H NMR (500 MHz, $CDCl_3$): δ 7.95 (dt, *J* = 2.5, 0.7 Hz, 1H), 7.38 (ddd, *J* = 8.5, 2.6, 0.5 Hz, 1H), 7.31 – 7.23 (m, 2H), 7.23 – 7.16 (m, 5H), 7.16 – 7.10 (m, 1H), 7.04 – 6.99 (m, 2H), 6.63 (dd, *J* = 8.5, 0.7 Hz, 1H), 4.18 (dd, *J* = 8.6, 7.2 Hz, 1H), 3.88 (s, 3H), 3.37 (dd, *J* = 13.6, 7.1 Hz, 1H), 3.29 (dd, *J* = 13.7, 8.6 Hz, 1H).

^{13}C NMR (101 MHz, $CDCl_3$): δ 162.8, 146.0, 144.1, 139.8, 138.6, 132.5, 129.2, 128.6, 128.3, 128.0, 126.6, 126.2, 110.7, 53.5, 50.0, 42.0.

FTIR (NaCl, thin film, cm^{-1}): 3027, 2943, 1606, 1571, 1492, 1453, 1393, 1291, 1029, 698.

HRMS (ESI-TOF, *m/z*): calc'd for $C_{20}H_{19}NO$ $[M+H]^+$: 290.1539; found: 290.1527.

2-methoxy-5-(3-methyl-1-phenylbutyl)pyridine (99)

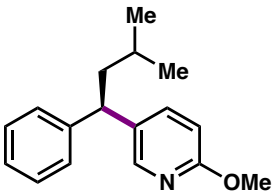

Prepared from 2-methoxy-5-iodopyridine (1 equiv, 47.0 mg, 0.2 mmol) and (1-chloro-3-methylbutyl)benzene (1.2 equiv, 44.0 mg, 0.24 mmol) following General Procedure 3. The crude residue was purified by column chromatography to yield **99** (30 mg, 74% yield) in 94% ee as a colorless oil.

$\mathbf{R}_f$ = 0.32 (silica gel, 10% EtOAc/Hex, UV).

Chiral SFC: (AD-H, 2.5 mL/min, 5% IPA in CO_2, λ = 254 nm): t_R (major) = 4.9 min, t_R (minor) = 5.6 min.

$\mathbf{[\alpha]_D^{25}}$ = +8.9° (c = 1.0, $CHCl_3$).

^{1}H NMR (500 MHz, $CDCl_3$): δ 8.07 (dt, *J* = 2.6, 0.7 Hz, 1H), 7.42 (dd, *J* = 8.6, 2.5 Hz, 1H), 7.32 – 7.24 (m, 2H), 7.25 – 7.20 (m, 2H), 7.20 – 7.15 (m, 1H), 6.67 (dd, *J* = 8.5, 0.7 Hz, 1H), 3.97 (t, *J* = 8.0 Hz, 1H), 3.91 (s, 3H), 1.89 (ddd, *J* = 8.4, 6.9, 1.4 Hz, 2H), 1.50 – 1.39 (m, 1H), 0.93 (d, *J* = 6.6 Hz, 6H).

^{13}C NMR (101 MHz, $CDCl_3$): δ 162.8, 145.8, 144.8, 138.4, 133.4, 128.7, 127.8, 126.4, 110.8, 53.5, 45.7, 44.9, 25.6, 22.8, 22.6.

FTIR (NaCl, thin film, cm^{-1}): 2955, 2868, 1605, 1572, 1489, 1466, 1452, 1393, 1286, 1259, 1029, 699.

HRMS (ESI-TOF, *m/z*): calc'd for $C_{17}H_{21}NO$ $[M+H]^+$: 256.1696; found: 256.1697.

5-(2-((*tert*-butyldimethylsilyl)oxy)-1-phenylethyl)-2-methoxypyridine (100)

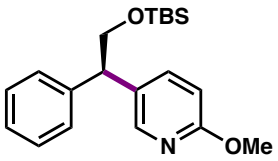

Prepared from 2-methoxy-5-iodopyridine (1 equiv, 47.0 mg, 0.2 mmol) and *tert*-butyl(2-chloro-2-phenylethoxy)dimethylsilane (1.2 equiv, 54.0 mg, 0.24 mmol) following General Procedure 3. The crude residue was purified by column chromatography to yield **100** (25 mg, 36% yield) in 94% ee as a colorless oil.

R_f = 0.50 (silica gel, 10% EtOAc/hexanes).

Chiral SFC: (AD-H, 2.5 mL/min, 5% IPA in CO_2, λ = 235 nm): t_R (major) = 2.9 min, t_R (minor) = 3.3 min.

$[\alpha]_D^{25}$ = +5.9° (c = 1.0, $CHCl_3$).

^{1}H NMR (400 MHz, $CDCl_3$): δ 8.08 (d, *J* = 2.5 Hz, 1H), 7.45 (dd, *J* = 8.6, 2.5 Hz, 1H), 7.33 – 7.25 (m, 3H), 7.25 – 7.17 (m, 3H), 6.67 (dd, *J* = 8.6, 0.7 Hz, 1H), 4.15 – 4.04 (m, 3H), 3.91 (s, 3H), 0.81 (s, 9H), -0.06 (s, 6H).

^{13}C NMR (101 MHz, $CDCl_3$): δ 163.0, 146.6, 142.0, 139.2, 130.9, 128.5, 128.5, 126.7, 110.4, 66.6, 53.5, 50.5, 25.9, 18.3, -5.4.

FTIR (NaCl, thin film, cm^{-1}): 2952, 2928, 1606, 1492, 1289, 1257, 1105, 1030.

HRMS (ESI-TOF, *m/z*): calc'd for $C_{20}H_{29}NO_2Si$ $[M+H]^+$: 344.2040; found: 344.2030.

tert-butyl-4-(2-(6-methoxypyridin-3-yl)-2-phenylethyl)piperidine-1-carboxylate (101)

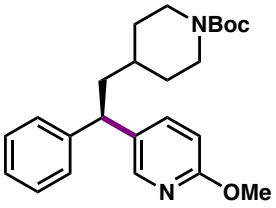

Prepared from 2-methoxy-5-iodopyridine (1 equiv, 47.0 mg, 0.2 mmol) and *tert*-butyl 4-(2-chloro-2-phenylethyl)piperidine-1-carboxylate (1.2 equiv, 78.0 mg, 0.24 mmol) following General Procedure 3. The crude residue was purified by column chromatography to yield **101** (48 mg, 60% yield) in 94% ee as a colorless oil.

R_f = 0.26 (silica gel, 10% EtOAc/Hexanes).

Chiral SFC: (AD-H, 2.5 mL/min, 15% IPA in CO_2, λ = 280 nm): t_R (major) = 7.6 min, t_R (minor) = 11.3 min.

$[\alpha]_D^{25}$ = +6.7° (c = 1.0, $CHCl_3$).

^{1}H NMR (400 MHz, $CDCl_3$): δ 8.05 (dd, *J* = 2.5, 0.7 Hz, 1H), 7.40 (dd, *J* = 8.6, 2.5 Hz, 1H), 7.33 – 7.23 (m, 2H), 7.24 – 7.15 (m, 3H), 6.66 (dd, *J* = 8.6, 0.7 Hz, 1H), 3.99 (t, *J* = 8.0 Hz, 2H), 3.89 (s, 3H), 2.56 (t, *J* = 12.2 Hz, 2H), 1.94 (ddd, *J* = 8.5, 6.7, 2.1 Hz, 2H), 1.69 (d, *J* = 12.9 Hz, 2H), 1.44 (s, 9H), 1.29 (dtd, *J* = 14.4, 7.4, 6.9, 3.8 Hz, 2H), 1.23 – 1.04 (m, 2H).

^{13}C NMR (101 MHz, $CDCl_3$): δ 162.9, 154.9, 145.6, 144.4, 138.2, 132.9, 128.8, 127.7, 126.5, 111.0, 79.3, 53.4, 44.6, 42.5, 33.5, 32.3, 32.1, 28.6.

FTIR (NaCl, thin film, cm^{-1}): 2922, 1690, 1604, 1491, 1423, 1393, 1365, 1285, 1244, 1166, 1122, 1029.

HRMS (ESI-TOF, *m/z*): calc'd for $C_{24}H_{32}N_2O_3$ $[M+H]^+$: 397.2486; found: 397.2473.

2-methoxy-5-(1-(dibenzo[*b,d*]furan-4-yl)propyl)pyridine (102)

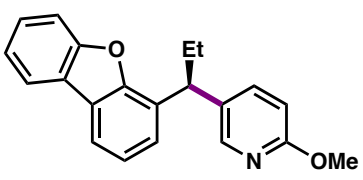

Prepared from 2-methoxy-5-iodopyridine (1 equiv, 47.0 mg, 0.2 mmol) and 4-(1-chloropropyl)dibenzo[*b,d*]furan (1.2 equiv, 59.0 mg, 0.24 mmol) following General Procedure 3. The crude residue was purified by column chromatography to yield **102** (30 mg, 48% yield) in 93% ee as a colorless oil.

R_f = 0.31 (silica gel, 10% EtOAc/Hex, UV).

Chiral SFC: (OB-H, 2.5 mL/min, 10% IPA in CO_2, λ = 254 nm): t_R (minor) = 6.5 min, t_R (major) = 7.2 min.

$[\alpha]_D^{25}$ = –97.0° (c = 1.0, $CHCl_3$).

^{1}H NMR (400 MHz, $CDCl_3$): δ 8.25 (dt, *J* = 2.5, 0.7 Hz, 1H), 7.92 (ddd, *J* = 7.7, 1.4, 0.7 Hz, 1H), 7.80 (dd, *J* = 7.3, 1.6 Hz, 1H), 7.62 – 7.54 (m, 2H), 7.45 (ddd, *J* = 8.3, 7.3, 1.4 Hz, 1H), 7.37 – 7.27 (m, 3H), 6.66 (dd, *J* = 8.5, 0.7 Hz, 1H), 4.42 (t, *J* = 7.9 Hz, 1H), 3.89 (s, 3H), 2.39 – 2.12 (m, 2H), 0.97 (t, *J* = 7.3 Hz, 3H).

^{13}C NMR (101 MHz, $CDCl_3$): δ 162.9, 156.1, 154.3, 146.2, 138.5, 132.3, 128.8, 127.2, 125.3, 124.6, 124.3, 123.1, 122.8, 120.8, 118.8, 111.9, 110.7, 53.4, 44.2, 27.6, 12.9.

FTIR (NaCl, thin film, cm^{-1}): 2964, 1605, 1572, 1489, 1451, 1422, 1394, 1291, 1184, 1027, 828, 752.

HRMS (ESI-TOF, *m/z*): calc'd for $C_{21}H_{19}NO_2$ $[M+H]^+$: 318.1489; found: 318.1486.

2.6.5 Mechanistic Experiments

2.6.5.1 Inhibitor Studies

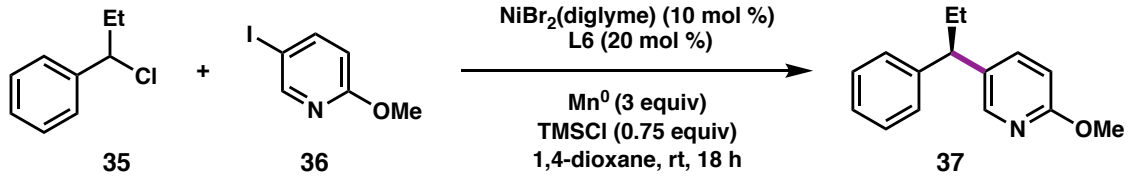

35 36 37

Control:	84% yield, 90% ee
50 mol % BHT:	83% yield, 89% ee
50 mol % DHA:	78% yield, 88% ee
50 mol % TEMPO:	72% yield, 91% ee

The experiment was conducted according to General Procedure 2 for cross-coupling, except that either BHT (0.025 mmol, 4.5 mg, 0.5 equiv), DHA (0.025 mmol, 5.5 mg, 0.5 equiv), or TEMPO (0.25 mmol, 3.9 mg, 0.5 equiv) were added prior to pumping into the glovebox. After 18 h, the reactions were light gray. The vials were opened and the reactions diluted with 20% Et_2O/hexanes and filtered through short basic alumina plugs. Analysis of the crude reaction mixture by ^1H NMR with 2,3,5,6-tetrachloronitrobenzene as a standard showed no inhibition.

2.6.5.2 Radical Clock Experiment

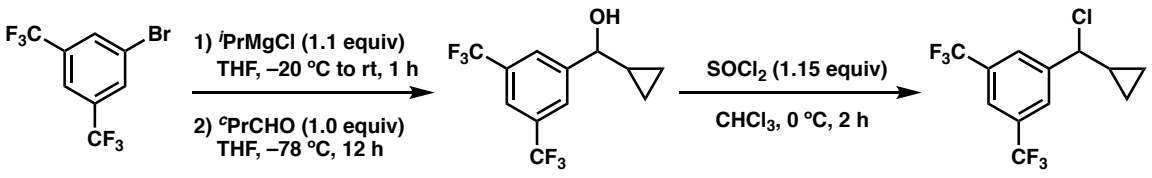

The aryl bromide (12 mmol, 2.07 mL, 1.0 equiv) was dissolved in 10 mL THF in a flame-dried round bottom flask and cooled to –20 ºC. ^{i}PrMgCl (13.2 mmol, 6.6 mL, 1.1 equiv) was added slowly and the reaction was warmed to 0 ºC for 1 hour. The aldehyde (12 mmol, 0.9 mL, 1.0 equiv) was dissolved in 30 mL dry THF in a flame-dried flask and

cooled to –78 ºC. The Grignard was added to the reaction flask slowly via cannula and the reaction was allowed to stir overnight, warming slowly to room temperature. The reaction was quenched with 30 mL sat. NH_4Cl and the aqueous layer was separated and extracted with 2 x 30 mL Et_2O. The combined organic layers were dried with Na_2SO_4, filtered and concentrated. The alcohol was purified by loading onto a silica plug and first eluting with hexane, then switching to Et_2O. Et_2O wash was concentrated to afford an off-white solid. (2.63 g, 77% yield).

R_f= 0.38 (silica gel, 20% EtOAc/hexanes, UV)

^{1}H NMR (400 MHz, $CDCl_3$): δ 7.91 (dq, *J* = 1.3, 0.6 Hz, 2H), 7.80 (t, *J* = 1.4 Hz, 1H), 4.11 (dd, *J* = 8.6, 2.9 Hz, 1H), 2.11 (d, *J* = 2.9 Hz, 1H), 1.25 – 1.14 (m, 1H), 0.78 – 0.64 (m, 2H), 0.58 – 0.44 (m, 2H).

^{13}C NMR (101 MHz, $CDCl_3$): δ 146.4, 131.69 (q, *J* = 33.2 Hz), 126.3, 123.5 (q, *J* = 273.8 Hz), 121.52 (t, *J* = 3.9 Hz), 19.8, 3.8, 3.6.

^{19}F NMR (282 MHz, $CDCl_3$): δ –62.8.

FTIR (NaCl, thin film, cm^{-1}): 3388, 1660, 1378, 1280, 1140, 1043, 901, 843, 683.

HRMS (EI+, m/z): calc'd for $C_{12}H_{10}F_6O$ $[M-F]^+$: 265.0652; found: 265.0658.

The alcohol (5.0 mmol, 1.42 g, 1 equiv) was dissolved in $CHCl_3$ (20 mL) in a flame-dried flask under N_2. The reaction was cooled to 0 ºC, then $SOCl_2$ (5.75 mmol, 0.42 mL, 1.15 equiv) was added. Reaction was allowed to stir for 2 hours, at which point monitoring by TLC showed the starting material was completely consumed. The reaction was concentrated and purified by silica gel chromatography (2% Et_2O/pentane) to afford the clean chloride as a clear oil (0.99 g, 65% yield). Care was taken to minimize exposure

to light or heat during reaction, concentration, and handling. The material was wrapped in foil and stored at –20 ºC.

R_f= 0.46 (silica gel, 5% EtOAc/hexanes, UV)

^{1}H NMR (300 MHz, $CDCl_3$): δ 7.98 – 7.88 (m, 2H), 7.87 – 7.82 (m, 1H), 4.36 (d, *J* = 9.2 Hz, 1H), 1.64 – 1.44 (m, 1H), 0.91 (dddd, *J* = 8.9, 7.9, 5.9, 4.7 Hz, 1H), 0.78 (dddd, *J* = 8.7, 7.8, 5.9, 4.7 Hz, 1H), 0.66 (ddt, *J* = 9.5, 5.8, 4.8 Hz, 1H), 0.48 (ddt, *J* = 9.4, 5.7, 4.7 Hz, 1H).

^{13}C NMR (101 MHz, $CDCl_3$): δ 144.3, 132.10 (q, *J* = 33.4 Hz), 127.5, 123.2 (q, *J* = 272.6 Hz), 122.30 (dt, *J* = 7.5, 3.5 Hz), 66.6, 19.7, 6.8, 6.4.

^{19}F NMR (282 MHz, $CDCl_3$): δ –62.9.

FTIR (NaCl, thin film, cm^{-1}): 3433, 1627, 1466, 1375, 1279, 1177, 899, 682.

HRMS (EI+, m/z): calc'd for $C_{12}H_9ClF_6$ $[M-F]^+$: 283.0313; found: 283.0351.

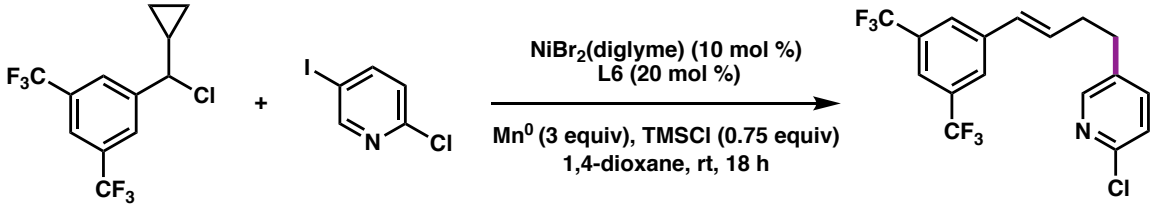

The cross coupling of radical clock substrate **113** was performed according to General Procedure 2, employing 2-chloro-5-iodopyridine (1 equiv, 12.0 mg, 0.05 mmol) and 1-(chloro(cyclopropyl)methyl)-3-(trifluoromethyl)benzene (1.2 equiv, 18.0 mg, 0.06 mmol). The crude reaction mixture contained the rearranged product **115** as the only cross-coupled product. No cyclopropyl peaks were remaining in the crude ^{1}H NMR. **115**

was reported as 57% yield after analysis of the crude reaction mixture by ^{1}H NMR with 2,3,5,6-tetrachloronitrobenzene as an internal standard.

R_f= 0.09 (silica gel, 5% Et_2O/10% PhMe/85% hexanes, UV)

^{1}H NMR (400 MHz, $CDCl_3$): δ 8.26 (dd, *J* = 2.5, 0.7 Hz, 1H), 7.71 (d, *J* = 4.2 Hz, 3H), 7.50 (dd, *J* = 8.1, 2.5 Hz, 1H), 7.27 (dd, *J* = 8.1, 0.7 Hz, 1H), 6.55 – 6.29 (m, 2H), 2.82 (dd, *J* = 8.5, 6.7 Hz, 2H), 2.58 (ddd, *J* = 9.3, 7.3, 6.1 Hz, 2H).

^{13}C NMR (101 MHz, $CDCl_3$): δ 149.7, 149.6, 139.3, 138.9, 135.4, 132.9, 132.02 (q, *J* = 33.1 Hz), 129.1, 126.11 – 125.87 (m), 124.2, 123.4 (q, *J* = 270.9 Hz), 120.81 (dt, *J* = 7.8, 3.9 Hz), 34.4, 31.8.

^{19}F NMR (282 MHz, $CDCl_3$): δ –63.0.

FTIR (NaCl, thin film, cm^{-1}): 2931, 2358, 1463, 1382, 1279, 1175, 1132.

HRMS (ESI-TOF, m/z): calc'd for $C_{17}H_{12}ClF_6N$ $[M+H]^+$: 380.0635; found: 380.0640.

2.6.6 Formal Synthesis of Sertraline

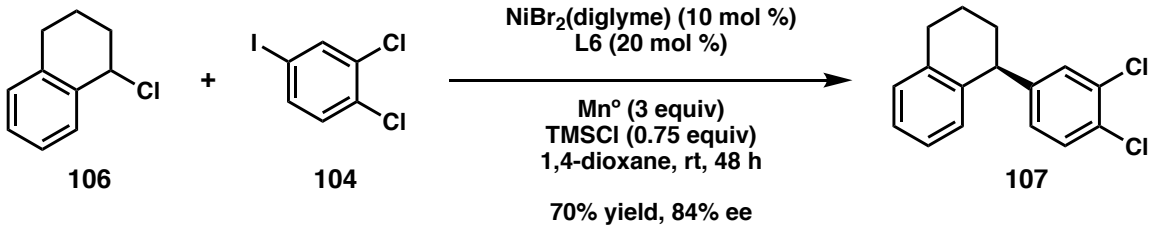

Prepared from 1,2-dichloro-4-iodobenzene (1 equiv, 55.0 mg, 0.2 mmol) and 1-chloro-1,2,3,4-tetrahydronaphthalene (2.4 equiv, 80.0 mg, 0.48 mmol) following General Procedure 3, stirring for 48 hours. The crude residue was purified by column chromatography to yield **107** (38 mg, 70% yield) in 84% ee as a colorless solid.

$\mathbf{R}_f$ = 0.26 (silica gel, 100% hexanes, UV).

Chiral SFC: (AD-H, 2.5 mL/min, 3% IPA in CO_2, λ = 235 nm): t_R (major) = 8.2 min, t_R (minor) = 10.6 min.

$\mathbf{[\alpha]_D^{25}}$ = +10.0° (c = 1.0, $CHCl_3$).

^{1}H NMR (500 MHz, $CDCl_3$): δ 7.34 (d, *J* = 8.3 Hz, 1H), 7.19 (d, *J* = 2.1 Hz, 1H), 7.18 – 7.12 (m, 2H), 7.09 – 7.02 (m, 1H), 6.92 (dd, *J* = 8.3, 2.1 Hz, 1H), 6.80 (dd, *J* = 7.7, 1.0 Hz, 1H), 4.11 – 4.05 (m, 1H), 2.98 – 2.78 (m, 2H), 2.20 – 2.10 (m, 1H), 1.92 – 1.70 (m, 3H).

^{13}C NMR (101 MHz, $CDCl_3$): δ 148.0, 138.1, 137.7, 132.3, 130.8, 130.3, 130.1, 130.0, 129.3, 128.4, 126.5, 126.0, 45.0, 33.2, 29.7, 20.8.

FTIR (neat, cm^{-1}): 2358, 2325, 2330, 1480, 1458, 885, 667, 621.

HRMS (FAB+, *m/z*): calc'd for $C_{16}H_{14}Cl_2$ $[(M+H) - H_2]^+$: 275.0394; found: 275.0386.

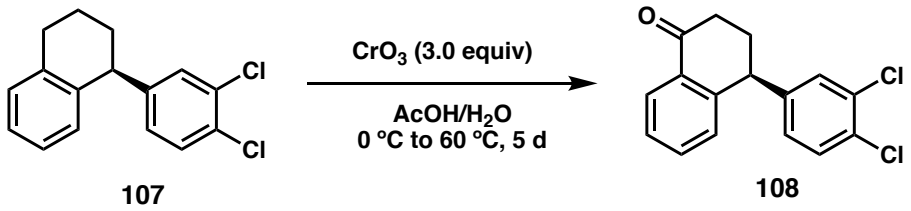

107 **108**

107 (6.5 mg, 0.023 mmol, 1 equiv) was dissolved in 0.25 mL of AcOH in a 1-dram vial and cooled to 0 ºC. The ice bath was removed and CrO_3 (7 mg, 0.070 mmol, 3 equiv) was added as an 8:2 solution in AcOH/H_2O (0.7 M). The reaction was allowed to warm to room temperature slowly, then heated to 60 ºC for 5 days. The reaction was quenched with a few drops of EtOH and then carefully neutralized with sat. $NaHCO_3$ solution. The aqueous layer was separated and extracted three times with EtOAc. The combined organic layers were dried with Na_2SO_4, filtered, and concentrated. The crude residue was purified by column chromatography to yield **108** (3.5 mg, 51% yield) in 84% ee as a white solid.

$\mathbf{R}_f$ = 0.33 (silica gel, 20% EtOAc/Hex, UV).

Chiral SFC: (OJ-H, 2.5 mL/min, 20% IPA in CO_2, λ = 254 nm): t_R (major) = 3.7 min, t_R (minor) = 4.0 min.

$\mathbf{[\alpha]_D^{25}}$ = +36.3° (c = 0.8, $CHCl_3$).

^{1}H NMR (500 MHz, $CDCl_3$): δ 8.12 (dd, *J* = 7.8, 1.5 Hz, 1H), 7.47 (td, *J* = 7.5, 1.5 Hz, 1H), 7.39 (dd, *J* = 8.2, 6.6 Hz, 2H), 7.22 (d, *J* = 2.1 Hz, 1H), 6.98 – 6.92 (m, 2H), 4.28 (dd, *J* = 8.2, 4.5 Hz, 1H), 2.77 – 2.60 (m, 2H), 2.48 (ddt, *J* = 13.4, 7.9, 4.6 Hz, 1H), 2.27 (dddd, *J* = 13.5, 9.3, 8.1, 4.5 Hz, 1H).

^{13}C NMR (101 MHz, $CDCl_3$): δ 197.6, 145.0, 144.1, 134.0, 132.9, 132.8, 131.1, 130.8, 130.7, 129.4, 128.1, 127.7, 127.5, 44.7, 36.7, 31.8.

2.6.7 SFC Traces of Racemic and Enantioenriched Products

37 (Table 2.11): racemic

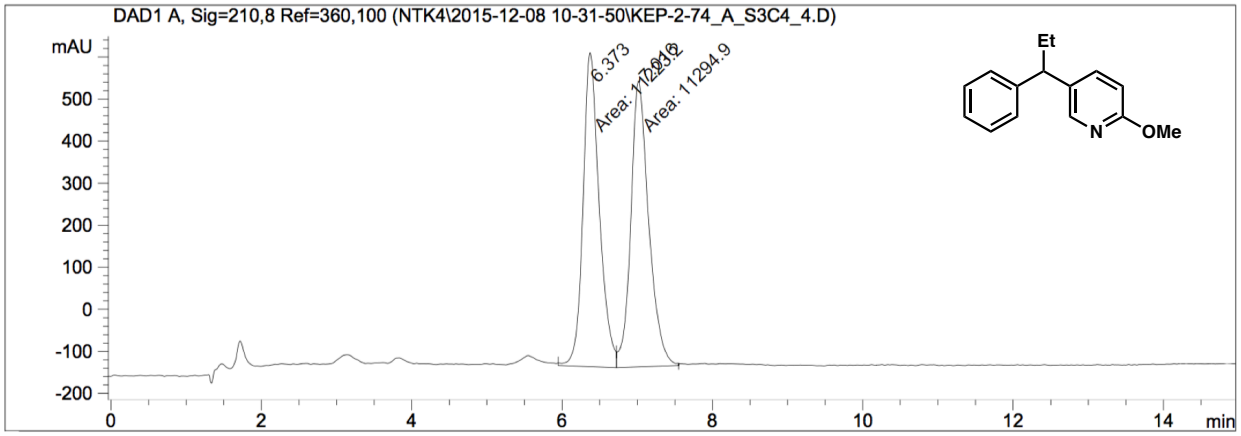

Peak #	RetTime [min]	Type	Width [min]	Area [mAU*s]	Height [mAU]	Area %
1	6.373	MM	0.2504	1.12232e4	746.91840	49.8408
2	7.016	MM	0.2768	1.12949e4	680.19781	50.1592

37 (Table 2.11): enantioenriched, 91% ee

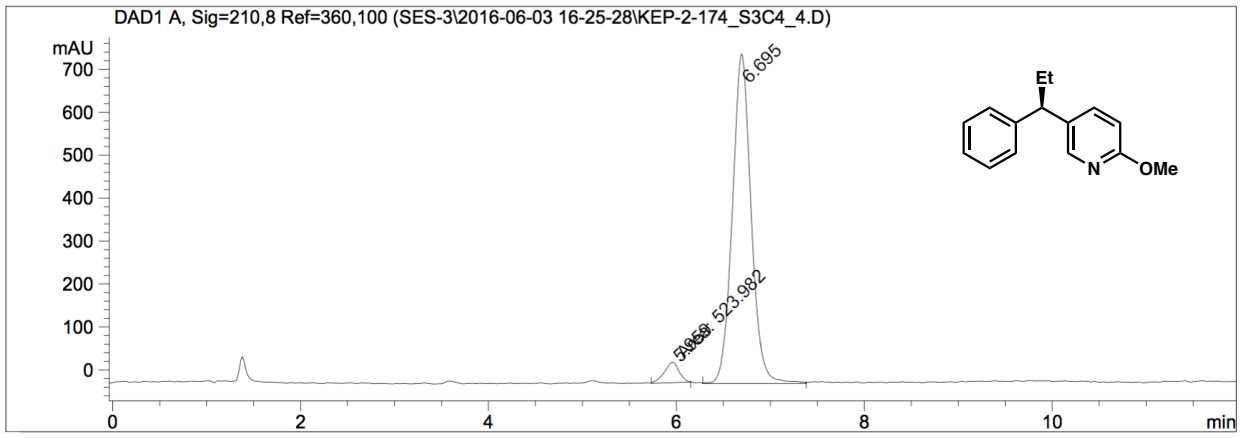

Peak #	RetTime [min]	Type	Width [min]	Area [mAU*s]	Height [mAU]	Area %
1	5.959	MM	0.1834	523.98187	47.63037	4.6799
2	6.695	VV	0.2104	1.06724e4	766.47681	95.3201

77 (Table 2.11): racemic

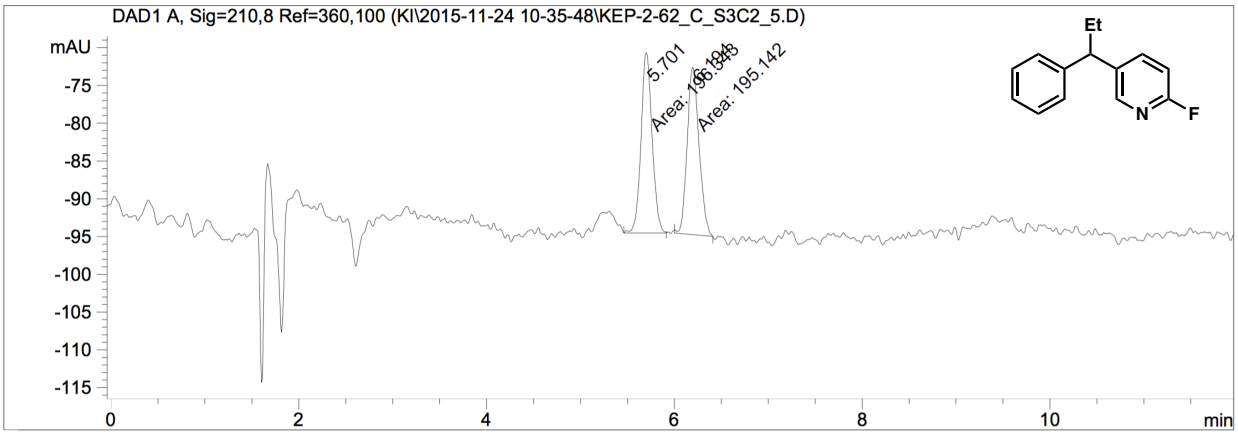

Peak #	RetTime [min]	Type	Width [min]	Area [mAU*s]	Height [mAU]	Area %
1	5.701	MM	0.1369	196.34299	23.90764	50.1534
2	6.194	MM	0.1463	195.14195	22.22900	49.8466

77 (Table 2.11): enantioenriched, 90% ee

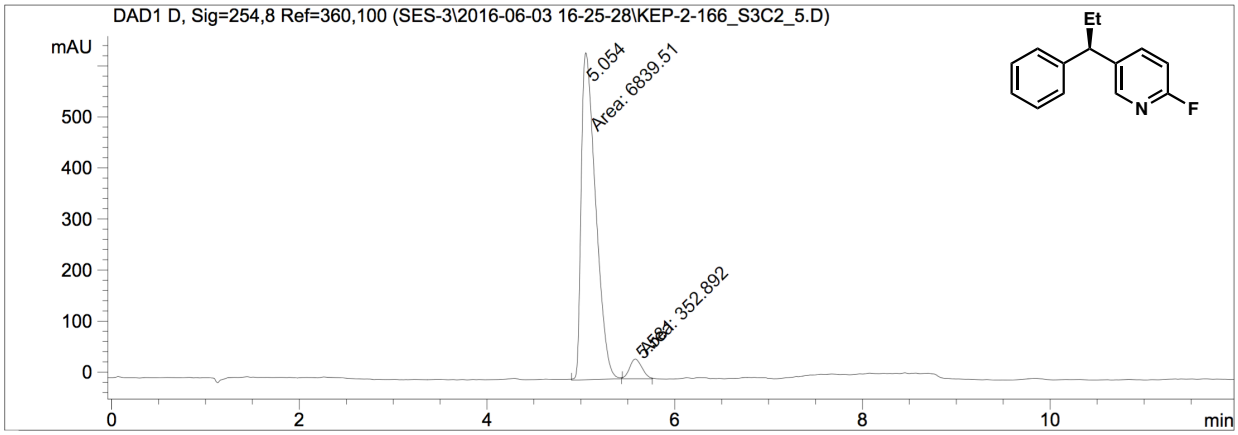

Peak #	RetTime [min]	Type	Width [min]	Area [mAU*s]	Height [mAU]	Area %
1	5.054	MM	0.1774	6839.51270	642.44238	95.0935
2	5.581	MM	0.1514	352.89209	38.86046	4.9065

78 (Table 2.11): racemic

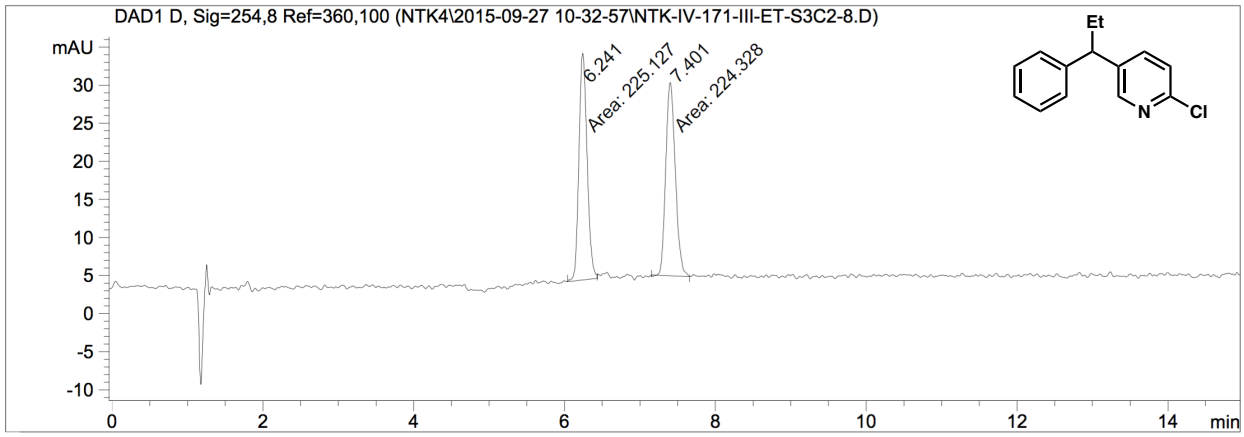

Peak #	RetTime [min]	Type	Width [min]	Area [mAU*s]	Height [mAU]	Area %
1	6.241	MM	0.1258	225.12733	29.83720	50.0889
2	7.401	MM	0.1469	224.32823	25.45803	49.9111

78 (Table 2.11): enantioenriched, 90% ee

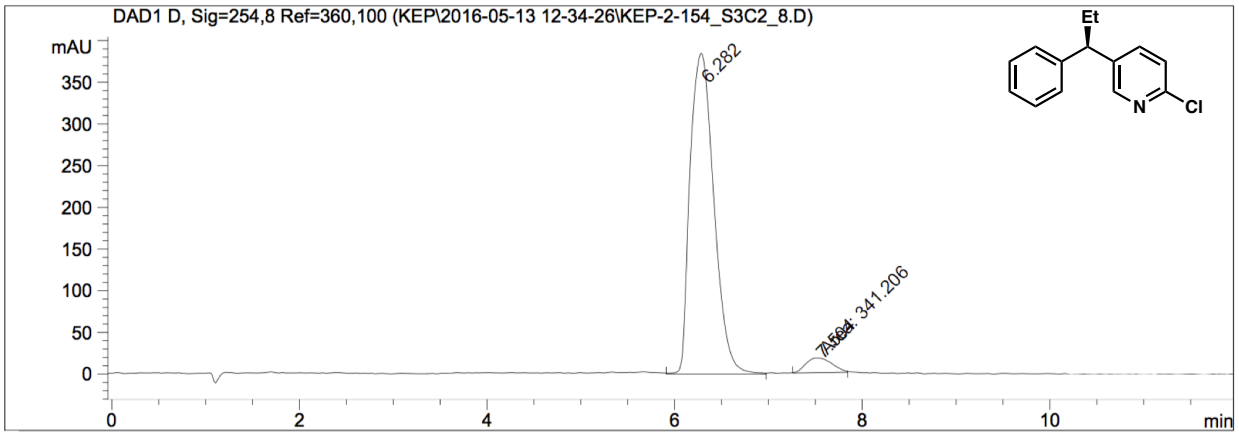

Peak #	RetTime [min]	Type	Width [min]	Area [mAU*s]	Height [mAU]	Area %
1	6.282	VV	0.2864	6799.51318	384.30942	95.2217
2	7.504	MM	0.3222	341.20612	17.64723	4.7783

79 (Table 2.11): racemic

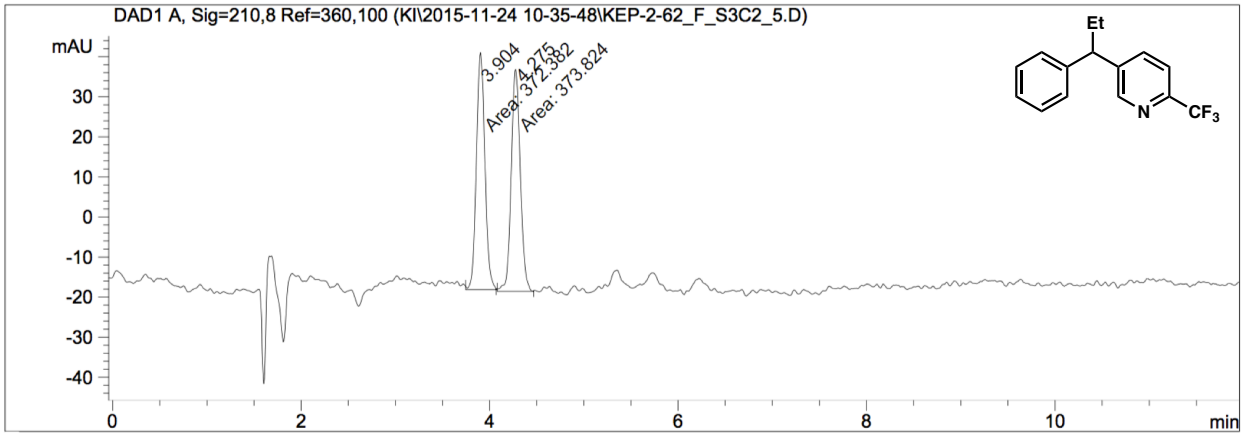

Peak #	RetTime [min]	Type	Width [min]	Area [mAU*s]	Height [mAU]	Area %
1	3.904	MM	0.1045	372.38202	59.37043	49.9034
2	4.275	MM	0.1119	373.82434	55.67645	50.0966

79 (Table 2.11): enantioenriched, 89% ee

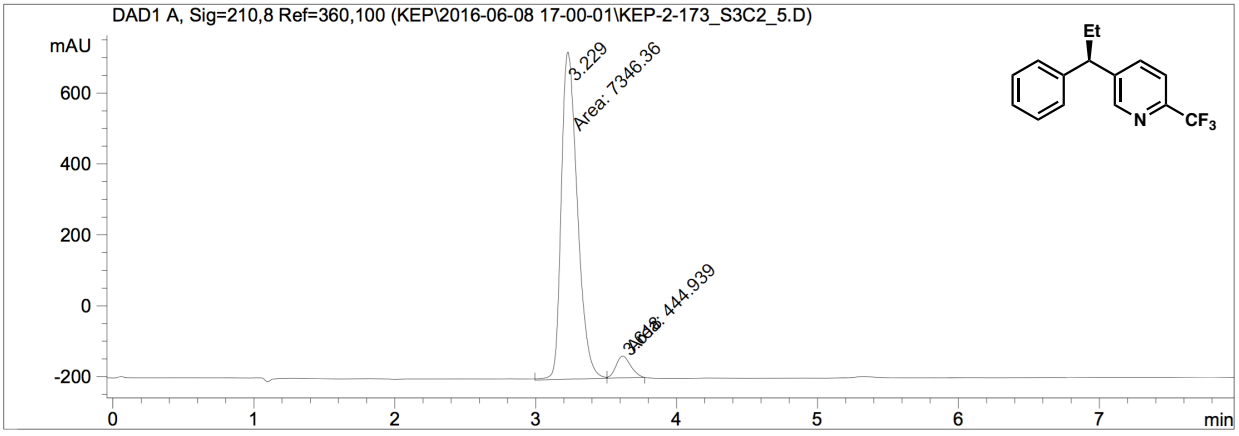

Peak #	RetTime [min]	Type	Width [min]	Area [mAU*s]	Height [mAU]	Area %
1	3.229	MM	0.1321	7346.35645	927.15521	94.2893
2	3.618	MM	0.1200	444.93854	61.81540	5.7107

80 (Table 2.11): racemic

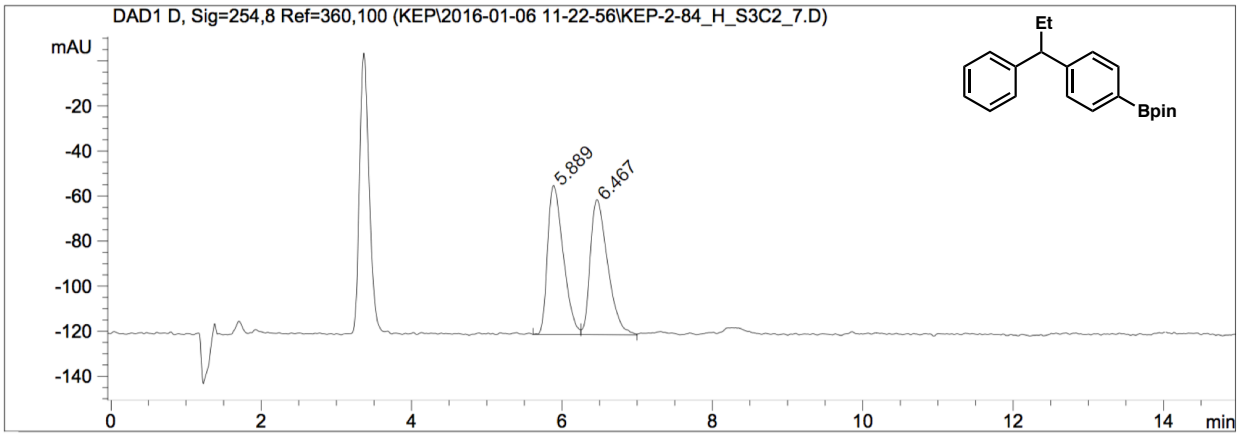

Peak #	RetTime [min]	Type	Width [min]	Area [mAU*s]	Height [mAU]	Area %
1	5.889	VV	0.2207	955.90326	66.10567	49.7597
2	6.467	VV	0.2441	965.13409	59.86779	50.2403

80 (Table 2.11): enantioenriched, 83% ee

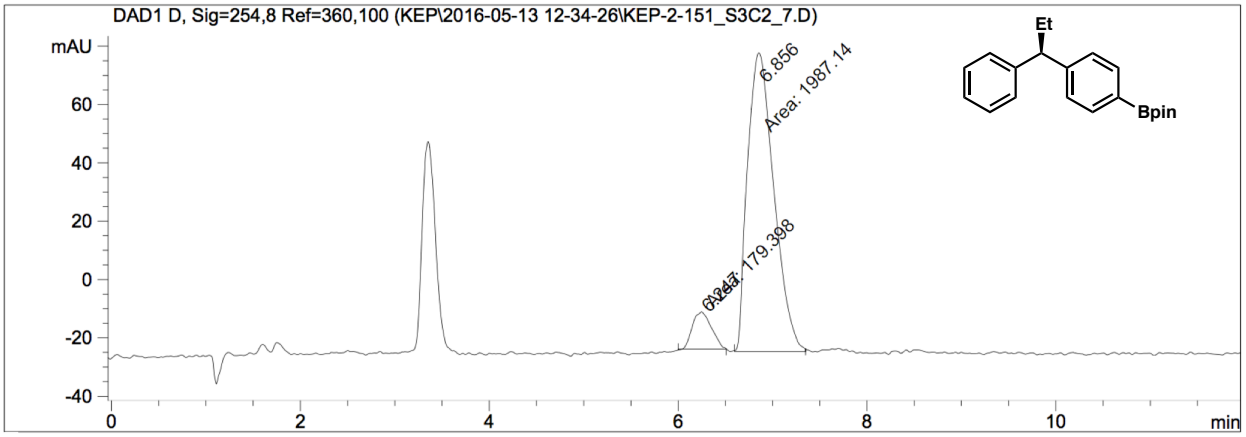

Peak #	RetTime [min]	Type	Width [min]	Area [mAU*s]	Height [mAU]	Area %
1	6.247	MM	0.2335	179.39758	12.80240	8.2804
2	6.856	MM	0.3232	1987.13965	102.47388	91.7196

81 (Table 2.11): racemic

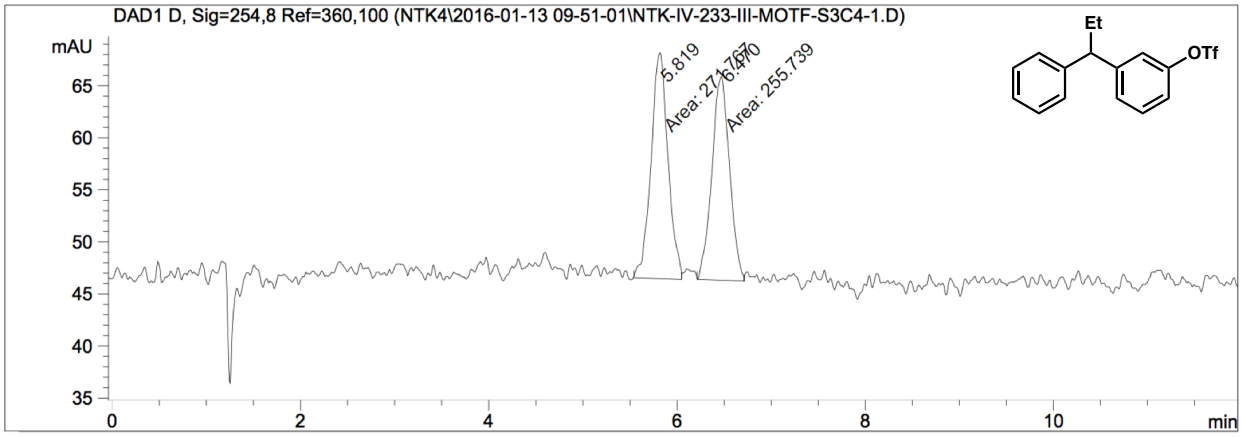

Peak #	RetTime [min]	Type	Width [min]	Area [mAU*s]	Height [mAU]	Area %
1	5.819	MM	0.2081	271.76694	21.76966	51.5192
2	6.470	MM	0.2176	255.73871	19.59052	48.4808

81 (Table 2.11): enantioenriched, 92% ee

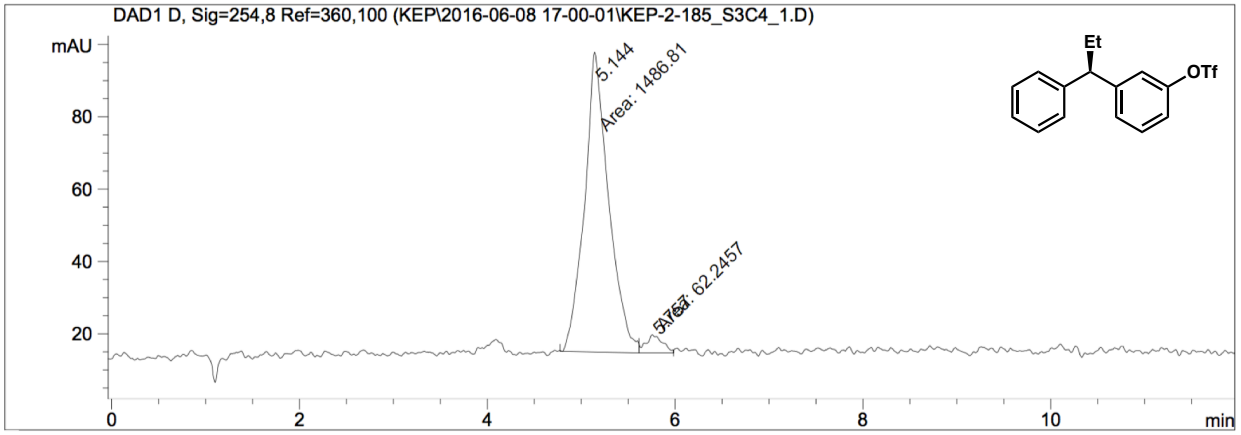

Peak #	RetTime [min]	Type	Width [min]	Area [mAU*s]	Height [mAU]	Area %
1	5.144	MM	0.2987	1486.80554	82.96041	95.9817
2	5.757	MM	0.2035	62.24570	5.09879	4.0183

82 (Table 2.11): racemic

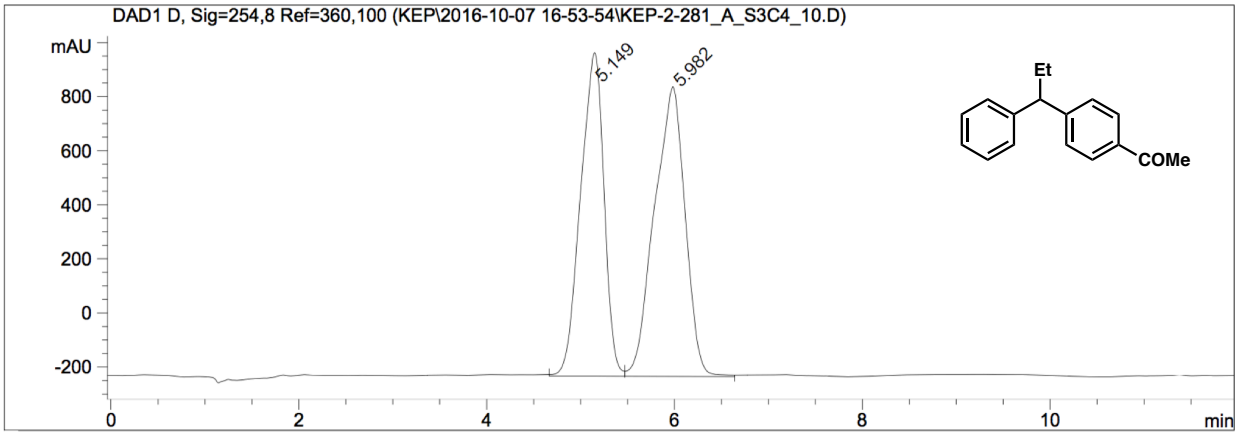

Peak #	RetTime [min]	Type	Width [min]	Area [mAU*s]	Height [mAU]	Area %
1	5.149	BV	0.2507	2.07723e4	1195.55908	46.0237
2	5.982	VV	0.3254	2.43617e4	1070.94434	53.9763

82 (Table 2.11): enantioenriched, 85% ee

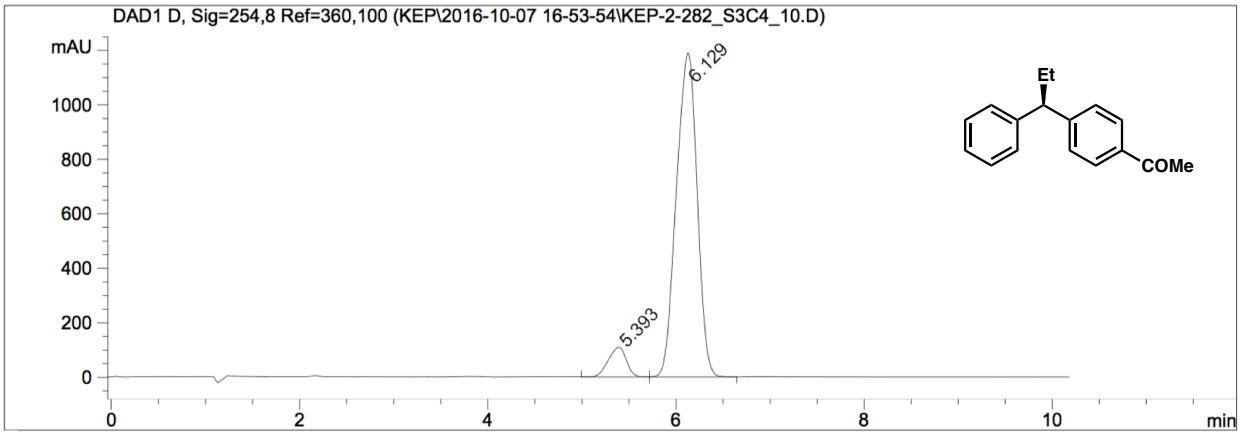

Peak #	RetTime [min]	Type	Width [min]	Area [mAU*s]	Height [mAU]	Area %
1	5.393	VV	0.2171	1477.27429	109.68082	7.4706
2	6.129	VV	0.2515	1.82972e4	1189.54590	92.5294

83 (Table 2.11): racemic

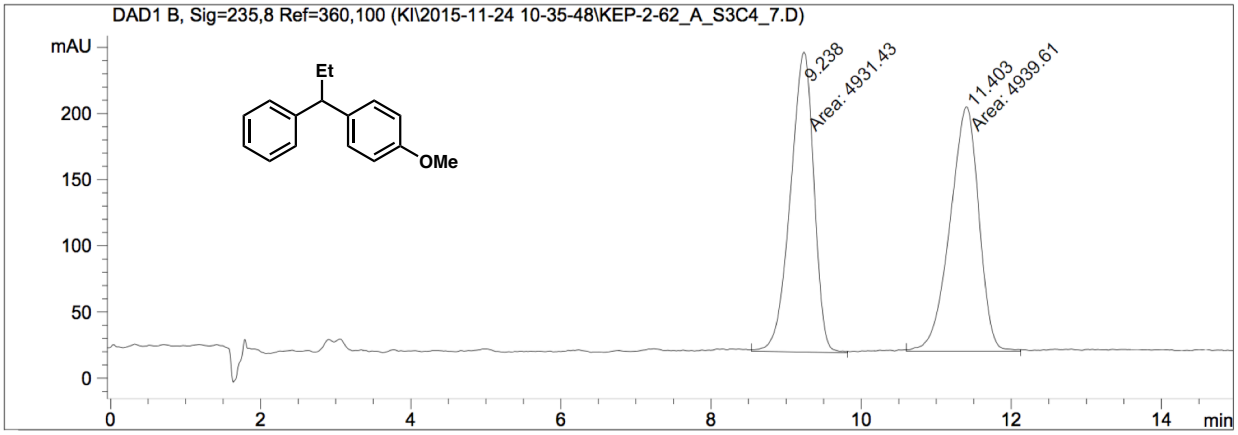

Peak #	RetTime [min]	Type	Width [min]	Area [mAU*s]	Height [mAU]	Area %
1	9.238	MM	0.3626	4931.42871	226.65631	49.9586
2	11.403	MM	0.4456	4939.61035	184.75740	50.0414

83 (Table 2.11): enantioenriched, 83% ee

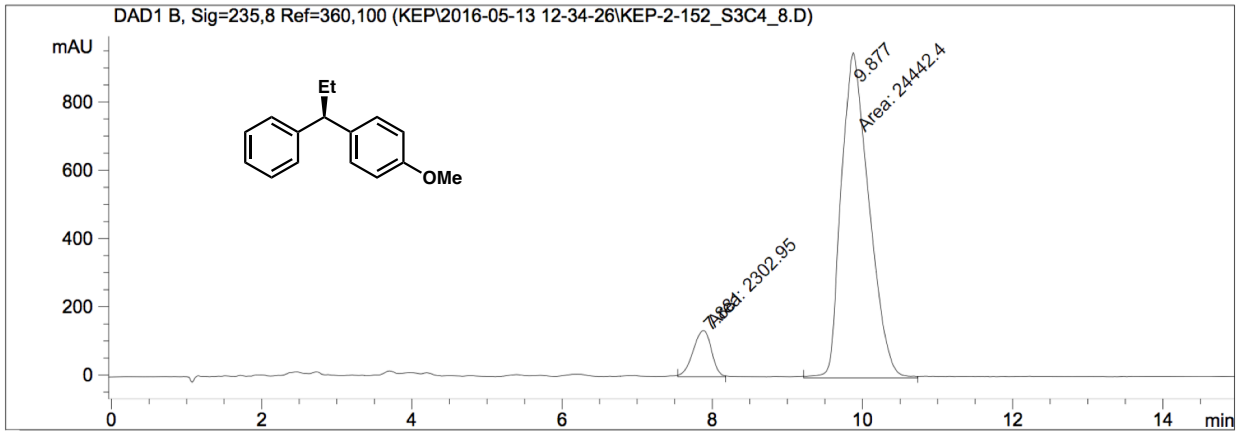

Peak #	RetTime [min]	Type	Width [min]	Area [mAU*s]	Height [mAU]	Area %
1	7.881	MM	0.2840	2302.95239	135.16910	8.6107
2	9.877	MM	0.4275	2.44424e4	952.97052	91.3893

84 (Table 2.11): racemic

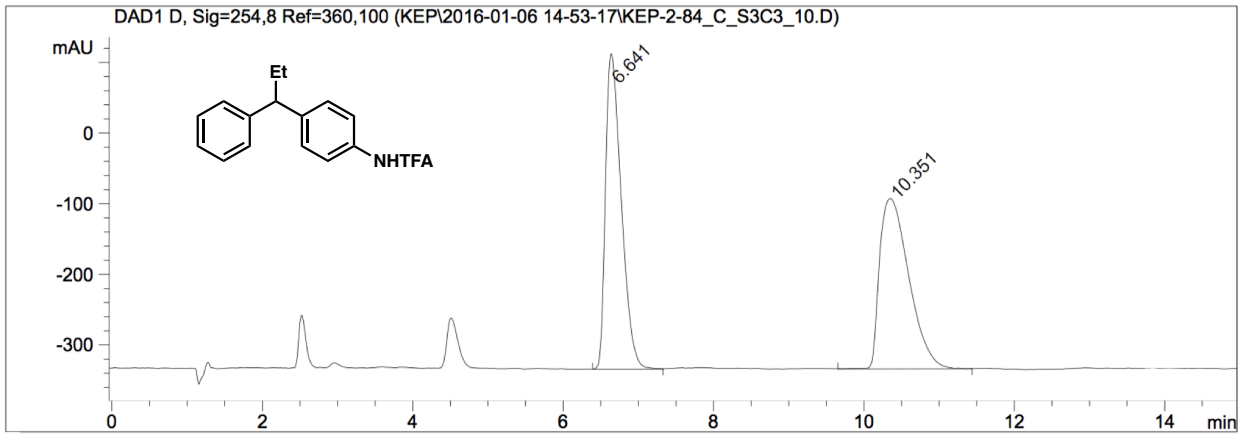

Peak #	RetTime [min]	Type	Width [min]	Area [mAU*s]	Height [mAU]	Area %
1	6.641	BV	0.2264	6517.64551	446.31766	49.9606
2	10.351	VB	0.4237	6527.92627	241.27650	50.0394

84 (Table 2.11): enantioenriched, 81% ee

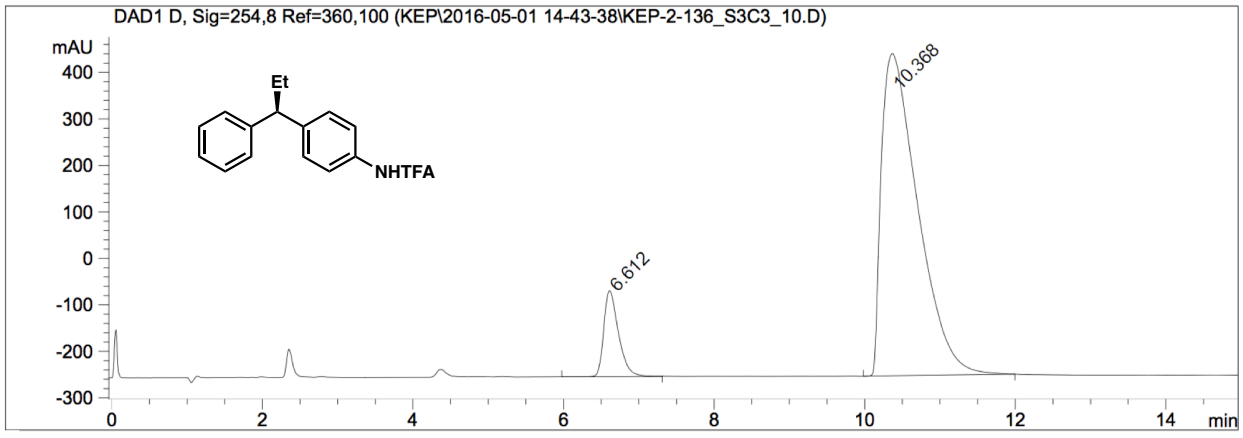

Peak #	RetTime [min]	Type	Width [min]	Area [mAU*s]	Height [mAU]	Area %
1	6.612	BB	0.2070	2511.82178	184.31891	9.7347
2	10.368	BBA	0.5081	2.32909e4	693.00104	90.2653

85 (Table 2.11): racemic

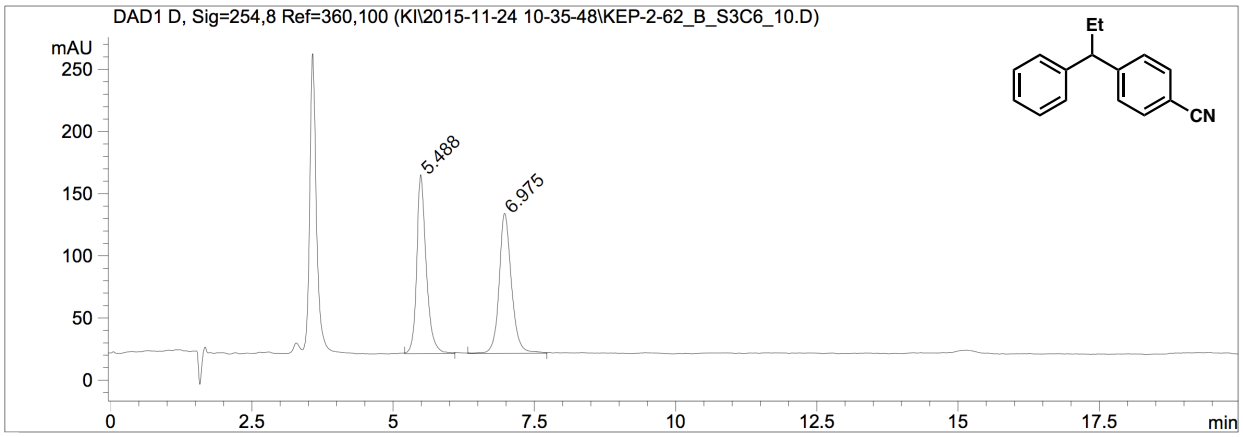

Peak #	RetTime [min]	Type	Width [min]	Area [mAU*s]	Height [mAU]	Area %
1	5.488	BB	0.1723	1681.73132	143.95172	49.4670
2	6.975	BB	0.2300	1717.97205	112.61301	50.5330

85 (Table 2.11): enantioenriched, 89% ee

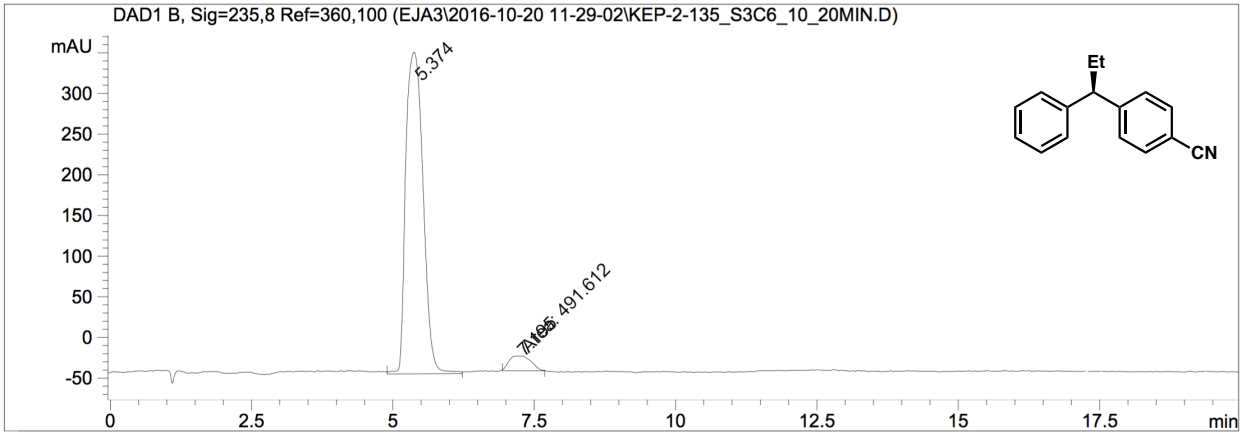

Peak #	RetTime [min]	Type	Width [min]	Area [mAU*s]	Height [mAU]	Area %
1	5.374	VB	0.3534	8457.98047	395.66473	94.5069
2	7.195	MM	0.4480	491.61188	18.28875	5.4931

86 (Table 2.11): racemic

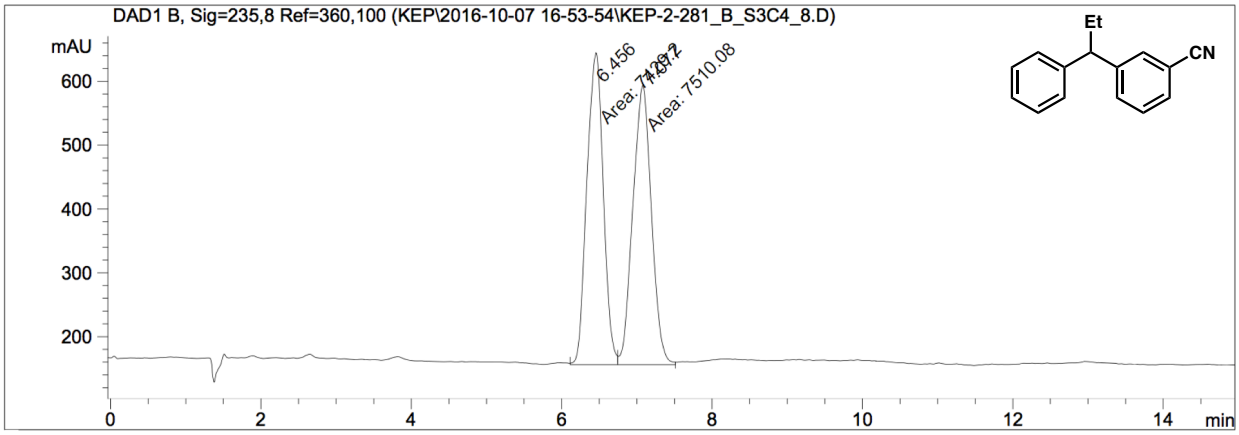

Peak #	RetTime [min]	Type	Width [min]	Area [mAU*s]	Height [mAU]	Area %
1	6.456	MM	0.2532	7429.20215	489.00641	49.7293
2	7.077	MM	0.2859	7510.07861	437.75015	50.2707

86 (Table 2.11): enantioenriched, 88% ee

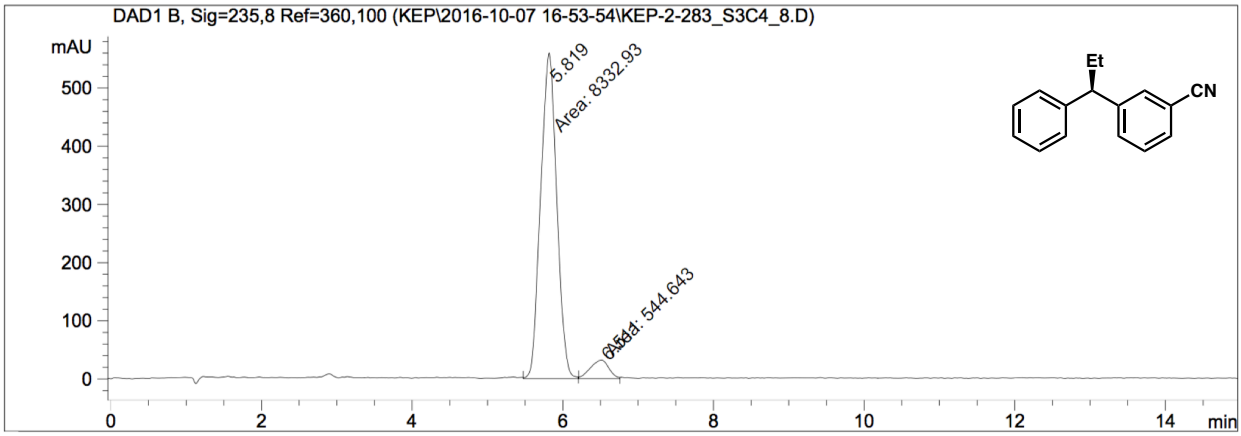

Peak #	RetTime [min]	Type	Width [min]	Area [mAU*s]	Height [mAU]	Area %
1	5.819	MM	0.2480	8332.93457	560.08173	93.8650
2	6.511	MM	0.2832	544.64307	32.05117	6.1350

87 (Table 2.11): racemic

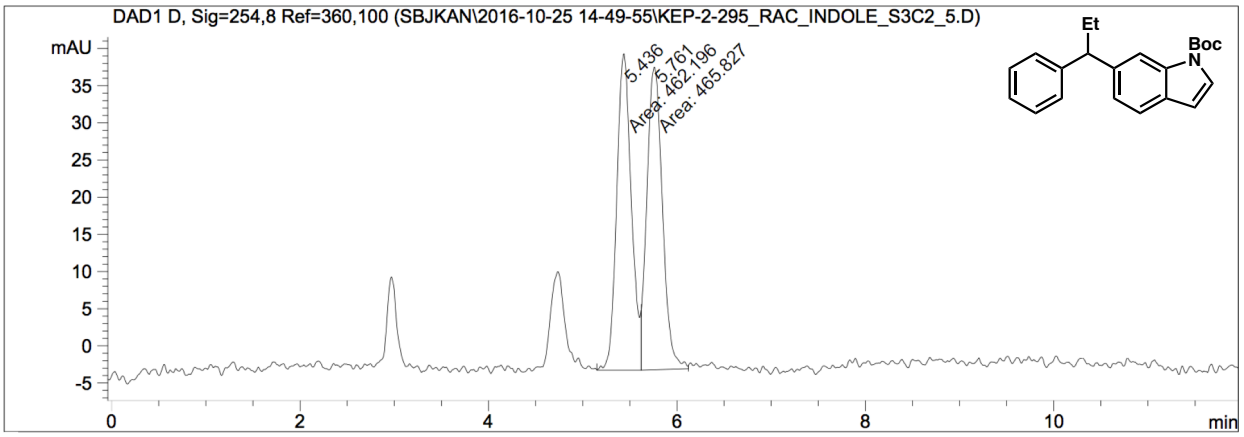

Peak #	RetTime [min]	Type	Width [min]	Area [mAU*s]	Height [mAU]	Area %
1	5.436	MM	0.1806	462.19641	42.65343	49.8044
2	5.761	MM	0.1903	465.82700	40.79035	50.1956

87 (Table 2.11): enantioenriched, 83% ee

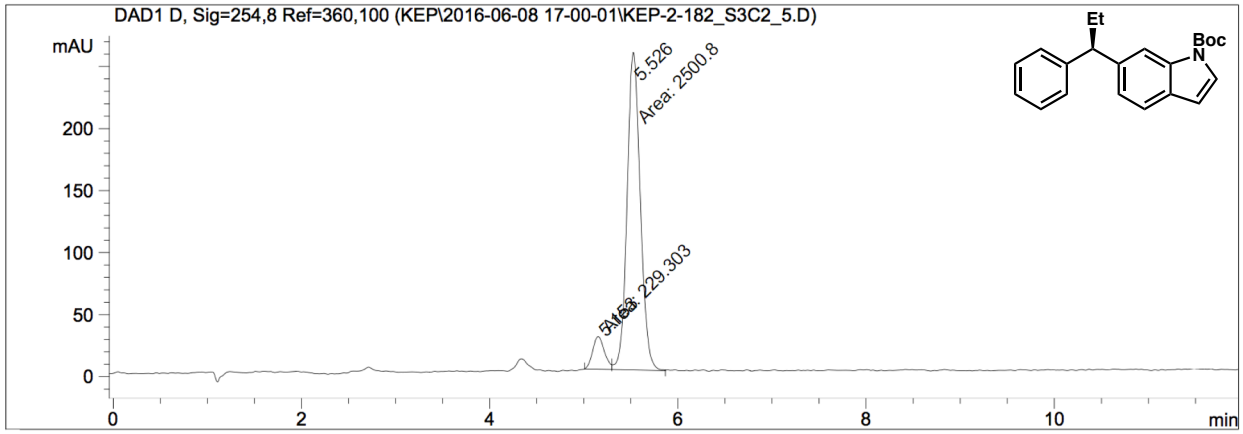

Peak #	RetTime [min]	Type	Width [min]	Area [mAU*s]	Height [mAU]	Area %
1	5.153	MM	0.1447	229.30257	26.41977	8.3991
2	5.526	MM	0.1625	2500.79614	256.55481	91.6009

88 (Table 2.11): racemic

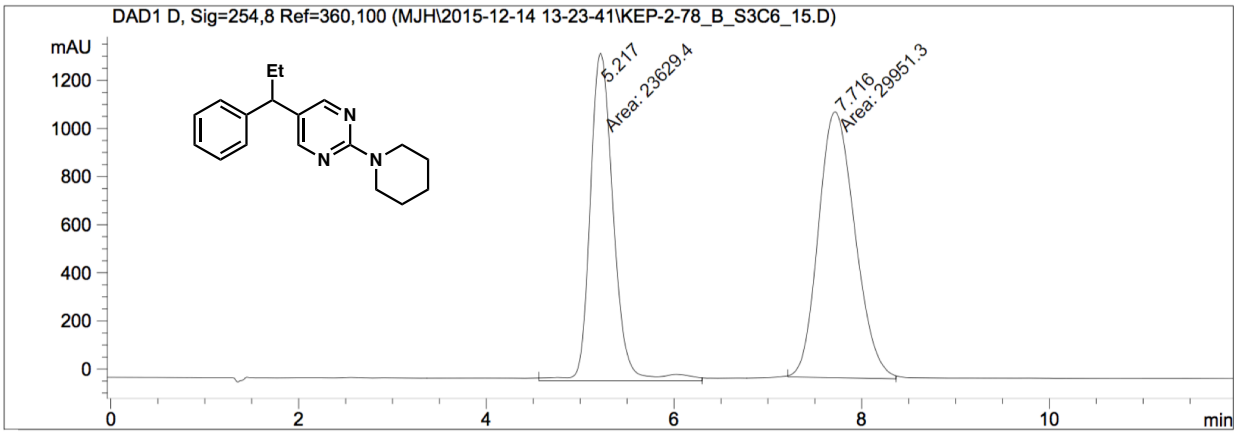

Peak #	RetTime [min]	Type	Width [min]	Area [mAU*s]	Height [mAU]	Area %
1	5.217	MM	0.2890	2.36294e4	1362.55078	44.1005
2	7.716	MM	0.4513	2.99513e4	1106.04492	55.8995

88 (Table 2.11): enantioenriched, 90% ee

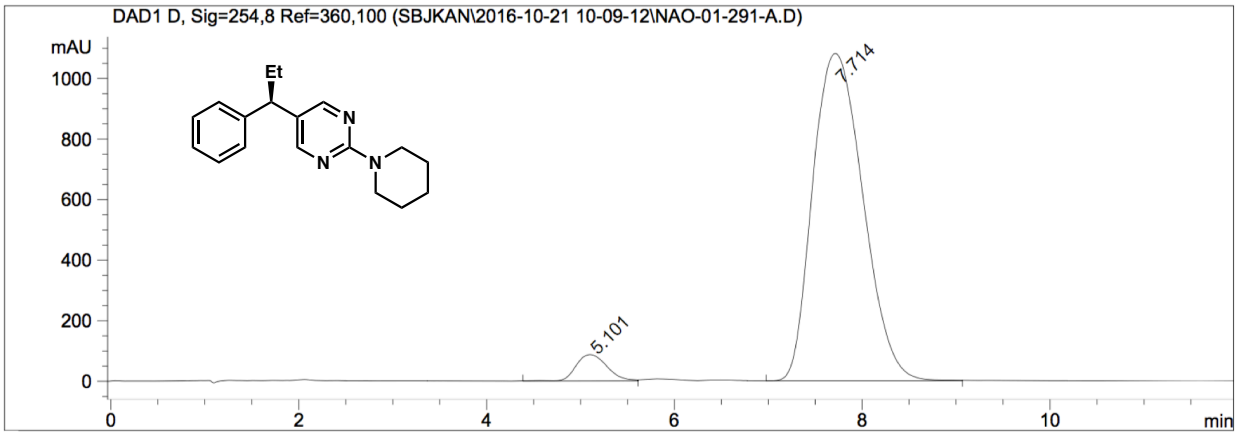

Peak #	RetTime [min]	Type	Width [min]	Area [mAU*s]	Height [mAU]	Area %
1	5.101	BV	0.3693	2020.01782	87.52279	4.7708
2	7.714	VB	0.6029	4.03216e4	1081.54956	95.2292

89 (Table 2.11): racemic

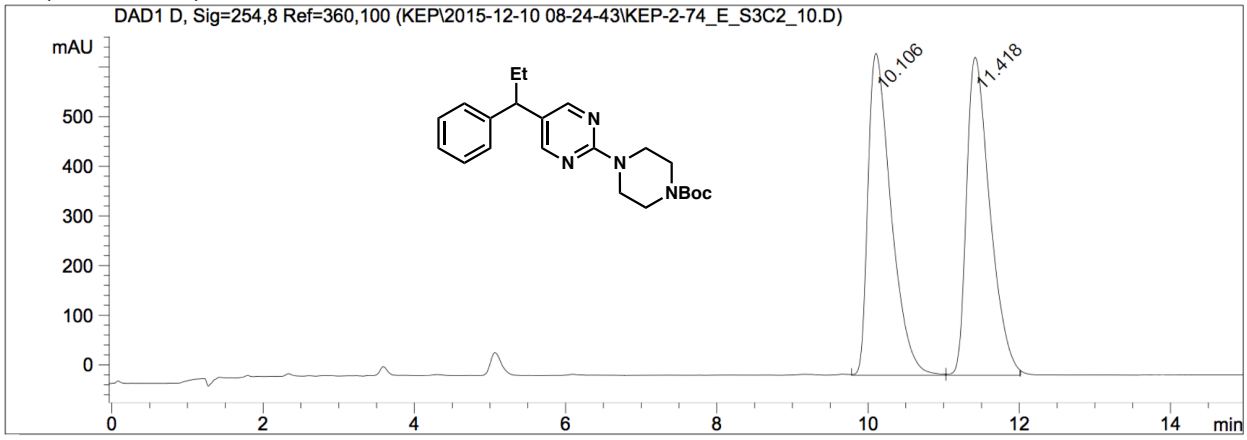

Peak #	RetTime [min]	Type	Width [min]	Area [mAU*s]	Height [mAU]	Area %
1	10.106	VV	0.3197	1.37647e4	648.30176	49.9751
2	11.418	VBA	0.3269	1.37784e4	640.60486	50.0249

89 (Table 2.11): enantioenriched, 91% ee

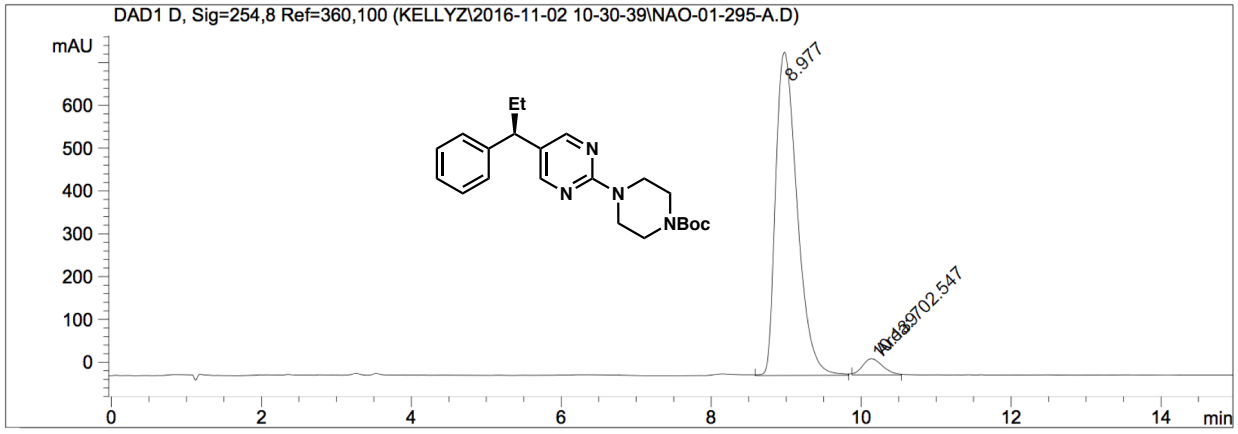

Peak #	RetTime [min]	Type	Width [min]	Area [mAU*s]	Height [mAU]	Area %
1	8.977	VV	0.3132	1.51019e4	755.54010	95.5548
2	10.139	MM	0.3080	702.54669	38.01196	4.4452

90 (Table 2.11): racemic

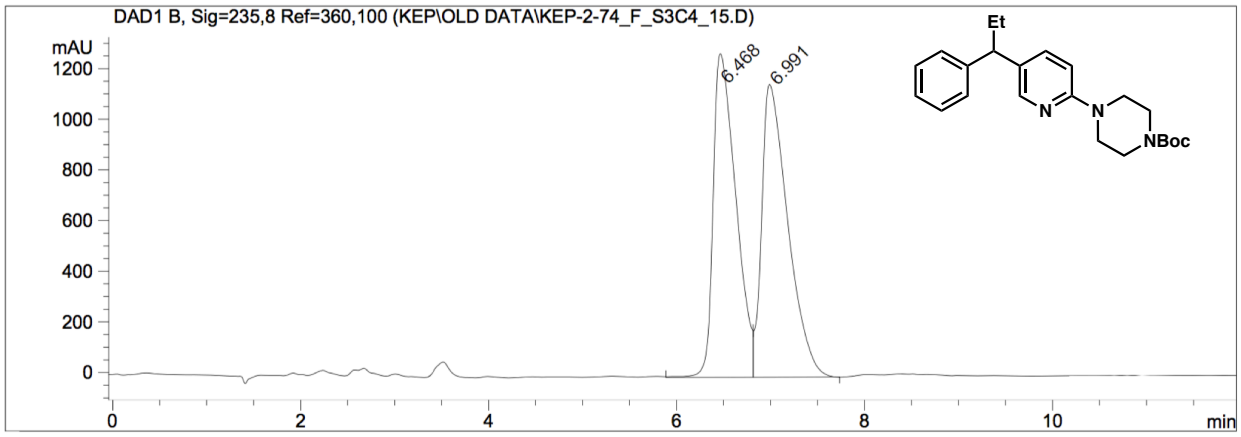

Peak #	RetTime [min]	Type	Width [min]	Area [mAU*s]	Height [mAU]	Area %
1	6.468	VV	0.2635	2.13999e4	1276.86255	48.9552
2	6.991	VV	0.2972	2.23133e4	1155.71497	51.0448

90 (Table 2.11): enantioenriched, 86% ee

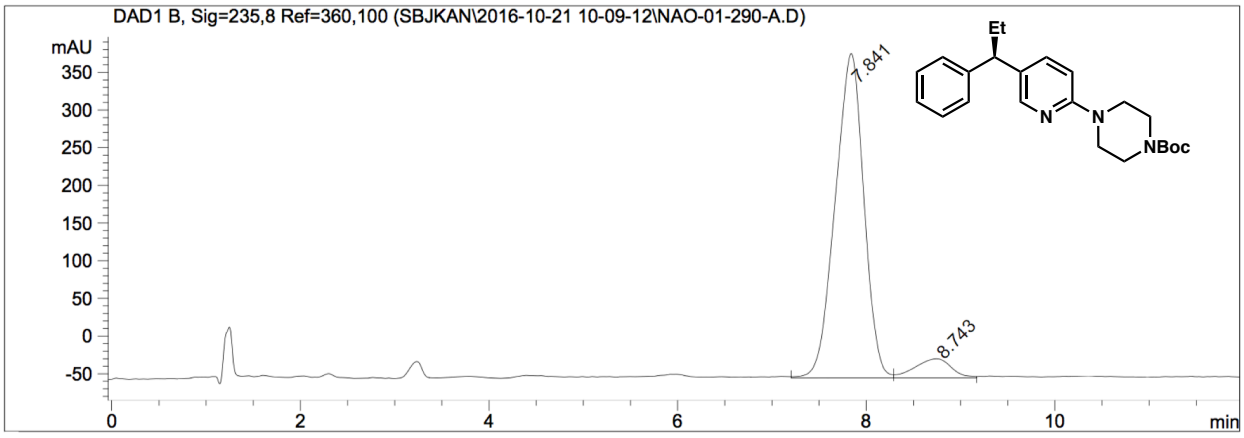

Peak #	RetTime [min]	Type	Width [min]	Area [mAU*s]	Height [mAU]	Area %
1	7.841	VV	0.3143	9084.12988	430.24960	93.1452
2	8.743	VV	0.3678	668.52216	25.34315	6.8548

91 (Table 2.12): racemic

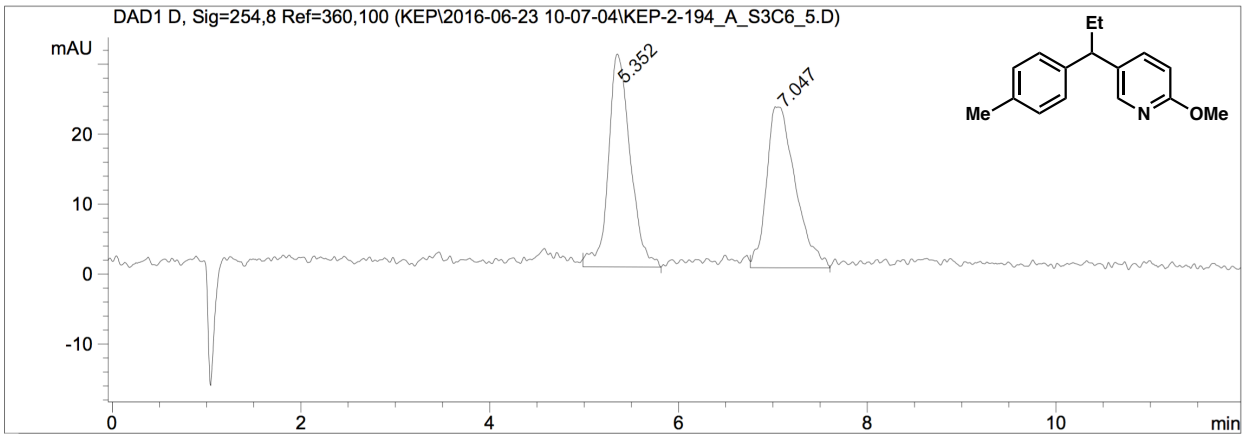

Peak #	RetTime [min]	Type	Width [min]	Area [mAU*s]	Height [mAU]	Area %
1	5.352	BV	0.2486	492.14969	30.44251	50.1656
2	7.047	VV	0.3051	488.90015	22.89762	49.8344

91 (Table 2.12): enantioenriched, 92% ee

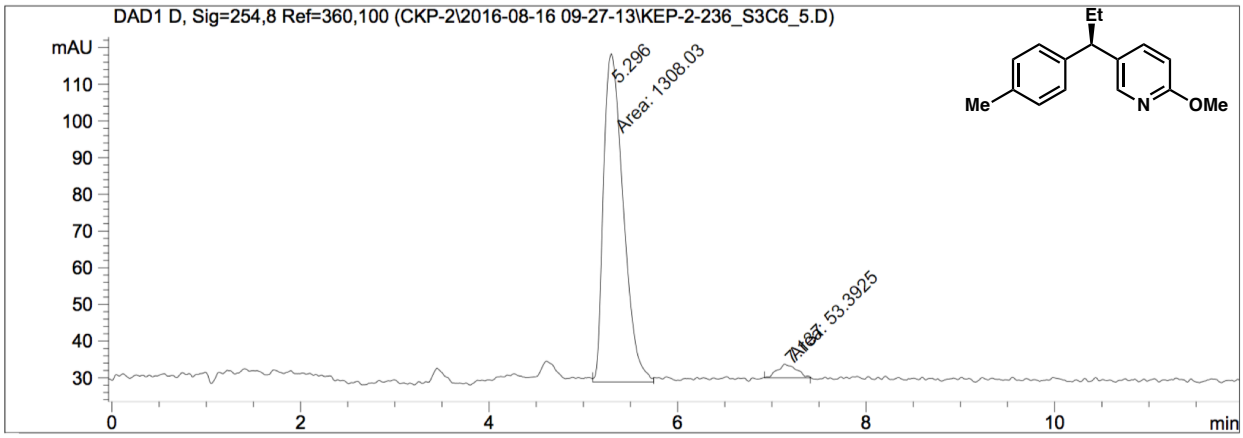

Peak #	RetTime [min]	Type	Width [min]	Area [mAU*s]	Height [mAU]	Area %
1	5.296	MM	0.2436	1308.03101	89.50471	96.0782
2	7.137	MM	0.2348	53.39251	3.78949	3.9218

92 (Table 2.12): racemic

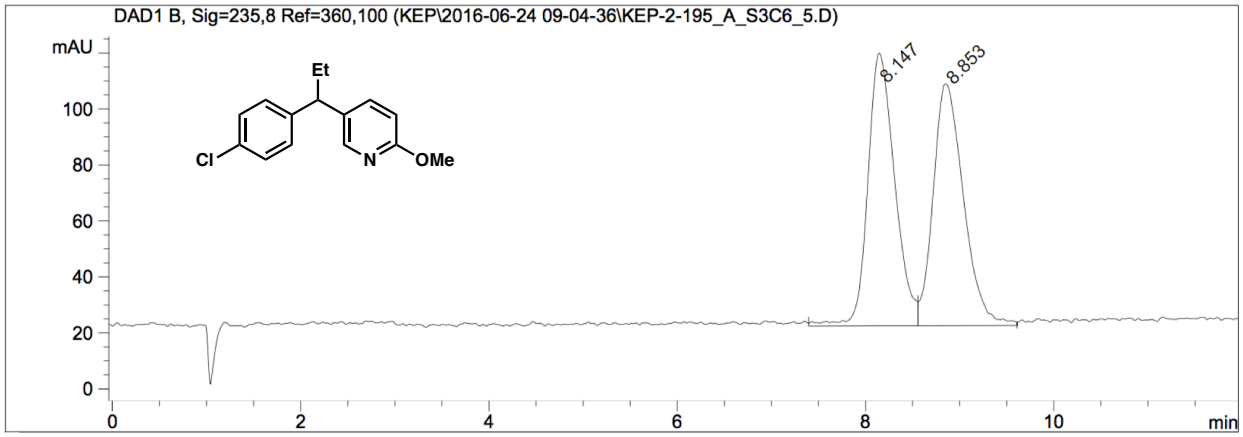

Peak #	RetTime [min]	Type	Width [min]	Area [mAU*s]	Height [mAU]	Area %
1	8.147	VV	0.3041	1937.56421	97.40051	50.0131
2	8.853	VV	0.3496	1936.54773	86.35545	49.9869

92 (Table 2.12): enantioenriched, 85% ee

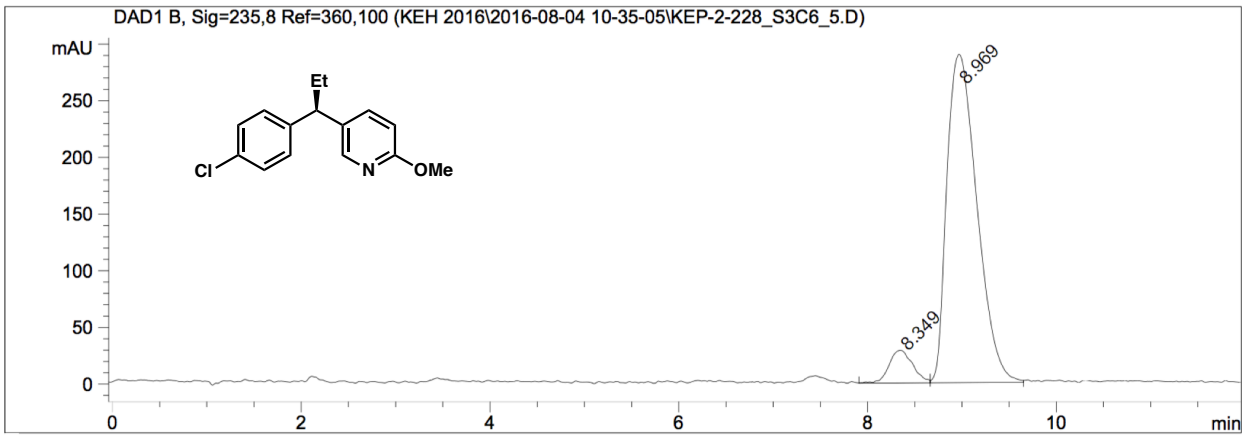

Peak #	RetTime [min]	Type	Width [min]	Area [mAU*s]	Height [mAU]	Area %
1	8.349	VV	0.2592	502.01791	28.81935	7.2551
2	8.969	VV	0.3586	6417.53760	289.55692	92.7449

93 (Table 2.12): racemic

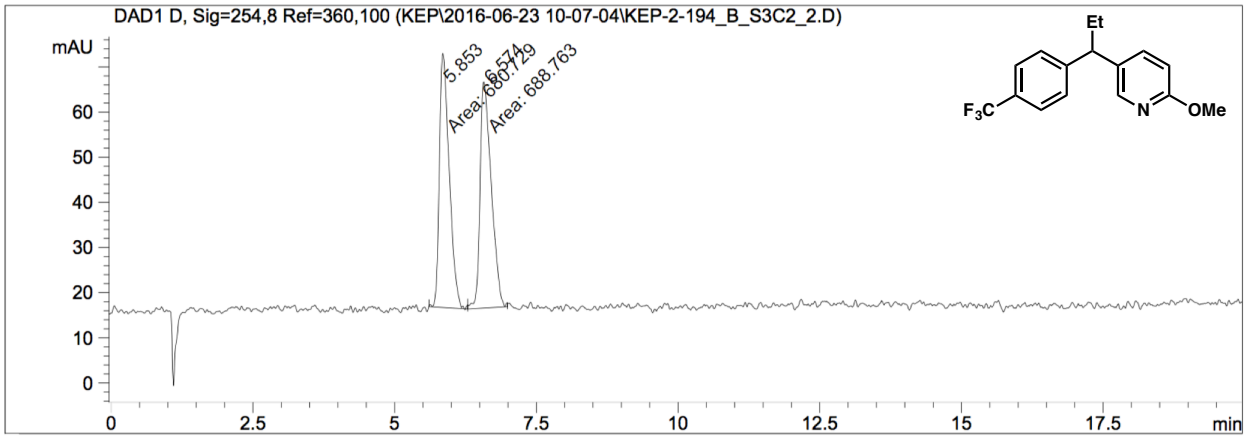

Peak #	RetTime [min]	Type	Width [min]	Area [mAU*s]	Height [mAU]	Area %
1	5.853	MM	0.2014	680.72894	56.33337	49.7067
2	6.574	MM	0.2290	688.76263	50.12506	50.2933

93 (Table 2.12): enantioenriched, 88% ee

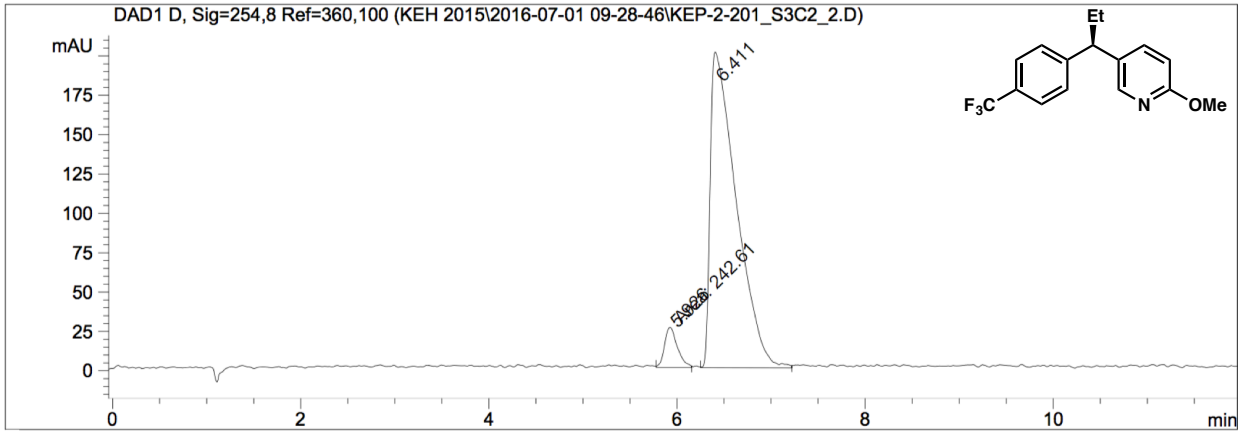

Peak #	RetTime [min]	Type	Width [min]	Area [mAU*s]	Height [mAU]	Area %
1	5.926	MM	0.1586	242.60960	25.49229	5.9009
2	6.411	VV	0.2976	3868.79395	200.08298	94.0991

74 (Table 2.12): racemic

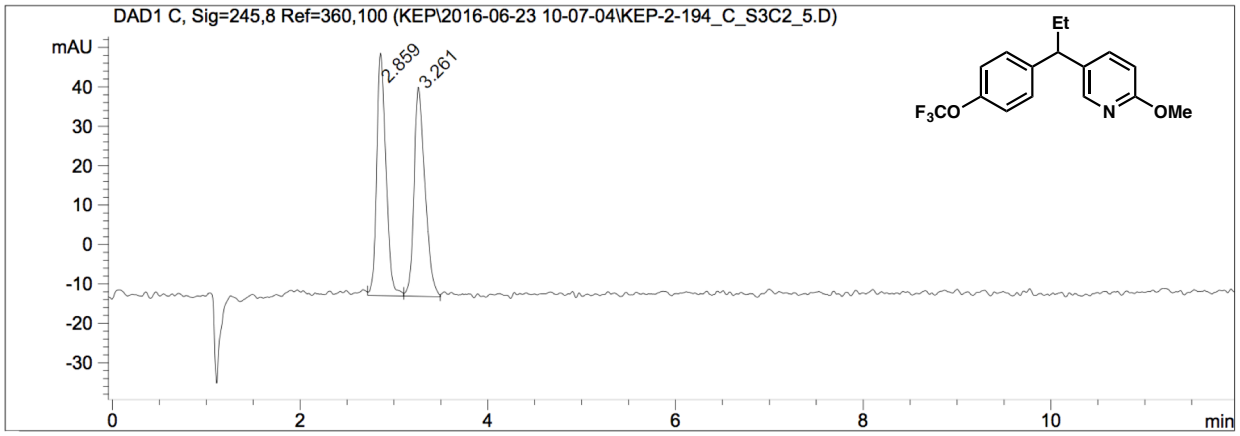

Peak #	RetTime [min]	Type	Width [min]	Area [mAU*s]	Height [mAU]	Area %
1	2.859	VV	0.1043	423.07886	61.46682	49.6391
2	3.261	VV	0.1230	429.23071	52.69527	50.3609

74 (Table 2.12): enantioenriched, 87% ee

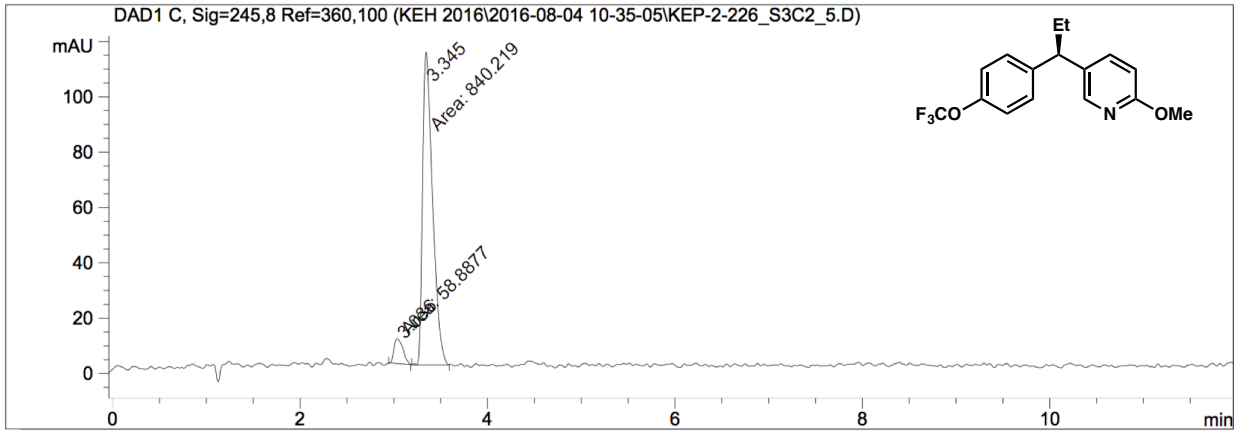

Peak #	RetTime [min]	Type	Width [min]	Area [mAU*s]	Height [mAU]	Area %
1	3.036	MM	0.1085	58.88769	9.04943	6.5496
2	3.345	MM	0.1231	840.21881	113.73206	93.4504

94 (Table 2.12): racemic

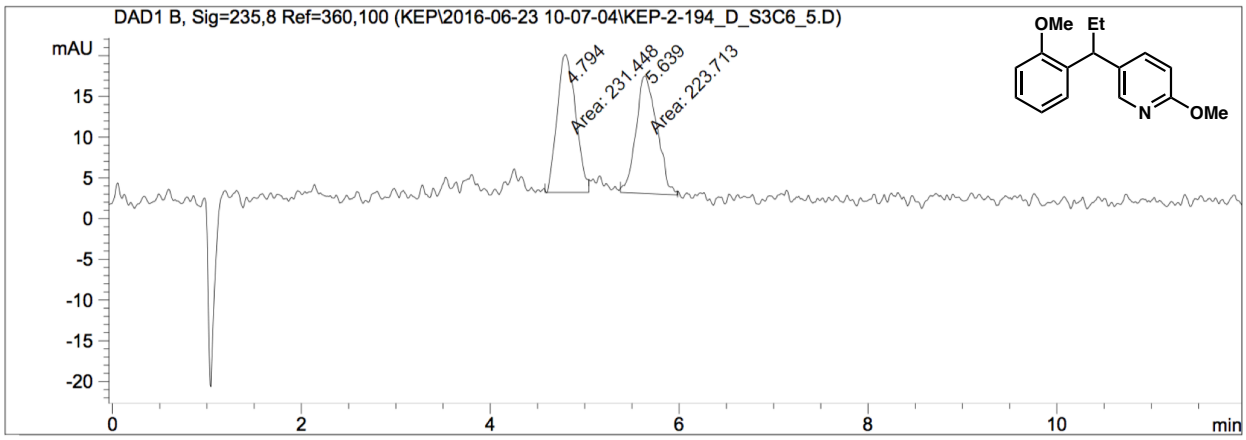

Peak #	RetTime [min]	Type	Width [min]	Area [mAU*s]	Height [mAU]	Area %
1	4.794	MM	0.2277	231.44783	16.93867	50.8497
2	5.639	MM	0.2590	223.71298	14.39786	49.1503

94 (Table 2.12): enantioenriched, 93% ee

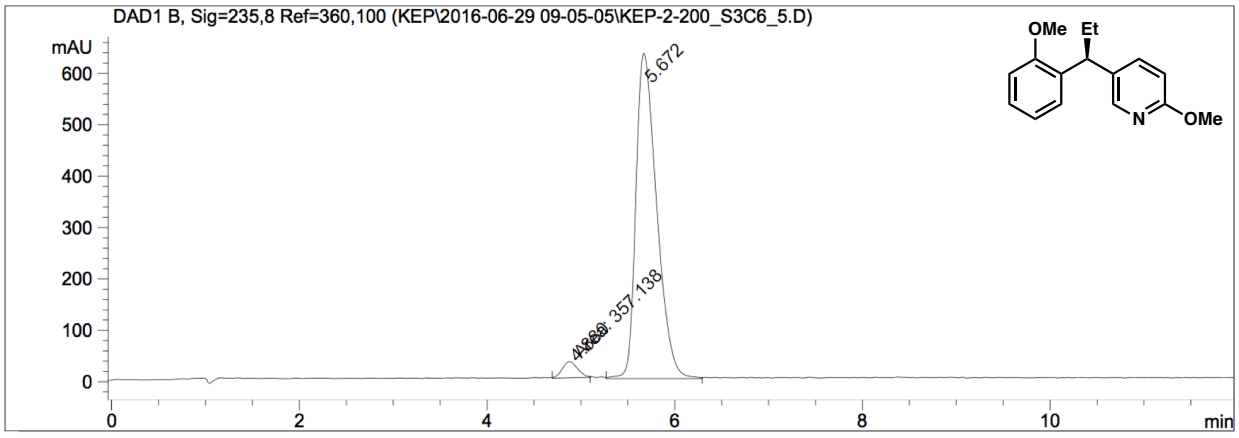

Peak #	RetTime [min]	Type	Width [min]	Area [mAU*s]	Height [mAU]	Area %
1	4.880	MM	0.1875	357.13812	31.74859	3.5278
2	5.672	VV	0.2402	9766.50586	632.42023	96.4722

95 (Table 2.12): racemic

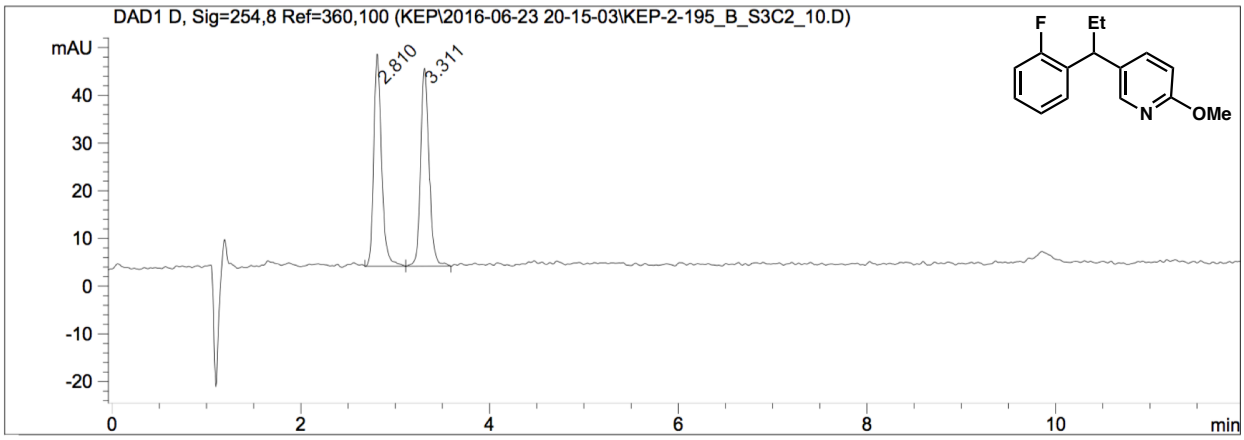

Peak #	RetTime [min]	Type	Width [min]	Area [mAU*s]	Height [mAU]	Area %
1	2.810	VV	0.0924	258.58182	44.11600	49.8675
2	3.311	VV	0.0972	259.95596	41.40617	50.1325

95 (Table 2.12): enantioenriched, 93% ee

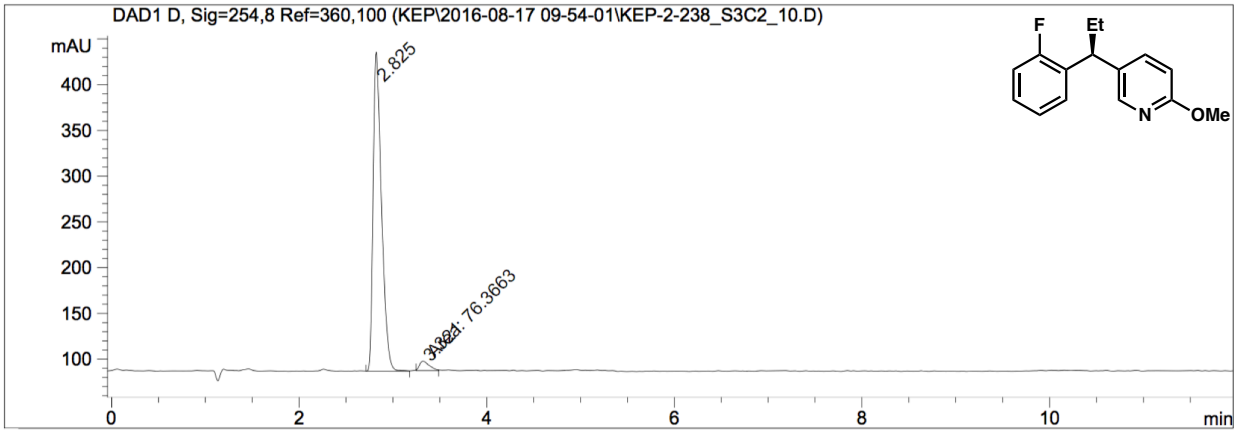

Peak #	RetTime [min]	Type	Width [min]	Area [mAU*s]	Height [mAU]	Area %
1	2.825	BV	0.0976	2180.79883	345.56207	96.6167
2	3.321	MM	0.1201	76.36634	10.59406	3.3833

96 (Table 2.12): racemic

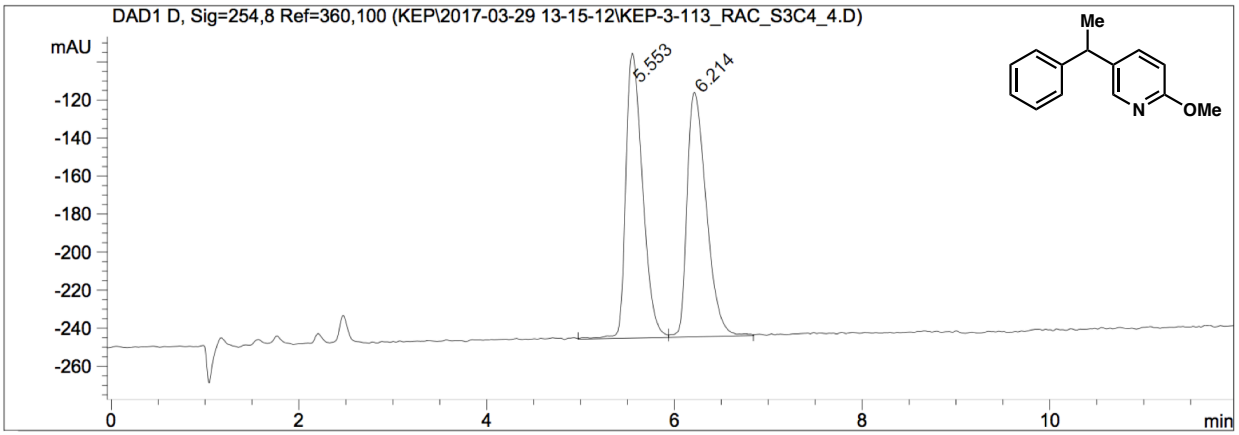

Peak #	RetTime [min]	Type	Width [min]	Area [mAU*s]	Height [mAU]	Area %
1	5.553	VV	0.1927	1857.50623	149.78943	50.2735
2	6.214	VB	0.2189	1837.29578	128.45862	49.7265

96 (Table 2.12): enantioenriched, 85% ee

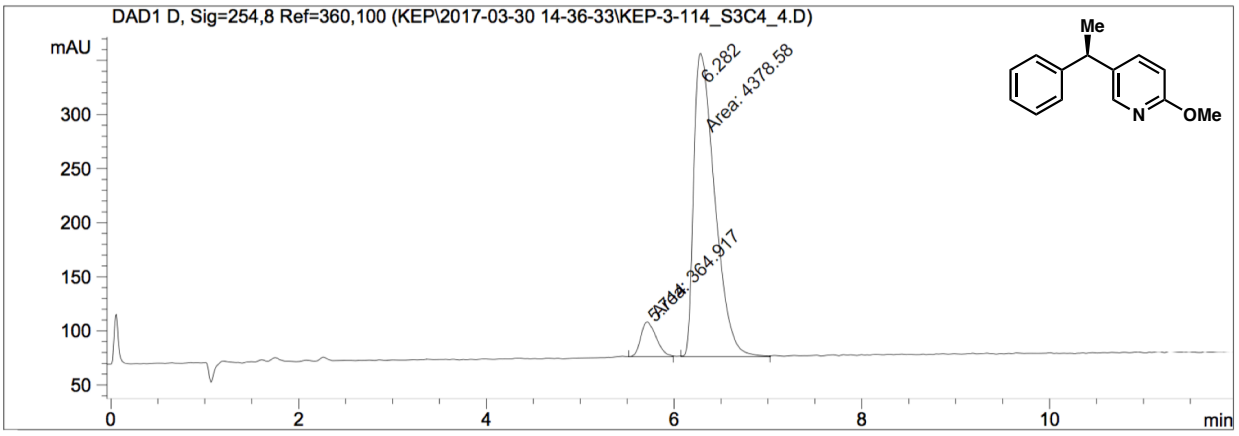

Peak #	RetTime [min]	Type	Width [min]	Area [mAU*s]	Height [mAU]	Area %
1	5.714	MM	0.1896	364.91733	32.08042	7.6930
2	6.282	MM	0.2601	4378.58398	280.57593	92.3070

97 (Table 2.12): racemic

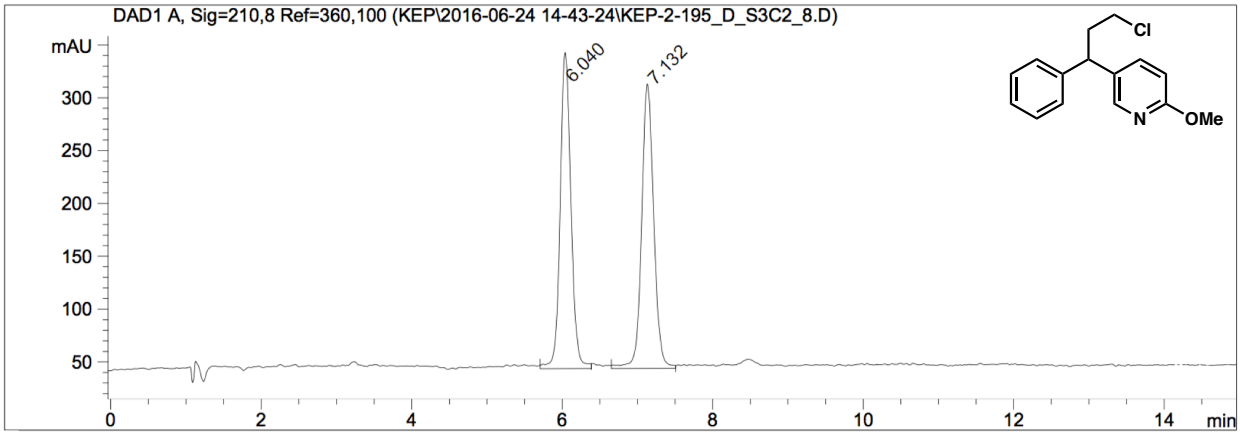

Peak #	RetTime [min]	Type	Width [min]	Area [mAU*s]	Height [mAU]	Area %
1	6.040	BB	0.1525	2986.70654	299.00430	49.6947
2	7.132	BV	0.1751	3023.40210	269.09836	50.3053

97 (Table 2.12): enantioenriched, 91% ee

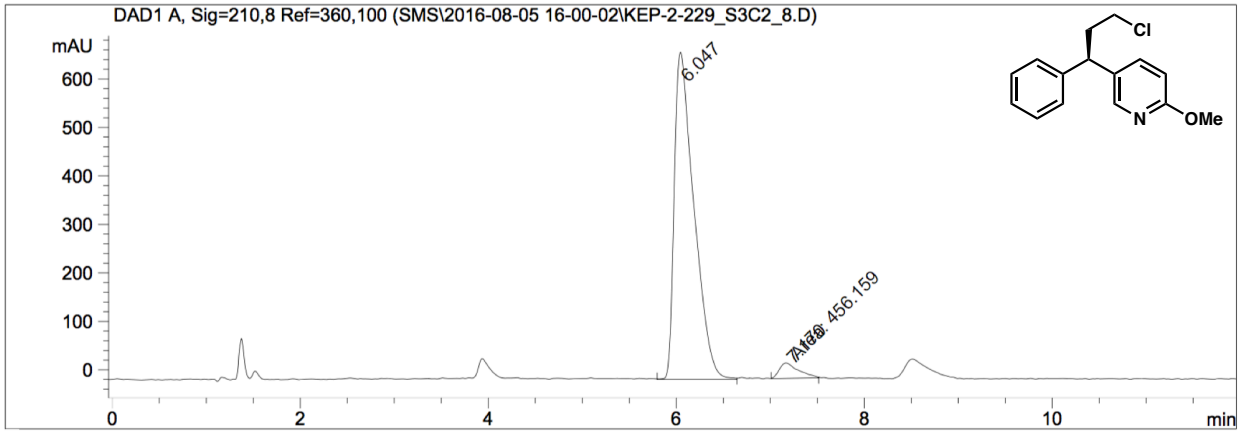

Peak #	RetTime [min]	Type	Width [min]	Area [mAU*s]	Height [mAU]	Area %
1	6.047	VV	0.2136	9809.45703	674.98010	95.5564
2	7.170	MM	0.2386	456.15921	31.86354	4.4436

98 (Table 2.12): racemic

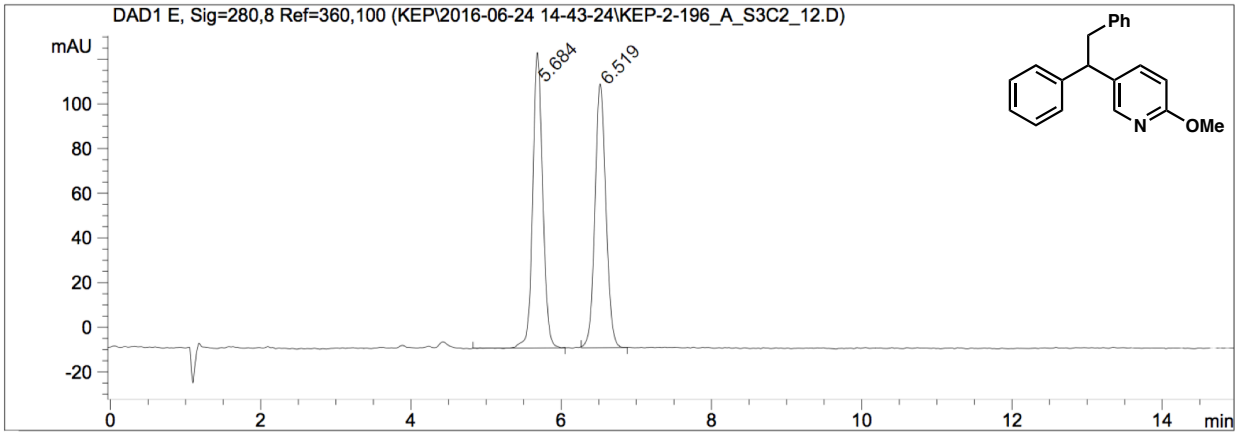

Peak #	RetTime [min]	Type	Width [min]	Area [mAU*s]	Height [mAU]	Area %
1	5.684	BB	0.1400	1223.06287	132.11612	50.4356
2	6.519	BB	0.1549	1201.93628	117.97483	49.5644

98 (Table 2.12): enantioenriched, 95% ee

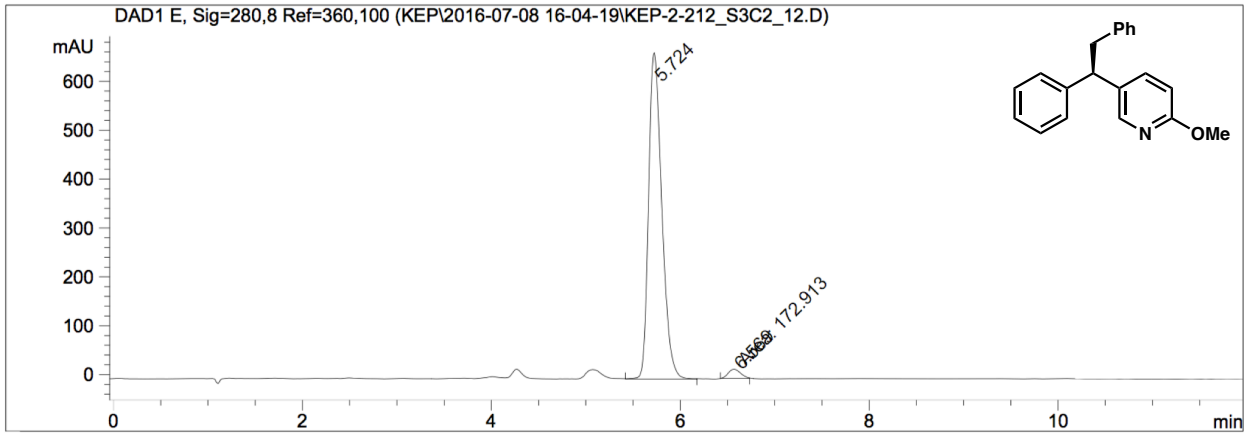

Peak #	RetTime [min]	Type	Width [min]	Area [mAU*s]	Height [mAU]	Area %
1	5.724	VB	0.1539	6510.68408	666.86530	97.4129
2	6.569	MM	0.1529	172.91284	18.84252	2.5871

99 (Table 2.12): racemic

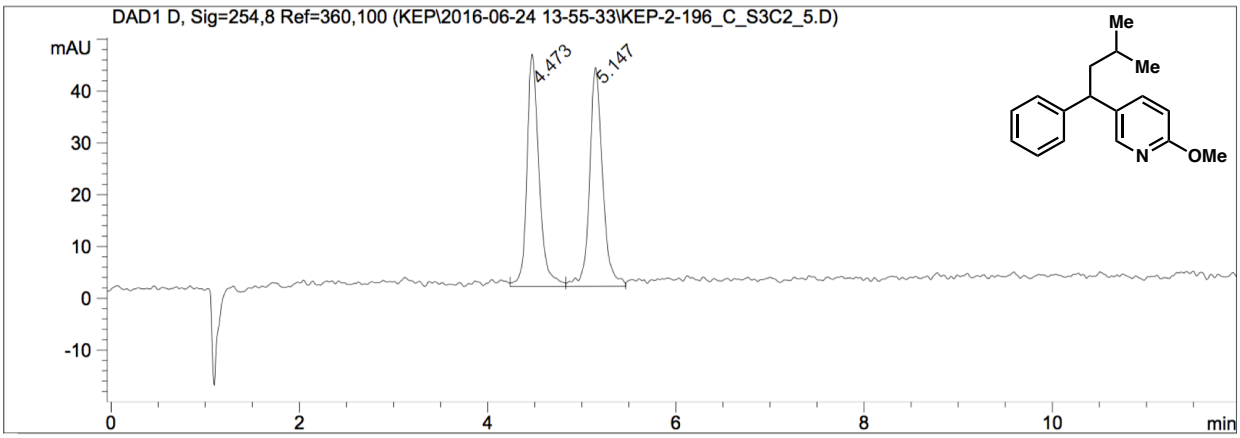

Peak #	RetTime [min]	Type	Width [min]	Area [mAU*s]	Height [mAU]	Area %
1	4.473	VV	0.1366	401.69574	44.82222	49.5490
2	5.147	VV	0.1451	409.00827	42.19704	50.4510

99 (Table 2.12): enantioenriched, 94% ee

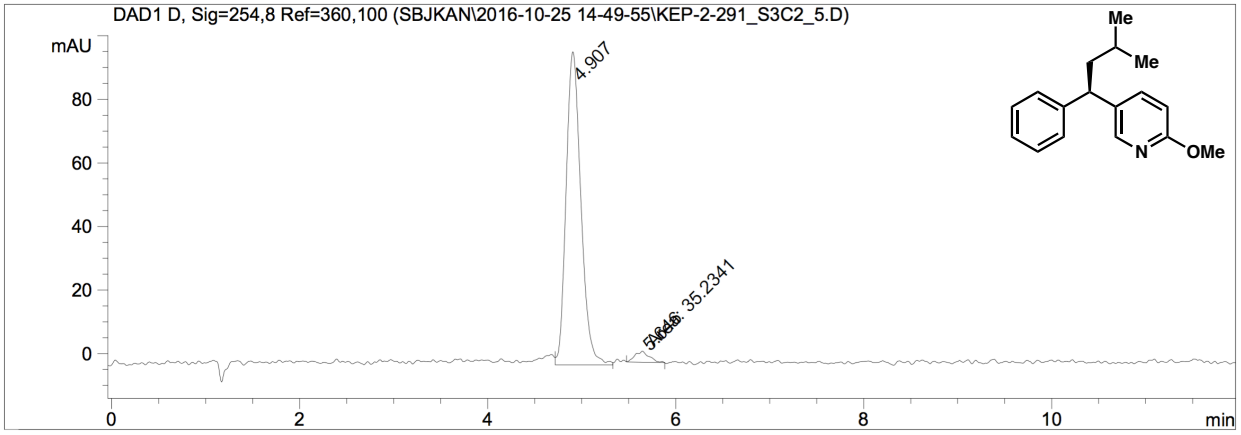

Peak #	RetTime [min]	Type	Width [min]	Area [mAU*s]	Height [mAU]	Area %
1	4.907	VV	0.1682	1080.82678	98.38535	96.8430
2	5.646	MM	0.1665	35.23412	3.52759	3.1570

100 (Table 2.12): racemic

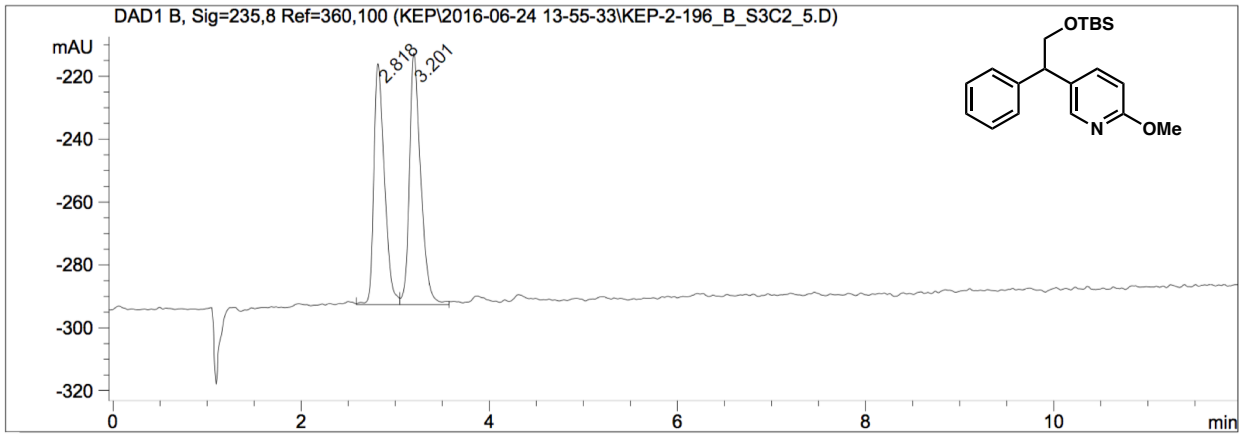

Peak #	RetTime [min]	Type	Width [min]	Area [mAU*s]	Height [mAU]	Area %
1	2.818	VV	0.1240	604.39984	76.62331	47.5039
2	3.201	VB	0.1257	667.91559	79.72723	52.4961

100 (Table 2.12): enantioenriched, 94% ee

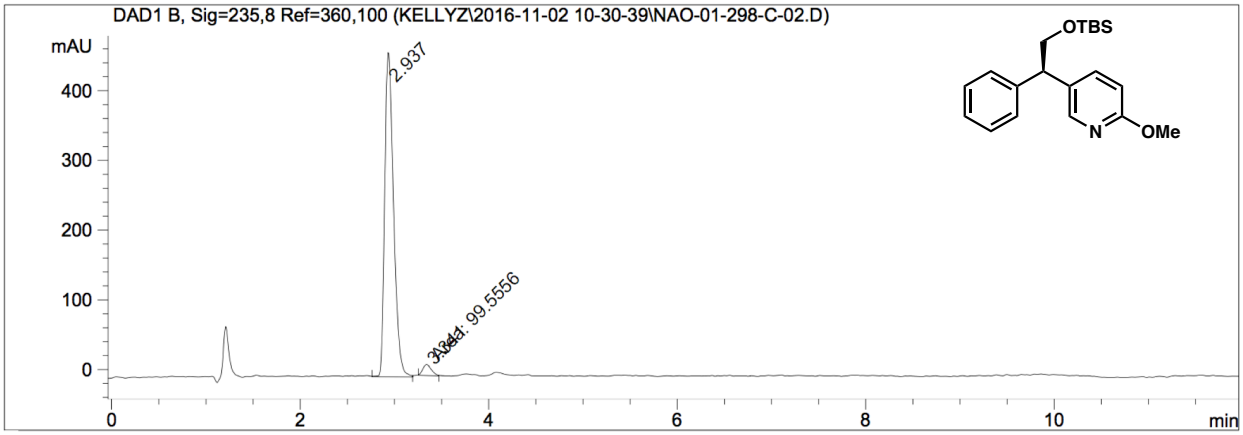

Peak #	RetTime [min]	Type	Width [min]	Area [mAU*s]	Height [mAU]	Area %
1	2.937	VV	0.1042	3032.79883	464.11722	96.8217
2	3.341	MM	0.1058	99.55560	15.68843	3.1783

101 (Table 2.12): racemic

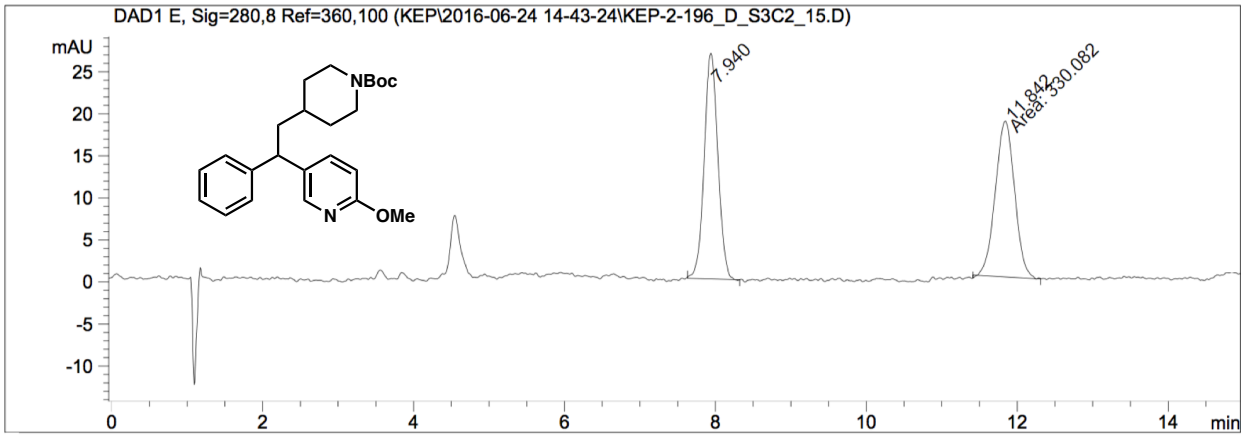

Peak #	RetTime [min]	Type	Width [min]	Area [mAU*s]	Height [mAU]	Area %
1	7.940	BB	0.1953	338.52716	26.80888	50.6315
2	11.842	MM	0.2963	330.08243	18.56997	49.3685

101 (Table 2.12): enantioenriched, 94% ee

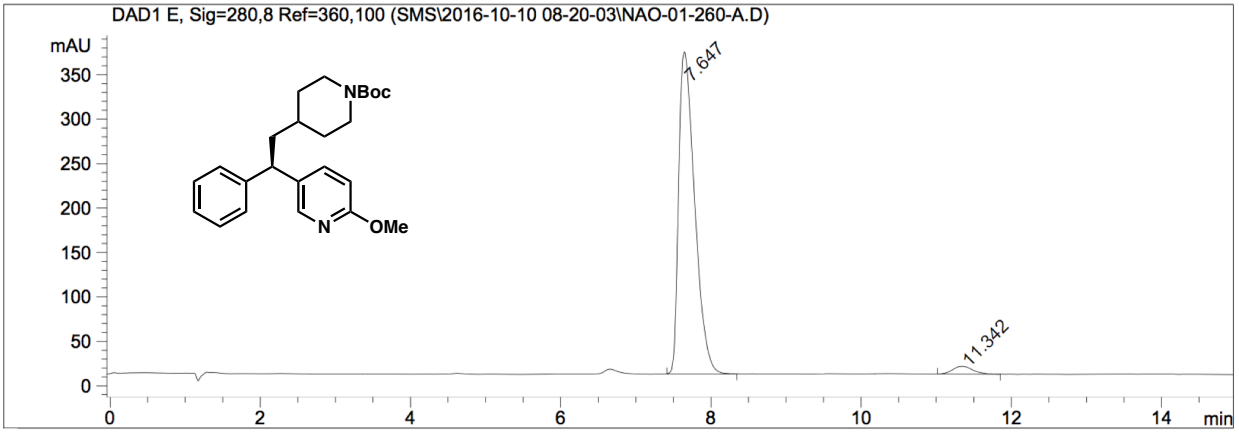

Peak #	RetTime [min]	Type	Width [min]	Area [mAU*s]	Height [mAU]	Area %
1	7.647	BB	0.2291	5372.29736	362.18082	97.0283
2	11.342	BB	0.2754	164.53700	8.91232	2.9717

102 (Table 2.12): racemic

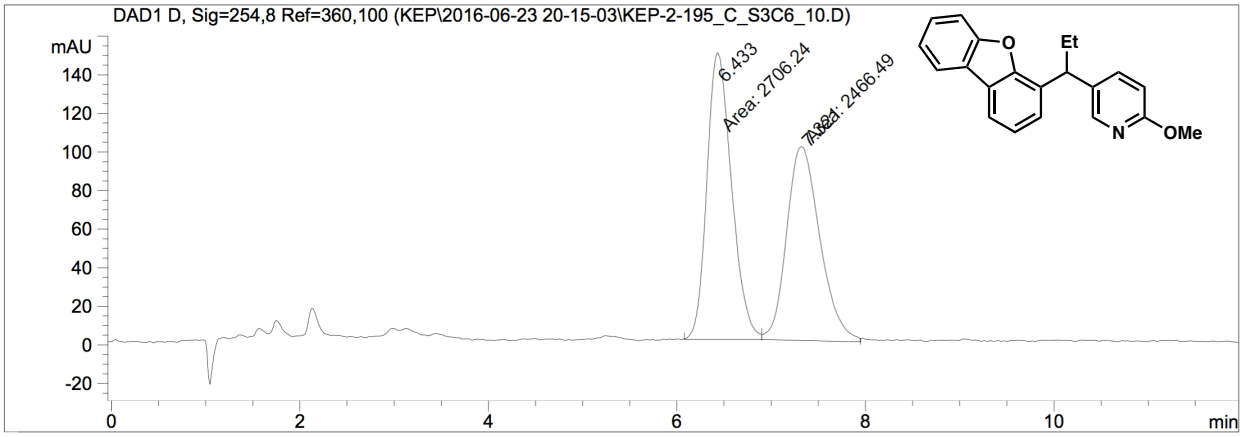

Peak #	RetTime [min]	Type	Width [min]	Area [mAU*s]	Height [mAU]	Area %
1	6.433	MM	0.3031	2706.24146	148.78586	52.3175
2	7.321	MM	0.4090	2466.48608	100.50787	47.6825

102 (Table 2.12): enantioenriched, 93% ee

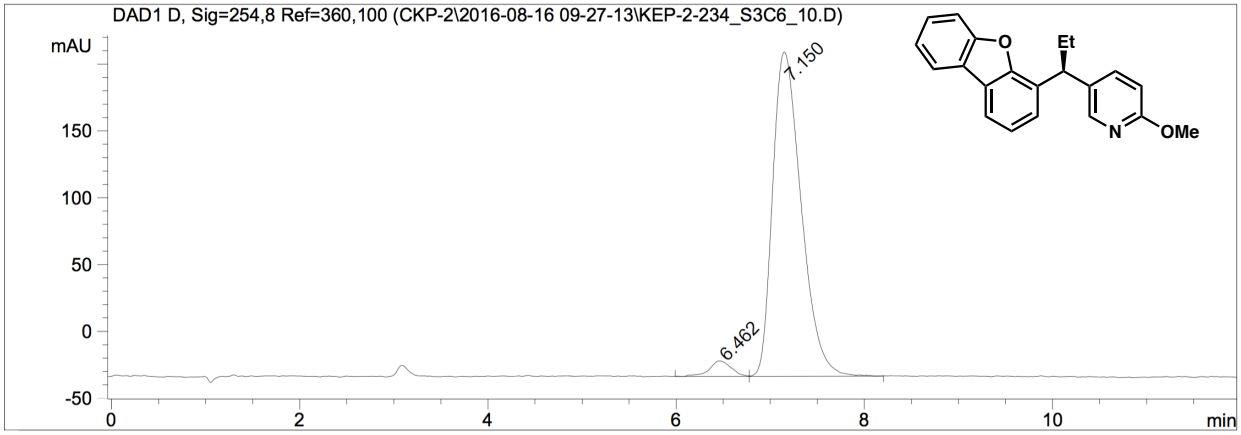

Peak #	RetTime [min]	Type	Width [min]	Area [mAU*s]	Height [mAU]	Area %
1	6.462	BV	0.2413	189.99944	11.70672	3.5725
2	7.150	VB	0.3266	5128.36816	242.62926	96.4275

107 (Scheme 2.7): racemic

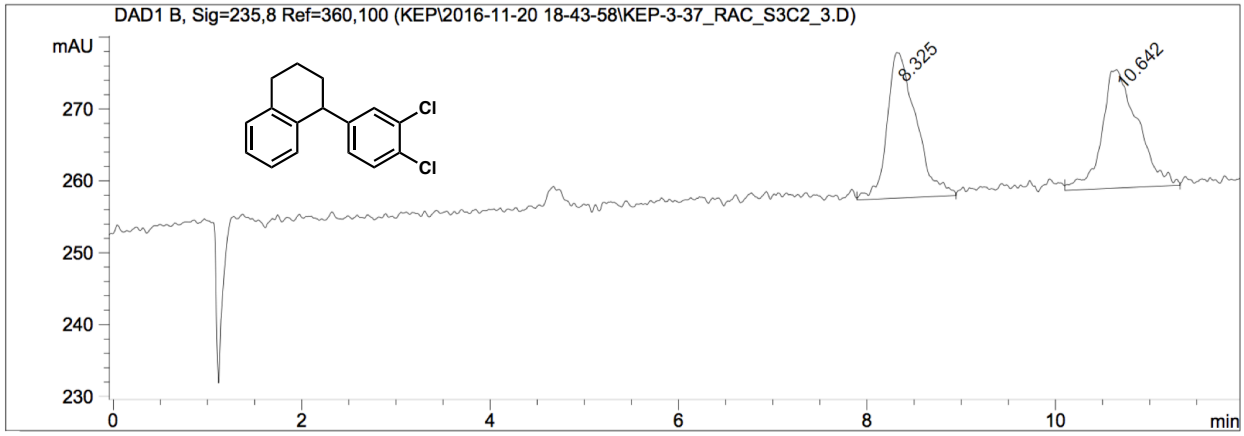

Peak #	RetTime [min]	Type	Width [min]	Area [mAU*s]	Height [mAU]	Area %
1	8.325	VV	0.3056	433.39096	20.25559	49.7137
2	10.642	VV	0.3314	438.38318	16.42403	50.2863

107 (Scheme 2.7): enantioenriched, 84% ee

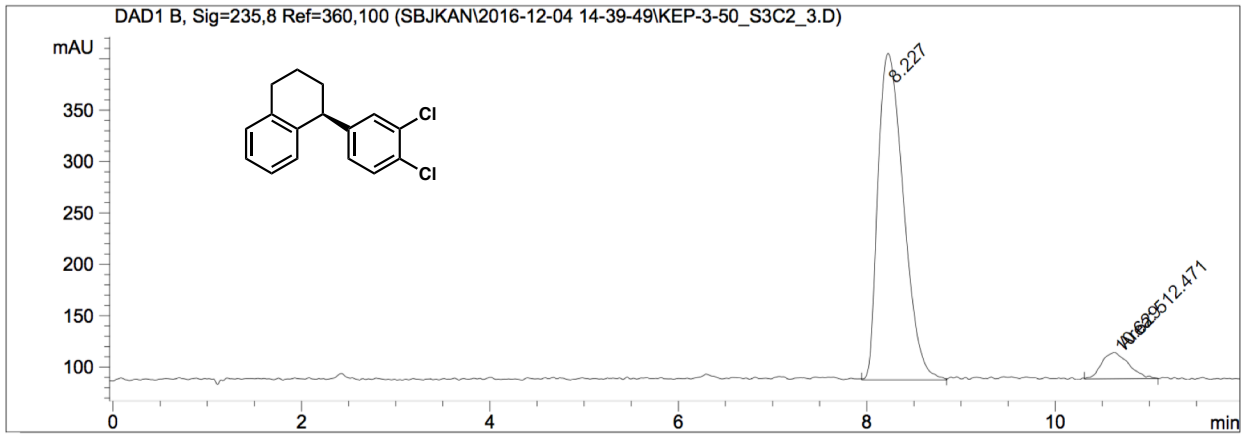

Peak #	RetTime [min]	Type	Width [min]	Area [mAU*s]	Height [mAU]	Area %
1	8.227	BV	0.3002	5989.72314	317.34003	92.1185
2	10.629	MM	0.3320	512.47150	25.72428	7.8815

108 (Scheme 2.7): racemic

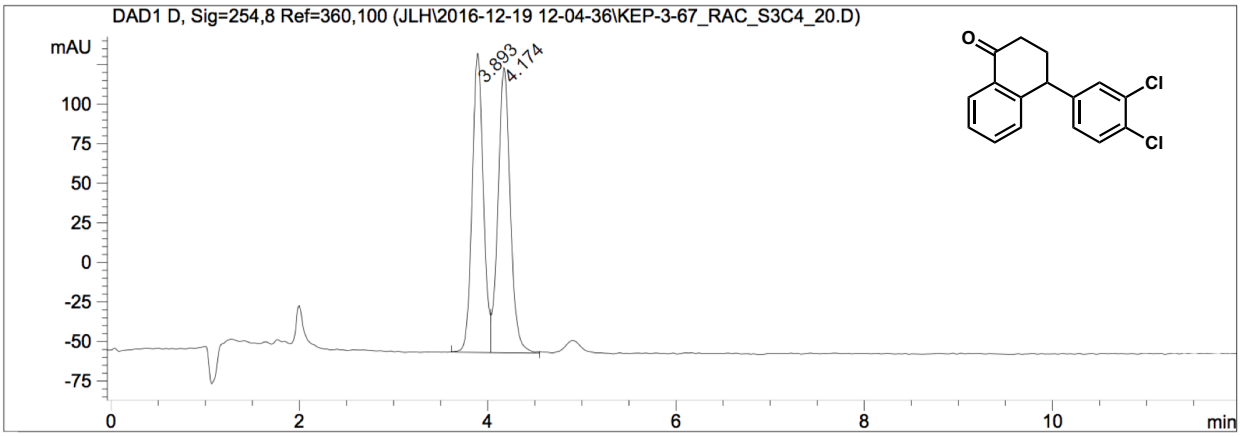

Peak #	RetTime [min]	Type	Width [min]	Area [mAU*s]	Height [mAU]	Area %
1	3.893	BV	0.1280	1552.17676	188.69421	48.6803
2	4.174	VB	0.1381	1636.33215	179.92238	51.3197

108 (Scheme 2.7): enantioenriched, 84% ee

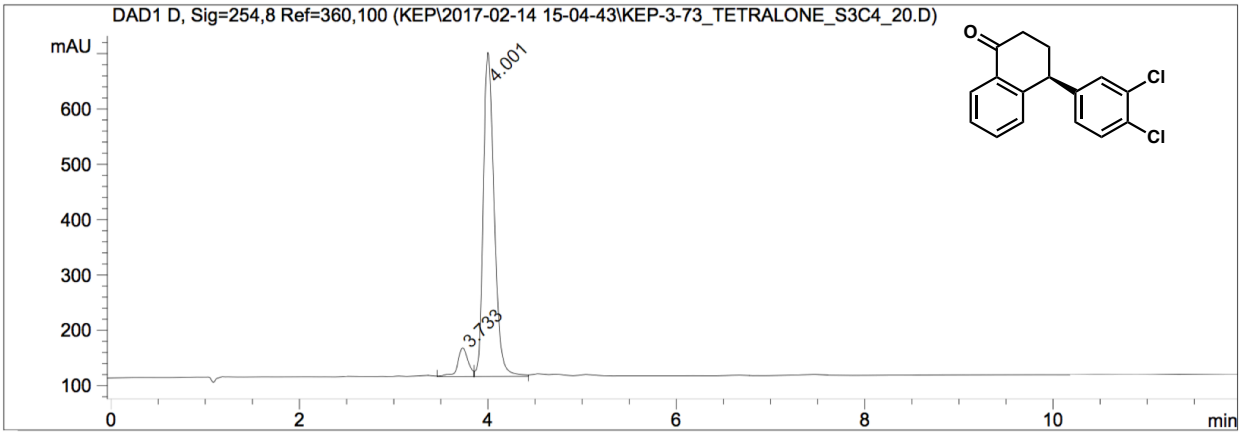

Peak #	RetTime [min]	Type	Width [min]	Area [mAU*s]	Height [mAU]	Area %
1	3.733	VV	0.1186	399.64880	51.48994	7.8135
2	4.001	VV	0.1262	4715.20508	583.70624	92.1865

2.7 NOTES AND REFERENCES

(1) Greene, M. A.; Yonova, I. M.; Williams, F. J.; Jarvo, E. R. *Org. Lett.* **2012**, *14*, 4293.

(2) Kleemann, A; Engel, J.; Kutscher, B.; Reichart, D. *Pharmaceutical Substances: Syntheses, Patents, Applications*, 4th edition; Stuttgart, Ed.; Thieme, 2001.

(3) Hills, C. J.; Winter, S. A.; Balfour, J. A. *Drugs* **1998**, *55*, 813.

(4) McRae, A. L.; Brady, K. T. *Expert Opin. Pharmacother.* **2001**, *2*, 883.

(5) Gordaliza, M.; Garcıa, P. A.; Miguel del Corral, J. M.; Castro, M. A.; Gomez-Zurita, M. A. *Toxicon* **2004**, *44*, 441.

(6) Logan, K. M.; Brown, M. K. *Angew. Chemie - Int. Ed.* **2017**, *56*, 851.

(7) Friis, S. D.; Pirnot, M. T.; Buchwald, S. L. *J. Am. Chem. Soc.* **2016**, *138*, 8372.

(8) Imao, D.; Glasspoole, B. W.; Laberge, V. S.; Crudden, C. M. *J. Am. Chem. Soc.* **2009**, *131*, 5024.

(9) Ohmura, T.; Awano, T.; Suginome, M. *J. Am. Chem. Soc.* **2010**, *132*, 13191.

(10) Yonova, I. M.; Johnson, A. G.; Osborne, C. A.; Moore, C. E.; Morrissette, N. S.; Jarvo, E. R. *Angew. Chemie - Int. Ed.* **2014**, *53*, 2422.

(11) Taylor, B. L. H.; Swift, E. C.; Waetzig, J. D.; Jarvo, E. R. *J. Am. Chem. Soc.* **2011**, *133*, 389.

(12) Wisniewska, H. M.; Swift, E. C.; Jarvo, E. R. *J. Am. Chem. Soc.* **2013**, *135*, 9083.

(13) Hatanaka, Y.; Hiyama, T. *J. Am. Chem. Soc.* **1990**, No. 112, 1193.

(14) Maity, P.; Shacklady-McAtee, D. M.; Yap, G. P. A.; Sirianni, E. R.; Watson, M. P. *J. Am. Chem. Soc.* **2013**, *135*, 280.

(15) Zhou, Q.; Srinivas, H. D.; Dasgupta, S.; Watson, M. P. *J. Am. Chem. Soc.* **2013**, *135*, 3307.

(16) Do, H.-Q.; Chandrashekar, E. R. R.; Fu, G. C. *J. Am. Chem. Soc.* **2013**, *135*, 16288.

(17) Article, E.; Ackerman, L. K. G.; Anka-lu, L. L.; Naodovic, M.; Weix, D. J. *Chem. Sci.* **2015**, *6*, 1115.

(18) Gutierrez, O.; Tellis, J. C.; Primer, D. N.; Molander, G. A.; Kozlowski, M. C. *J. Am. Chem. Soc.* **2015**, *137*, 4896.

(19) Pfaltz, A.; Woodmansee, D. H. *Chem. Commun.* **2011**, *47*, 7912.

(20) Wang, X.; Guram, A.; Caille, S.; Hu, J.; Preston, J. P.; Ronk, M.; Walker, S. *Org. Lett.* **2011**, *13*, 1881.

(21) Sorgel, Sebastian; Tokunaga, Norihito; Sasaki, Keigo; Okamoto, Kazuhiro; Hayashi, T. *Org. Lett.* **2008**, *10*, 589.

(22) Itoh, T.; Mase, T.; Nishikata, T.; Iyama, T.; Tachikawa, H.; Kobayashi, Y.; Miyaura, N. *Tetrahedron* **2006**, *62*, 9610.

(23) Defieber, C.; Stephenson, C. R. J.; Carreira, E. M. *J. Am. Chem. Soc.* **2005**, *127*, 10850.

(24) Nishikata, T.; Yamamoto, Y.; Gridnev, I. D.; Miyaura, N. *Organometallics* **2005**, *24*, 5025.

(25) Ackerman, L. K. G.; Anka-Lufford, L. L.; Naodovic, M.; Weix, D. J. *Chem. Sci.* **2015**, *6*, 1115.

(26) Tellis, J. C.; Primer, D. N.; Molander, G. A. *Science* **2014**, *345*, 433.

(27) Kadunce, N. T.; Reisman, S. E. *J. Am. Chem. Soc.* **2015**, *137*, 10480.

(28) Cherney, A. H.; Kadunce, N. T.; Reisman, S. E. *J. Am. Chem. Soc.* **2013**, *135*, 7442.

(29) Everson, D. A.; Jones, B. A.; Weix, D. J. *J. Am. Chem. Soc.* **2012**, *134*, 6146.

(30) Johnson, K. A.; Biswas, S.; Weix, D. J. *Chem. Eur. J.* **2016**, *22*, 7399.

(31) Müller, D.; Umbricht, G.; Weber, B.; Pfaltz, A. *Helv. Chim. Acta* **1991**, *74*, 232.

(32) Cherney, A. H.; Reisman, S. E. *J. Am. Chem. Soc.* **2014**, *136*, 14365.

(33) Hofstra, J. L.; Cherney, A. H.; Ordner, C. M.; Reisman, S. E. *J. Am. Chem. Soc.* **2018**, *140*, 139.

(34) Suzuki, N.; Hofstra, J. L.; Poremba, K. E.; Reisman, S. E. *Org. Lett.* **2017**, *19*, 2150.

(35) Tang, T. P.; Volkman, S. K.; Ellman, J. A. *J. Org. Chem.* **2001**, *66*, 8772.

(36) Broggi, J.; Terme, T.; Vanelle, P. *Angew. Chemie - Int. Ed.* **2014**, *53*, 384.

(37) Poremba, K. E.; Kadunce, N. T.; Suzuki, N.; Cherney, A. H.; Reisman, S. E. *J. Am. Chem. Soc.* **2017**, *139*, 5684.

(38) Woods, B. P.; Orlandi, M.; Huang, C. Y.; Sigman, M. S.; Doyle, A. G. *J. Am. Chem. Soc.* **2017**, *139*, 5688.

(39) Khouzam, H. R.; Ernes, R.; Gill, T.; Roy, R. *Compr. Ther.* **2003**, *29*, 47.

(40) Bianco, G. G.; Ferraz, H. M. C.; Costa, A. M.; Costa-Lotufo, L. V.; Pessoa, C.; de Moraes, M. O.; Schrems, M. G.; Pfaltz, A.; Silva, L. F. J. *ChemInform* **2009**, *40*, 2561.

(41) Lautens, M.; Rovis, T. *J. Org. Chem.* **1997**, *62*, 5246.

(42) Vukics, K.; Fodor, T.; Fischer, J.; Fellegvári, I.; Lévai, S. *Org. Process Res. Dev.* **2002**, *6*, 82.

(43) Welch, W. M.; Harbert, C. A.; Koe, B. K.; Kraska, A. R. U. S. No Title. Patent 4536518 A, 1985.

(44) Spavins, J. C. Patent 4855500 A, 1989.

(45) Beckwith, A. L. J.; Bowry, V. W. *J. Am. Chem. Soc.* **1994**, *116*, 2710.

(46) Halgren, T. A.; Roberts, J. D.; Horner, J. H.; Martinez, F. N.; Tronche, C.; Newcomb, M. *J. Am. Chem. Soc.* **2000**, *122*, 2988.

(47) Biswas, S.; Weix, D. J. *J. Am. Chem. Soc.* **2013**, *135*, 16192.

(48) Lundin, P. M.; Esquivias, J.; Fu, G. C. *Angew. Chemie - Int. Ed.* **2009**, *48*, 154.

(49) Lou, S.; Fu, G. C. *J. Am. Chem. Soc.* **2010**, *132*, 1264.

(50) Lou, S.; Fu, G. Cr. *J. Am. Chem. Soc.* **2010**, *132*, 5010.

(51) Liang, Y.; Fu, G. C. *J. Am. Chem. Soc.* **2014**, *136*, 5520.